RESIDENT'S ATLAS OF OCT ANGIOGRAPHY

RESIDENT'S ATLAS
OF

OCT
ANGIOGRAPHY

BY
ADAM WYLĘGAŁA
RETCO & CMW PRESS

Resident's atlas of OCT Angiography

Author: Adam Wylęgała

Editor: Sławomir Teper MD PhD.

Correction: Translmed

Cover design: Filip Wylęgała

ISBN: 978-83-954140-0-8

Katowice 2019

DTP and printing:
KMSTUDIO Agencja Wydawniczo-Reklamowa
e-mail: kmstudio@poczta.fm

Contents

Disclaimer

Due to rapid advances in medical science and knowledge and as new devices enter the market or old ones receive software upgrades, part of the information in this book may become obsolete. In their effort to provide the most accurate information, the author and editor of this work has consulted sources believed to be reliable and appropriate at the time of the writing of this book. As always in science, readers are strongly encouraged to consult the information found in this book together with other sources. It is important to know that Optical Coherence Tomography Angiography (OCTA) is a novel technology and that these results from large randomized multicenter trials have not yet been published; hence, it is still doubtful whether these results can be used in daily clinical practice. Neither the author, nor the editor nor the publisher nor any other party involved, guarantees any information contained in this book and cannot be held liable for any errors resulting from missed diagnoses or false treatment based on the information found herein. Patients seeking health information in this book should seek professional advice from healthcare professionals. Product names of the software and machines are registered trademarks and proprietary names. Therefore, these names cannot be considered as being in the public domain.

Disclosures: Adam Wylęgała received speaker honorary from Carl Zeiss, he has a patent pending for the OCTA algorithm. Polish patent office P.418979.

Abbreviations

AMD	– Age related macular degeneration.
BCVA	– Best corrected visual acuity
CNV	– Choroidal neovascularization.
CRVO	– Central retinal vein occlusion
CSR	– Central serous retinopathy
DCP	– Deep capillary plexus
DVC	– Deep vascular complex
FAZ	– Foveal avascular zone
GCL	– Ganglion cell layer
ICP	– Intermediate capillary plexus
NVD	– Neovascularization on a disc
OCTA	– Optical coherence tomography angiography
OCT	– Optical coherence tomography
SSAD	– Split spectrum amplitude decorrelation
PED	– Pigment epithelial detachment
RAP	– Retinal Angiomatous Proliferation
RNFL	– Retinal nerve fibre layer
RP	– Retinitis pigmentosa
RPCP	– Radial peripapillary nerve plexus
SVC	– Superficial vascular complex
SVP	– Superficial vascular plexus
SD-OCT	– Spectral-domain OCT
SS-OCT	– Swept-source OCT

Foreword

When I started the period of my residency, OCT was just entering the market. It soon turned out that the introduction of this method is a revolution that will forever change ophthalmology. Today, it is difficult to imagine the treatment of retinal diseases without OCT. The gradually developed potential of this method was manifested by the introduction of further hardware and software improvements. One of the greatest achievements in the development of this technology is OCT-A – angiography without contrast media. Up to now, the imaging of the flow in the retinal vessels was possible only in an invasive way. Each invasive examination has many limitations, side effects and contraindications so it is impossible to perform such tests in specific groups of patients and in specific clinical situations. It increases risk and costs. OCT-A is not a flawless method, but it eliminates many of the above problems. For the next generation of ophthalmologists it will be a routine diagnostic procedure. The author's enthusiasm and involvement in the cognition of this method are proof of the widely open possibilities for scientific development from the beginning of the ophthalmologic career path. The interpretation of angio-OCT, maybe beyond the assessment of the superficial plexus in healthy people, is not easy. It is worth starting to get to know the OCT-A from the very beginning – the principles of operation, the guidelines for obtaining an image suitable for evaluation and the principles of interpretation of the results. This book is an introduction that will allow you to start the adventure with OCT-A. It is dedicated to residents in ophthalmology and specialists who want to get acquainted with OCT-A and introduce this method into their practice. The author focused on the most important issues and the most common diseases.

I believe it is a very good starting point.

There is still a lot of questions to answer:

1. Will the OCT and OCT-A algorithms assess leakage from blood vessels?
2. Will the quantitative data obtained with OCT-A be clinically significant enough to change the treatment of retinal disorders?
3. Will OCT-A eliminate the need for fluorescein angiography?
4. Will OCT-A eliminate the need to perform indocyanine angiography?
5. Will OCT-A allow to unambiguously assess the nature and speed of the blood flow or the components of the flowing blood?

I believe that the Author will take part in getting answers to the above questions and I wish him that.

Sławomir Teper M.D. Ph.D. Editor

Preface

"It is becoming increasingly clear that Nature operates according to a completely different plan than previously thought".

Nearly a hundred years ago, the creator of quantum electrodynamics, Paul Dirac, described the destruction of old knowledge by the new. This destruction led to the creation of new theories and unprecedented development in science and technology, without which GPS, smartphones and most of the devices used today in ophthalmology, including OCT, would not be possible. I am convinced that the introduction of OCT angiography in general is one such creative destruction that may replace fluorescein angiography and broaden our understanding of retinal disease.

My adventure with OCT angiography started in October 2015 when Topcon technicians upgraded our OCT Triton with an angiography function. At the beginning, the program was slow, images were full of motion artifacts and they were 0.5 GB in size and so, to the horror of our IT specialist, after 3 months there was no free disc space on our server. Today, of all cases diagnosed with vascular AMD we perform fluorescein angiography in only 15%. Once my boss had seen my presentation during an international conference in China, he asked me if I could write an OCTA atlas for residents. This was a fascinating yet long (9643 min of word editing and 32 hours of image hunting) journey for me. It was my intention to create a concise pocket atlas, so I realize that some chapters are very superficial, e.g. the one on optic discs or the principles of OCTA. I cannot overstate how much I have learned about OCT and OCTA during this time. I can only hope that I have been able to pass on my knowledge clearly and concisely.

I would like to express my gratitude to Magdalena Hunt MD and Bogumiła Sędziak-Marcinek MD, two residents from Railway Hospital who helped me to find interesting cases.

1. Principles of Optical Coherence Tomography Angiography (OCTA)

Most people reading this book will probably skip this chapter; however, experts in this field agree that due to the as yet still developmental nature of OCTA it is essential to understand how OCTA works. I can only encourage you to read and understand the principles of how the computer creates images of vessels. OCTA is an addition to already existing OCT platforms. The first paper about OCTA was published in 2006, and it took almost 10 years from that time to bring it to the bedside. So what is OCT? Let us decipher its meaning: *optical* means that light is used, *coherence* describes the fact that the light used in this technique has the same phase so, if you delay it by 1/2 the time of the phase duration you can create destructive interference (this is how noise canceling in headphones works), while *tomography* means that we will visualize slices of the human body. Similar to the principles of ultrasound imaging, OCT generates pictures of tissue slices by using the interference that arises when superimposing reference light and backscattered light in an interferometer to obtain an amplitude profile scan (A-Scan) of a sample. The lateral deflection of the sample beam generates slice images. A "brightness-mode scan," (B-scan) from which three-dimensional volume images can be generated, is created by acquisition of multiple A-scans in the transverse direction of the beam of light. The measurement of the interference spectrum on a *spectrometer* is called spectral-domain OCT (SD-OCT), or if a rapid tunable laser *sweeps* the wavelength over a given time period then it is called swept-source OCT (SS-OCT).

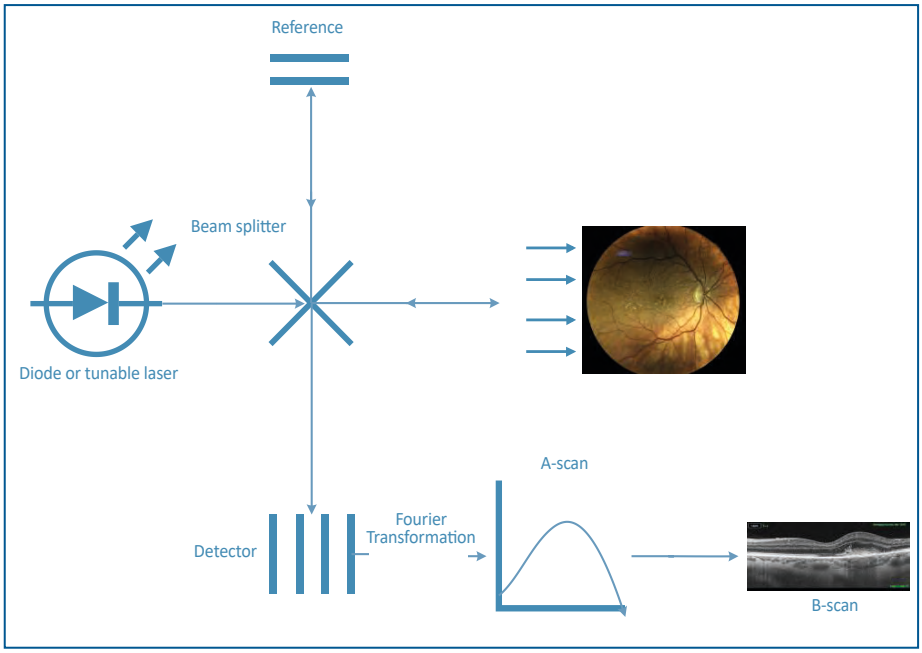

Figure 1-1. Drawing of the OCT technology. Swept source uses tunable laser while SD-OCT superluminescente diode. A CMOS camera in SS-OCT or CCD camera in SD-device can act as a detector.

The idea of OCTA is based on the detection and analysis of the reflection behavior of moving particles in a static environment. By comparing two or more consecutively recorded B-scans of the same position of the retina, a contrast between the moving blood flow within the vessels and the static surrounding tissue can be created via a software-based image processing step. Such an idea can obviously lead to the creation of false information because it is only *generally* true that the all the motion comes from the movement of blood. For example, it is estimated that our eyes make up to 200 000 movements per day, or the eyes move with the movement of the head, or that there is a movement of the body associated with the beating of the heart. This created a huge problem for the inventor of OCTA. I have already mentioned that OCTA creates 3D images by taking multiple B-scans of the different locations that will be displayed, but in order to generate OCTA B-scans the device has to acquire multiple OCT B-scans of the *same* location and the changes in pixels are analyzed. OCTA images are created by algorithms that compare differences in OCT signal amplitude or phase or both.

Another method is utilized by algorithms measuring speckle variance. Speckles are nothing more than noise and in most electronic devices are a disturbing factor (white noise on a TV screen); however, in some OCTA their *changes* can be analyzed. Most devices use OCT split spectrum amplitude decorrelation (SSAD), where the wave spectrum is divided into many narrow bands, which are then used to compute reflectance amplitude decorrelations in a single voxel over time. In swept-source devices another algorithm is employed – OCTARA (OCTA Ratio Analyses, Topcon) based not on decorrelation but on intensity ratio analyses.

OCT machines detect the flow of erythrocytes which, due to their concave structure, act as a mirror. This effect can be seen when there is diffused blood in the anterior chamber of an eye; so, with a slit lamp you can see bright spots that are erythrocytes.

An OCTA image is generated by a B-scan starting at one edge of the imaged region followed by the A-scans that are acquired as the beam of coherent light scans in the transverse direction across the required location. OCTA scans are also thresholded based on the OCT signal. So, if an OCTA signal is low, it means either that the flow is low or that the OCT signal is low, which can happen e.g. under drusen or both. Another possibility is that the flow, especially in the choroid, is too fast and this leads to fringe washout of the OCT signal. SD devices are susceptible to a so-called roll of phenomena, which means that the sensitivity farther from the system's zero-delay is smaller. Most devices are set to image vitreoretinal spaces correctly which means that the retinal features are displayed with high resolution while the choriocapillaris are not. However, if there is a choriocapillaris scan protocol in your device, you should try to use it for visualizing the sub-RPE areas.

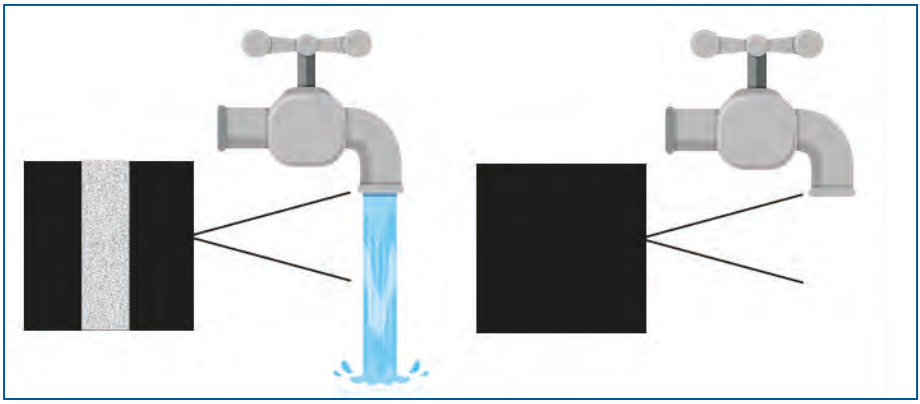

Figure 1-2. OCTA can detect motion in a static environment.

Regarding the time required by the OCTA: every B-scan is composed of a certain number of A-scans and every OCTA device has a number of A-scans per second, e.g. DRI OCT Triton makes 100 000 A-scans/s, Optopol Flux 250 000 A-scans/s and prototype vertical cavity surface emitting lasers can make up to 500 000 A-scans/s. The total time of a B-scan is called the acquisition time. As I mentioned, OCTA images are composed of several B-scans of the same location. (Some prototypes do not really need to have multiple B-scans but that is a topic for the second edition.) This means that the beam must always scan back to the primary position. This is called flyback and the time required to do this accounts for around 10%-20% of the whole B-scan time. Flyback time plus acquisition time equals interscan time which is the time between the completion of a B-scan and the start of a new scan. Why is this important? Interscan determines the sensitivity. The longer the interscan time the more blood will flow thorough vessels and the more detailed will be the visualization of the structure of smaller vessels. The obvious drawback is that this will mean that more artifacts coming from eye motion will also be captured. In contrast, a shorter time will generate less sensitive results but also less artifacts. Just like the specificity and sensitivity of a diagnostic test. Therefore, as a compromise variable interscan time analysis (VISTA) was developed. As the blood flowing through the arteries and capillaries does not have the same speed, another problem emerges. If the A-scan registers certain blood cells, in order to register the flow these same cells must be in a different location when the A-scan is repeated. We can imagine that the longer the interscan time the more distance the cells are going to move and a slower flow will be detected. However, if the interscan time is too long, it may happen that the blood cells are detected by the first scan and when the repeat scan commences these cells will already be outside the beam range of the OCT device and such a fast flow will not be detected. A regular OCT has a beam range of 20 μm.

Does OCTA quantify blood flow? The short answer is- in future it could be possible, currently it is not. As we know from physiology, blood does not flow in a constant manner but rather in a pulsatile way. This is one problem, a second one is that it takes a very limited number of B-scans (2-4) to create an OCTA image so the output information is rather binary: yes, there is a flow or no, there is not. It is very challenging to obtain statistical data from such a small number of repeated measurements. So we will probably have to wait a few more years to have reliable flow measurements. Right now, we have to rely on maps showing vessels.

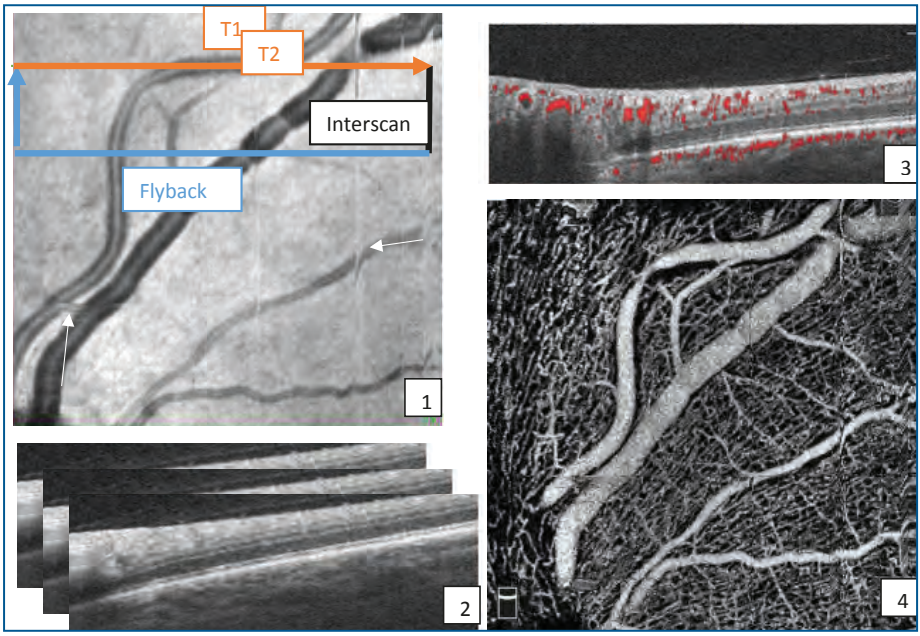

Figure 1-3. Schematic of how OCTA images are created. 1. T1 is the acquisition time of the B-scan. As the scanning beam flies back to the first position (where it previously was) and rescans the same location. There is also an interscan time which is the time between T1 and T2. 2. Multiple A-scans create a B-scan. 3. After multiple B-scans of the same location are generated, differences in specific parameters are measured from which an OCTA B-scan is created. 4. From OCTA B-scans such impressive images can be formed. Note the detailed structure of the RPCP. These images are taken with Angiovue (Optovue, USA) and this machine scans in X and Y axes, so the bars can be seen on the SLO image (arrows).

Another important issue is the blood flow through the retina. As OCTA is quite new, some nomenclature discrepancy exists. The whole retina has a dual blood supply with the outer being (mostly) supplied by the choriocapillaris, and the inner by the branches of the central retinal artery. The vascular complex that is above the inner nuclear layer (within the Inner Plexiform layer (IPL), Ganglion cell layer (GCL) and partially in the retinal nerve fiber layer (RNFL)) is called superficial (SVC). In contrast, the vascular plexus located within the inner nuclear and outer plexiform layer is called the deep vascular complex (DVC). While this classification is easy for machines as segmentation is done among specific boundaries it is not histologically true. At the time of writing, 4 retinal vascular plexuses are distinguished histologically. The layer

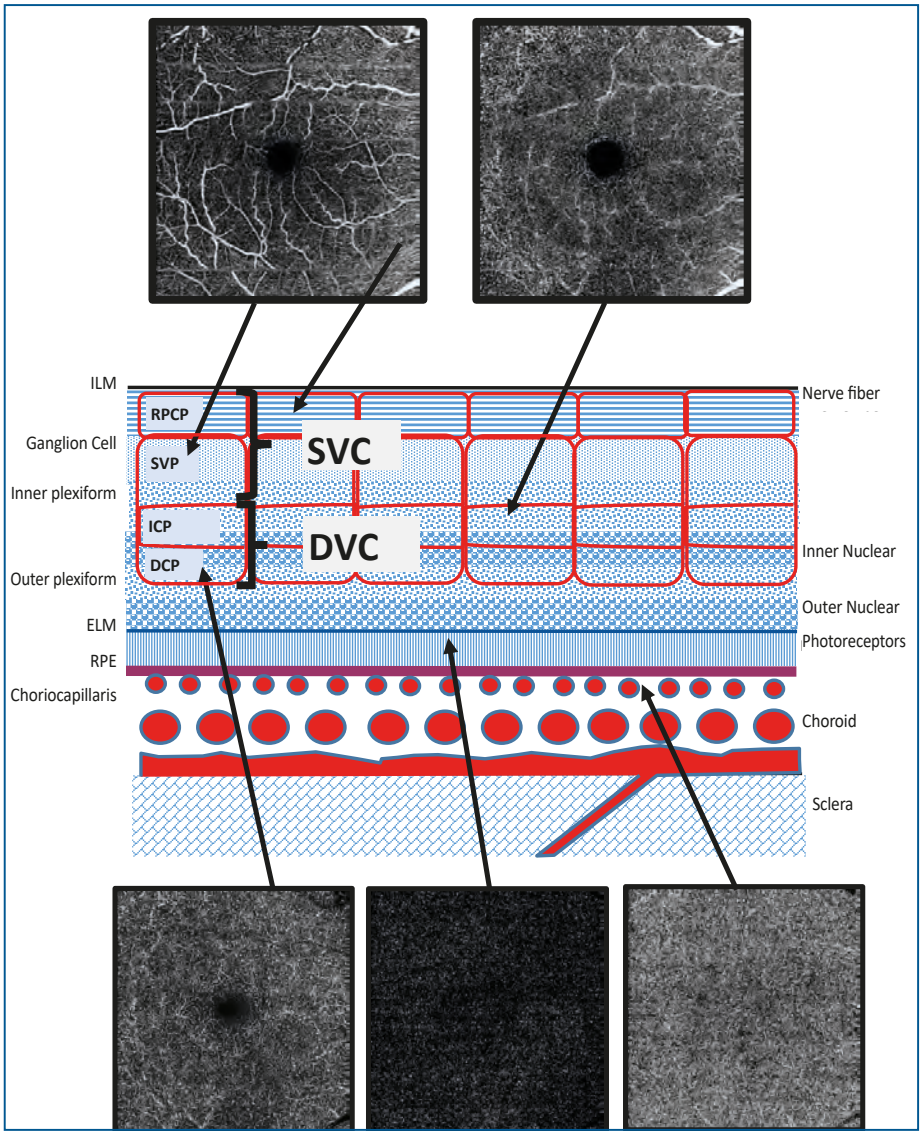

Figure 1-4. Graph describing the blood flow of the retina. SVC is composed of the blood flowing from the central retinal artery, and then through anastomoses to another plexus – ICP – and then DCP. DCP and ICP vascular plexuses have lobular configurations, whereas the radial peripapillary nerve plexus RPCP runs parallel with the axons of the RNFL. SVC – superficial vascular complex SVP superficial vascular plexus, ICP – intermediate capillary plexus, DVC – deep vascular plexus, DCP deep capillary plexus, RPCP – retinal peripapillary nerve fiber layer.

of vessels closest to the vitreous, mostly in the GCL and partially in the IPL, is called the superficial vascular plexus. The ones located within outer parts of the IPL and inner parts of INL are called the intermediate capillary plexus. Whereas, all capillaries in the outer plexiform layer and outer INL are called the deep capillary plexus. There is a fourth vascular plexus located within the RNFL running parallel to the axons of ganglion cells and this is called the radial peripapillary capillary plexus (RPCP). In older publications you can find the use of superficial vascular plexus and deep vascular plexus composed of smaller plexuses this is not entirely logical because the 2 plexuses are forming complex. That is why we will follow this nomenclature.

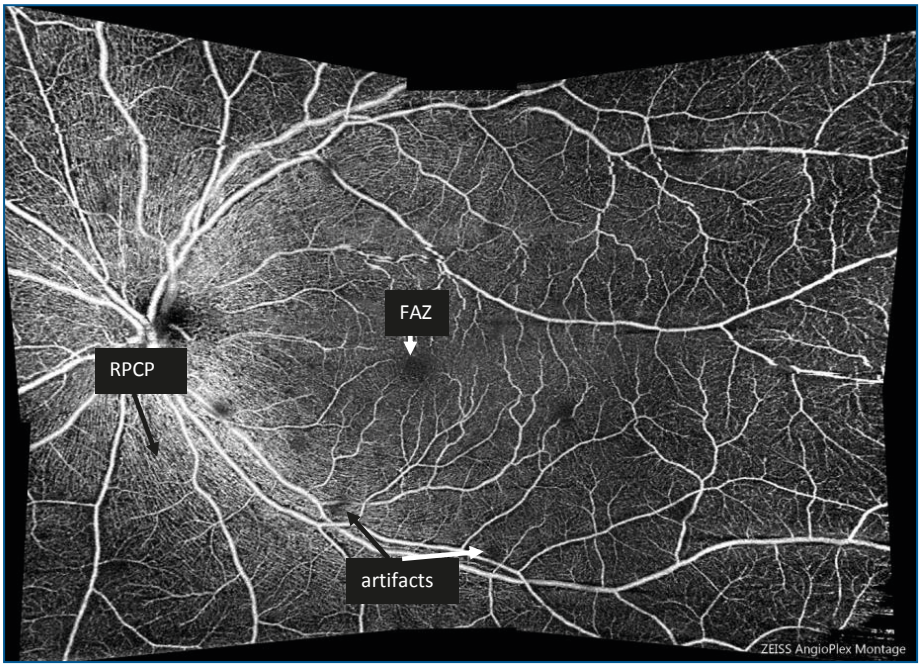

Figure 1-5. 14×10 mm Wide-field montage of OCTA images of a healthy 37-year-old female. FAZ foveal avascular zone, RPCP radial peripapillary capillary plexus. This type of image can be used to visualize neovascularization elsewhere. FAZ area in healthy eyes varies among the different device and it is usually around 0.35 mm^2.

Key points

OCT measures the time delay of a light and how much a certain tissue scatters or absorbs light.

Multiple A-scans are converted into B-scans, while multiple B-scans create 3-D images. Multiple B-scans of the 3D slice create the OCTA image. Images of the same locations are compared for changes in specific parameters and on this basis the software detects flow. There are four retinal capillary plexuses: radial peripapillary, superficial, intermediate and deep. OCTA currently does not precisely measure blood flow but gives general information about a flow or a lack thereof.

2. Standard reports from 3 devices used in this book

In this book OCTA images from three different devices will be presented: DRI OCT Triton, (Topcon, Tokyo, Japan), Cirrus 5000 (Zeiss Medictec, Dublin, CA, USA) and Angiovue (Optovue inc, Freemont, USA). Each machine is slightly different and visualizes the CNV in a different manner. Angiovue has very few artifacts; however, it is very hard to see RPCP on a regular 6×6 mm scan, unlike with Cirrus or Triton. Angiovue software is also quite confusing and it takes a long time to learn. The main advantage of Triton is the presence of fundus camera which enables the examiner to assess the fundus simultaneously and merge the fundus photo with the OCTA. Moreover SS-OCT has a deeper penetration but lower resolution. Cirrus has a very intuitive interface and the largest scan resolution.

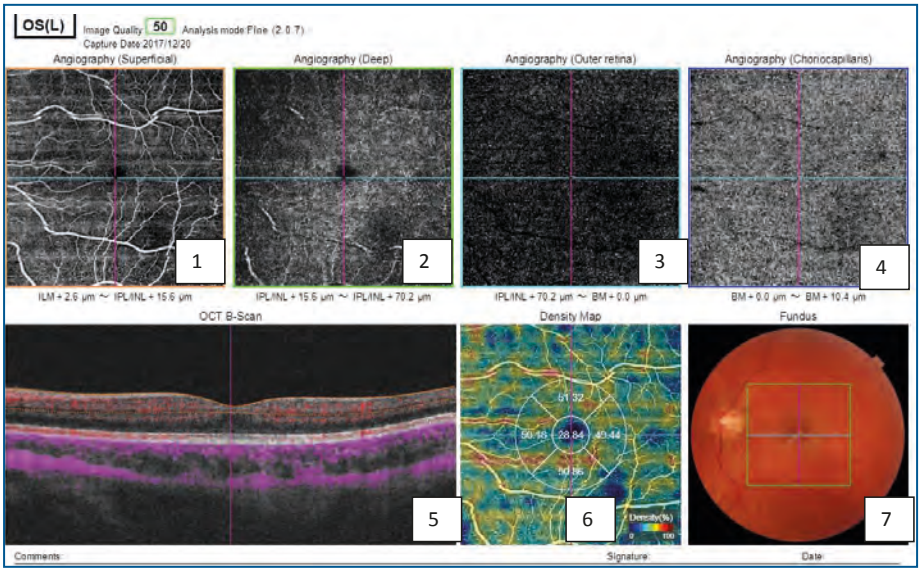

Figure 2-1. Topcon Triton boasts a 100 kHz Swept-source system and fundus camera option with potential fluorescein angiography in the most complex version. It takes up to 12×12 mm

scans; however, they take a while and are almost impossible without mydriasis and cooperation. In theory, the use of infrared light enables a greater penetration but it lacks the resolution that SD-OCT has. Top left to right: 1. superficial complex 2. deep complex 3. outer retina 4. choriocapillaris. Bottom left to right 5. B-scan color-coded with flow intensity 6. different types of map, i.e. SLO, ganglion cell thickness, RNFL, here density map of the superficial segment 7. fundus photo. On the density map there is a visible semi-EDTRS circle with a 1-millimeter-diameter circle at the center, four quarters within 3-millimeter-diameter circles. It is in the same position as EDTRS circles are on the OCT B-scans describing central macular thickness.

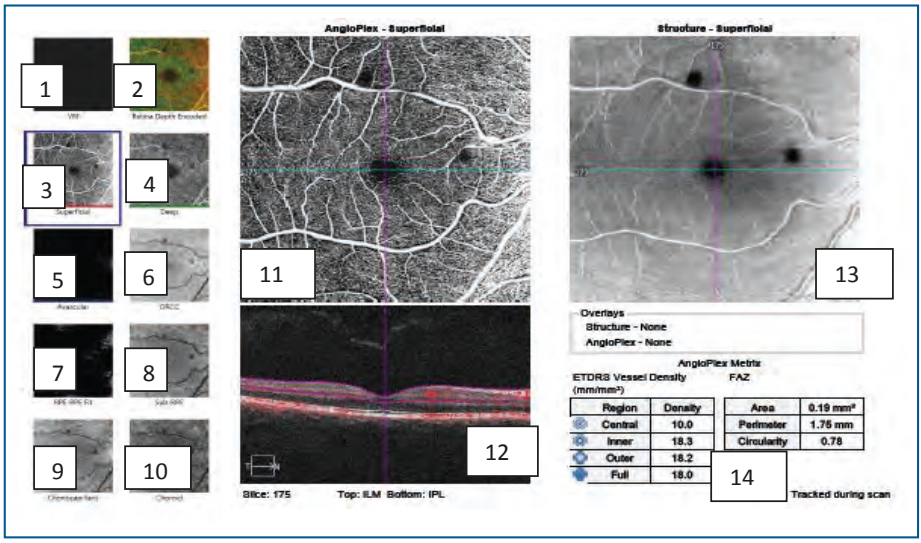

Figure 2-2. Cirrus 5000 from Zeiss has the highest resolutions of all of the 3 devices 6×6 mm has a 512×512 while Triton has 320×320 that makes the observations of the RPCP on almost all 6×6 mm scans what is hard on Triton and on Optovue system. This system has the highest number of automatic segmentations. Moreover, it can create merged images of 14×14 mm; again, mydriasis and patient cooperation are necessary. On the left are small icons representing different scans 1. VRI – vitreous retinal interface used for neovascularization on a disc 2. color-coded merge image 3. superficial 4. deep 5. avascular 6. ORCC – outer retina choriocapillaris – very useful for CNV types I and II 7. RPE and RPE fit, so also helpful for better visualization of CNV 9. sub-RPE 10. choriocapillaris and choroid 11. selected OCTA images from the icons on the left 12. B-SCAN scan with color-coded flow, it is possible to code sub-RPE as green and above RPE as red. 13. SLO image 14. metric analysis with EDTRS circle vessel density in 4 quadrants and FAZ measurement area, perimeter and circularity. Circularity is the measure of how close an object is to a perfect circle which has a value of 1. The lower the value the less round the FAZ is. Black dots are artifacts from dirt on the lens.

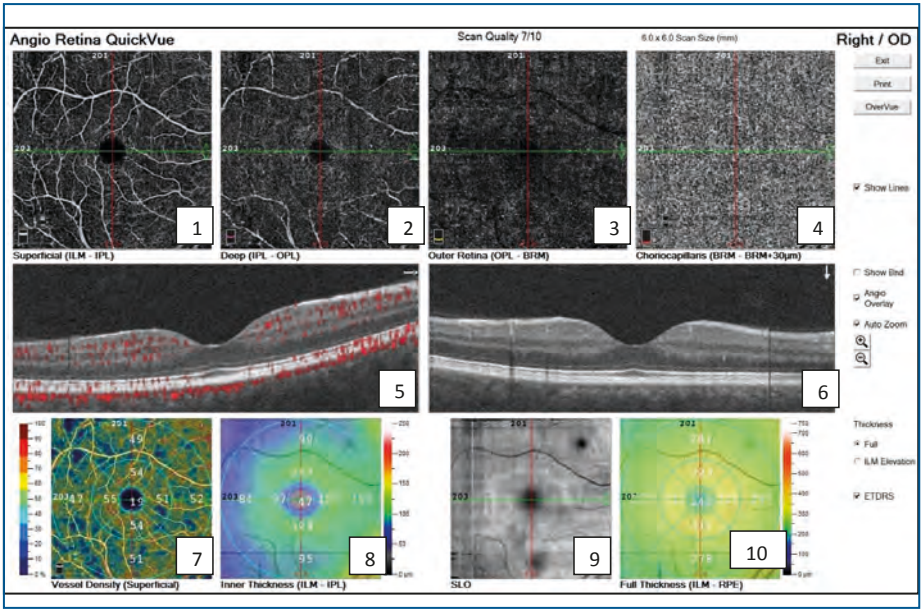

Figure 2-3. This report comes from Angiovue by Optopvue. It is similar to the one seen in the Topcon device, although in this device there is a full EDTRS circle and the outer circle has a 6 mm diameter and instead of a color fundus photo there is a SLO photo. Top from left to right 1. superficial 2. deep 3. outer retina 4. choriocapillaris 5. B-SCAN with flow 6. B-SCAN 7. density map with EDTRS 8. inner thickness map 9. SLO image 10. full-thickness color map. There is also the possibility to create a montage image and follow progression and perform the same flow analysis. There is also a color-coded map. This device also features a metric solution where it is possible to measure changes in density or CNV size.

3. Fifteen rules to keep you out of trouble

3.1. Have a good technician

In our private practice and clinic, we are lucky to have been working with a technician who performs OCT scans since 2002 when we bought our very first Zeiss Stratus (the first machine in eastern Europe). Since then, she has performed more than 2 million scans and is probably the most experienced technician in the whole country. As in our clinic we have a reading center for south Poland, I see how important is it to have a good technician, especially since it takes a long time to take a 12×12 mm OCTA scan. All scans in this book performed on Cirrus and Triton were conducted by her, for which I am very grateful. The patient must be well positioned, have the eyelid wide open and must not be distracted by any light, sound or movement. So, it should preferably be a dark room not a corridor where everybody is constantly walking. As patients tend to blink, it is advisable for them to have their eyes shut while you prepare for the exam or wait till the next examination is ready. It is also crucial to inform the patient that it does not hurt, has no known side effects and is short. Sometimes mydriasis is necessary.

3.2. Know your device

Although similar at first glance, every machine is different, and has unique functions that are imbedded to allow you better diagnosis of diseases. After you start using a new device, it is worth spending an evening getting acquainted with the software and trying to get the best out of it. It is also worth reading the manual. Then you will be able to discover new functions which might be hidden deep in the programs.

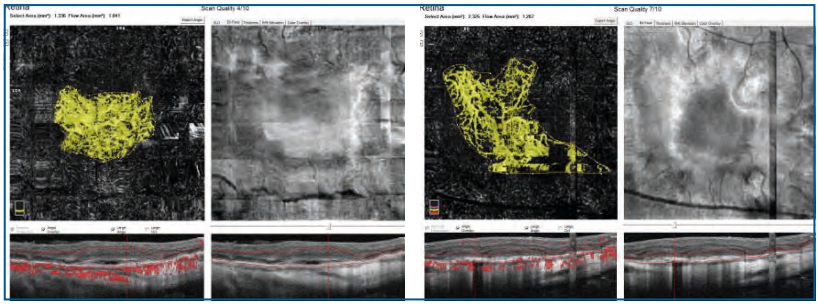

Figure 3-1. Comparison of OCTA reports. Angiovue has an option to automatically calculate the size of a CNV and to compare it. However, there is also a function that allows you to do this manually in cases with poor image quality. Example of the use of a comparative analysis of two scans during therapy with a one month follow. Here, the CNV area grew from 1.367 to 2.325 mm^2. Frequently, it is hard to clearly delineate the lesion, as in the first two follow up photos. So, this method needs to be used cautiously.

3.3. Not everything white is a vessel

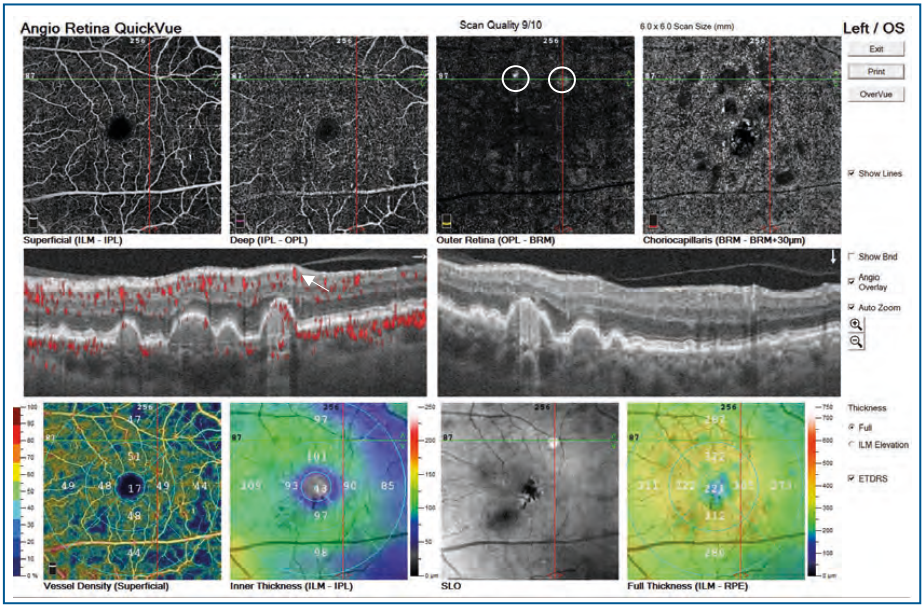

Figure 3-2. OCTA report on left eye. Image from a 74-year-old female with multiple soft drusen. Note that some of these are generating motion contrast in the outer retina which should be devoid of vessel (circles). Note that large retinal vessels (white arrow) generate shadowing through the capillary. Moreover, there is a loss of choriocapillaris under drusen, as seen in the choriocapillaris image.

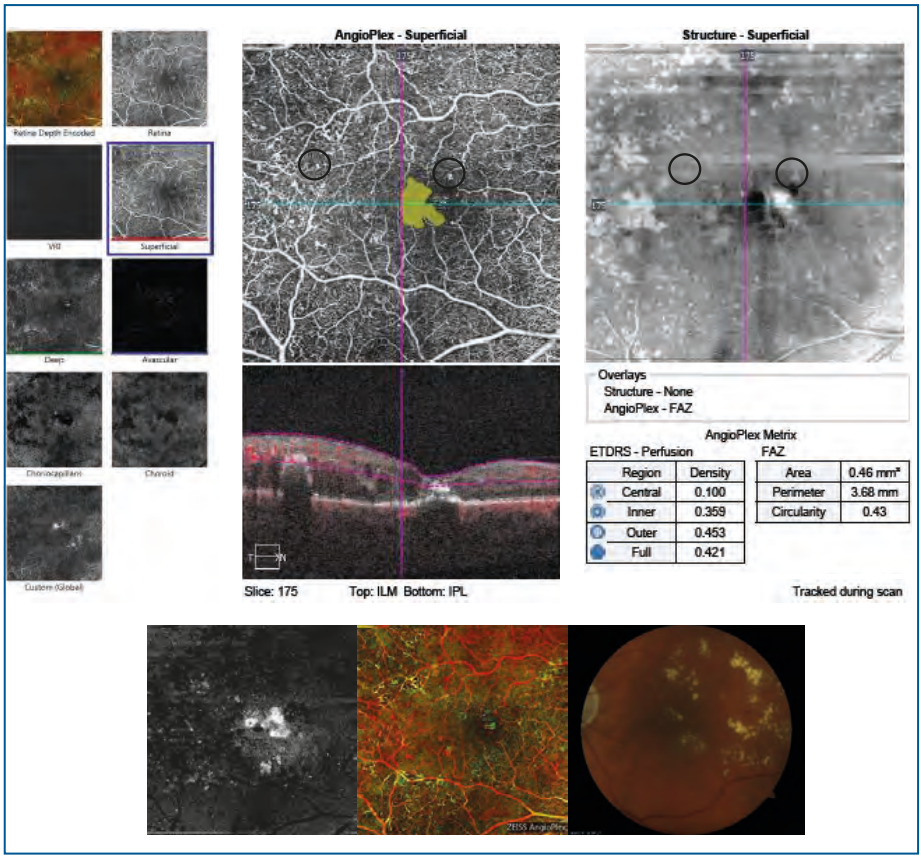

Figure 3-3. Multimodal image of left eye. This diabetes t 2 patient has multiple hard exudates that imitate blood flow and are displayed as white points (black circles). Please note the distorted FAZ (yellow fill), a feature of diabetic retinopathy with a circularity of 0.43, meaning it is not completely round. On a color fundus photo, cystoid macular edema is visible with multiple hard exudates from leaking microaneurysms. In this case, it is also worth looking at the en-face as cysts and hard exudates are even more prominent. Usually, the difference between lipid/protein aggregates and vascular abnormalities lies in the surrounding area and shape. Exudates are usually circular and are not connected to vessels, and their size is not comparable to the surrounding vessels. Generally, hard exudates are hyper-reflective on B-scans but on OCT-A this varies. Those superficially located may not be seen, while deeper ones can create a signal; however, sometimes abnormal vessels that are close to them can be the cause of this signal. It seems that the algorithm creates these changes.

3.4. Watch out for segmentation errors

Always check segmentation for possible errors. Since the introduction of OCTA, the second biggest problem has been erroneous segmentation. This is especially visible if there are structures pushing parts of the retina, e.g. macular edema.

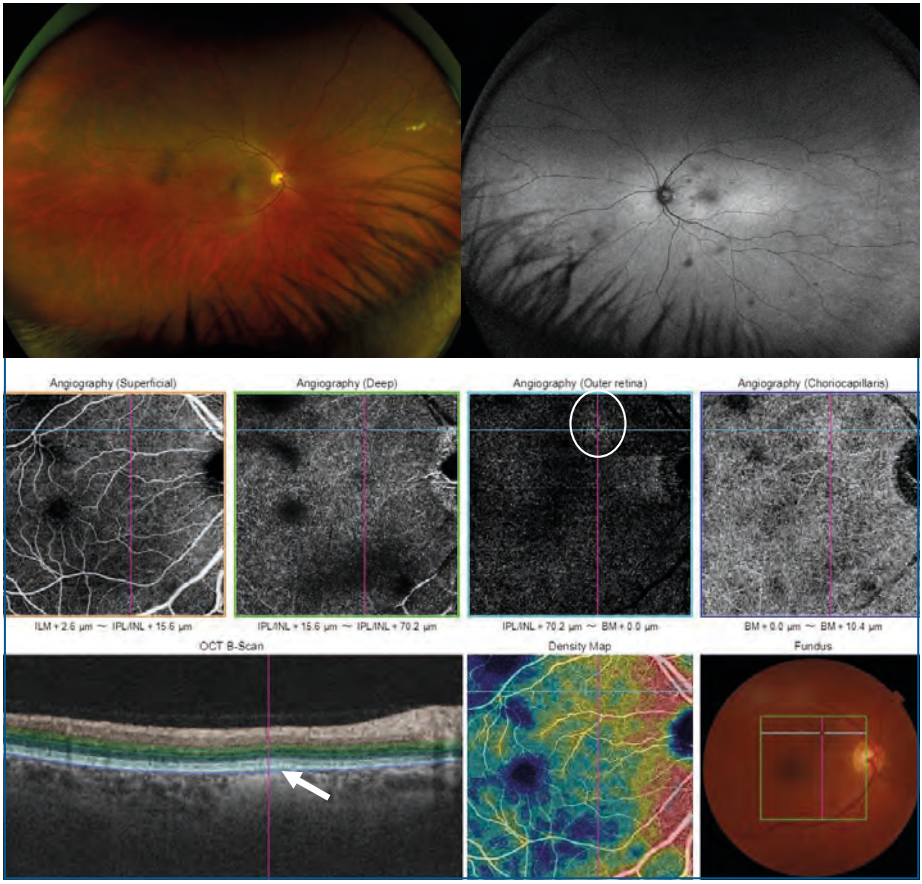

Figure 3-4. The segmentation shown in the above image displays a possible error. In this 54-year-old male with multiple choroidal naevi, multimodal imaging was undertaken. As one nevus is pushing the outer layers up (arrow), the segmentation captures parts of the choriocapillaris and displays this in the outer retina segment (circle). The blue line on the B-scan is relatively flat.

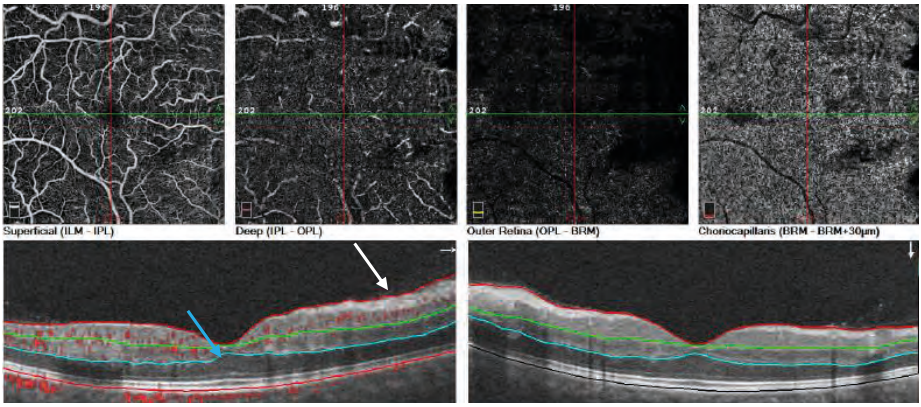

Figure 3-5. OCTA images of right eye. 55-year-old male. The presence of a mild epiretinal membrane (white arrow) can cause a wavy segmentation line (blue line and white arrow), as in this patient with superficial vessels displayed in the deep complex.

3.5. CNV does not have to be in the macula

A.

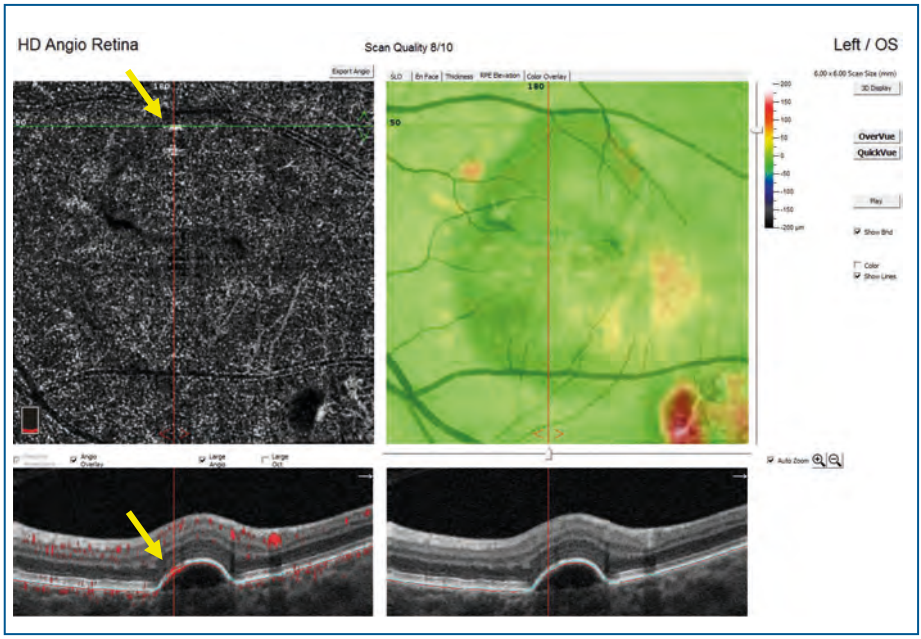

B.

Figure 3-6. Multimodal imaging of left fundus. In these images from a 64-year-old female with RPE detachment (PED), A. white lines (yellow arrow) are seen in the outer retina that correlate with an increased flow in the B-scan within the elevated flow (yellow arrow) that is an artifact however, if you look down; B. in the bottom right corner you can see CNV (white arrow) that corresponds to a hyper-reflective lesion on the B-scan. En-face OCTA image shows CNV (arrow) on a B-scan, presence of intraretinal fluid with absence of subretinal fluid and absence of ellipsoid zone as well as empty space with less visible choroid under PED.

3.6. Even if an OCTA scan does not show any new finding, look for progression

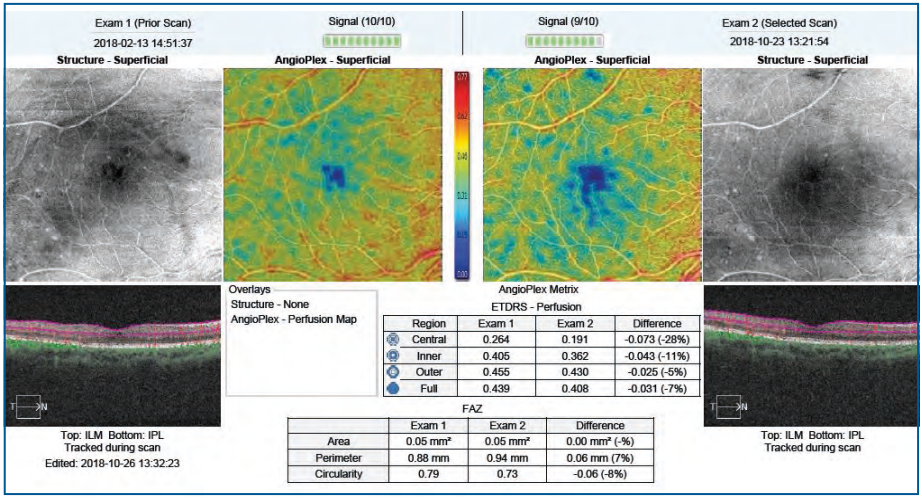

Figure 3-7. OCTA images do not provide any new information regarding this 71-year-old female with diabetes type 2; however, if you look at the changes of perfusion then a change of perfusion is observed at 8 months. Most devices are already equipped with a change analysis feature. This is not only very useful when treating CNV but also when seeking to show progression of ischemic conditions such as diabetic retinopathy. Not only did the perfusion change but also the accompanying FAZ became larger and less circular. Furthermore, if you are in doubt over something in the scan, ask for another scan

3.7. Atrophy does not prevent CNV

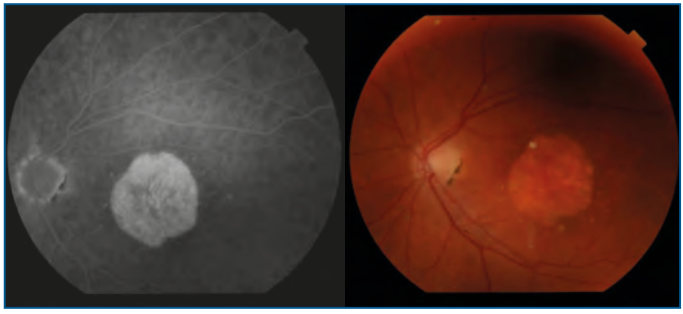

Figure 3-8. Fundus photos and fluorescein angiogram of a patient with macular atrophy; no leakage is found.

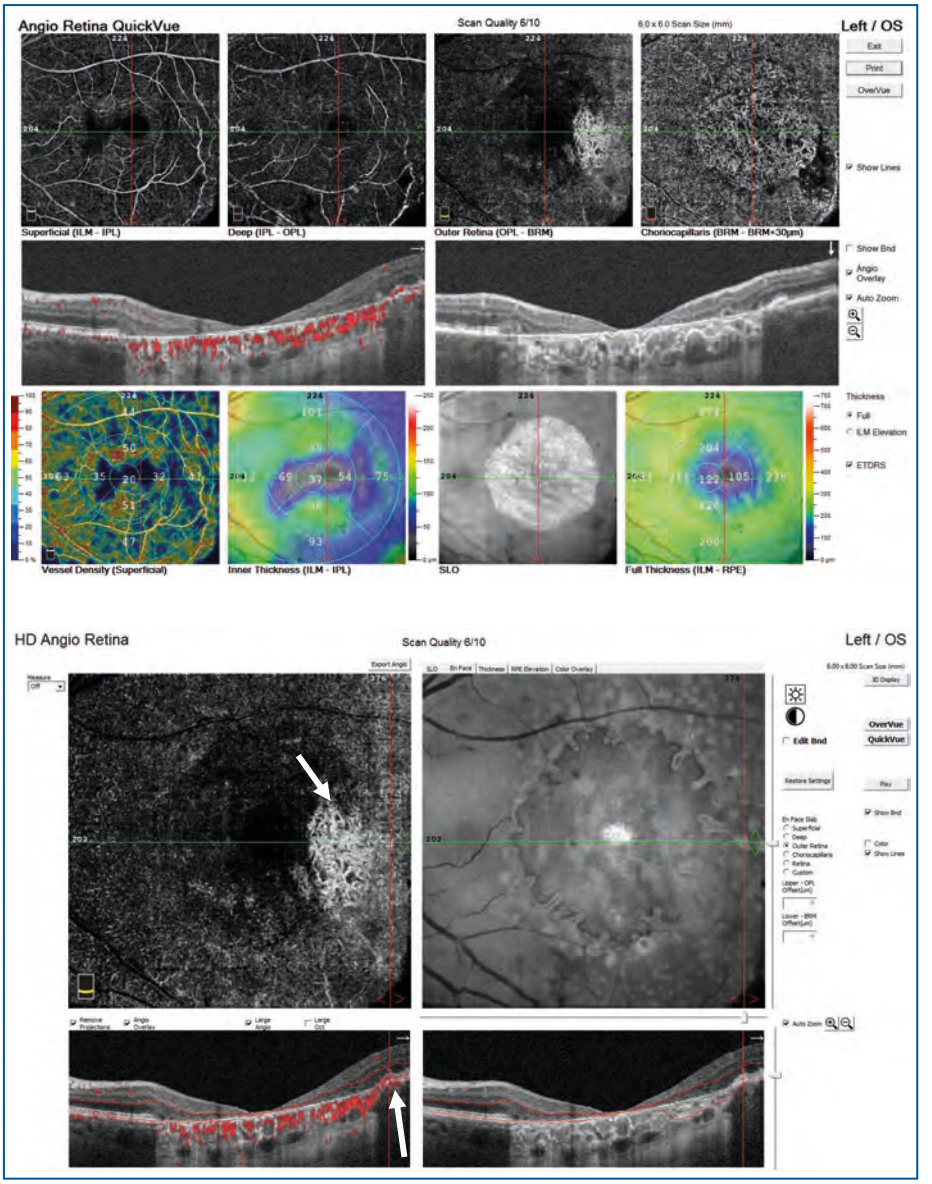

Figure 3-9. OCTA report on left eye. It is usually reversed: a patient with CNV is treated with anti-VEGF and, on the basis of a re-evaluation of the IVAN study, he/she has a 25% chance of developing macular atrophy two years after its initiation. However, it may happen that you see an atrophy and yet there is still an active lesion.

3.8. Low BCVA prevents a good OCTA scan

Other factors that can affect patient fixation are: mental state, age, and neck stiffness. A patient has to stare for up to several minutes, ideally with as little blinking as possible, so it may be wise to advise him/her to have his/her eyes shut while the technician prepares the machine for the scan.

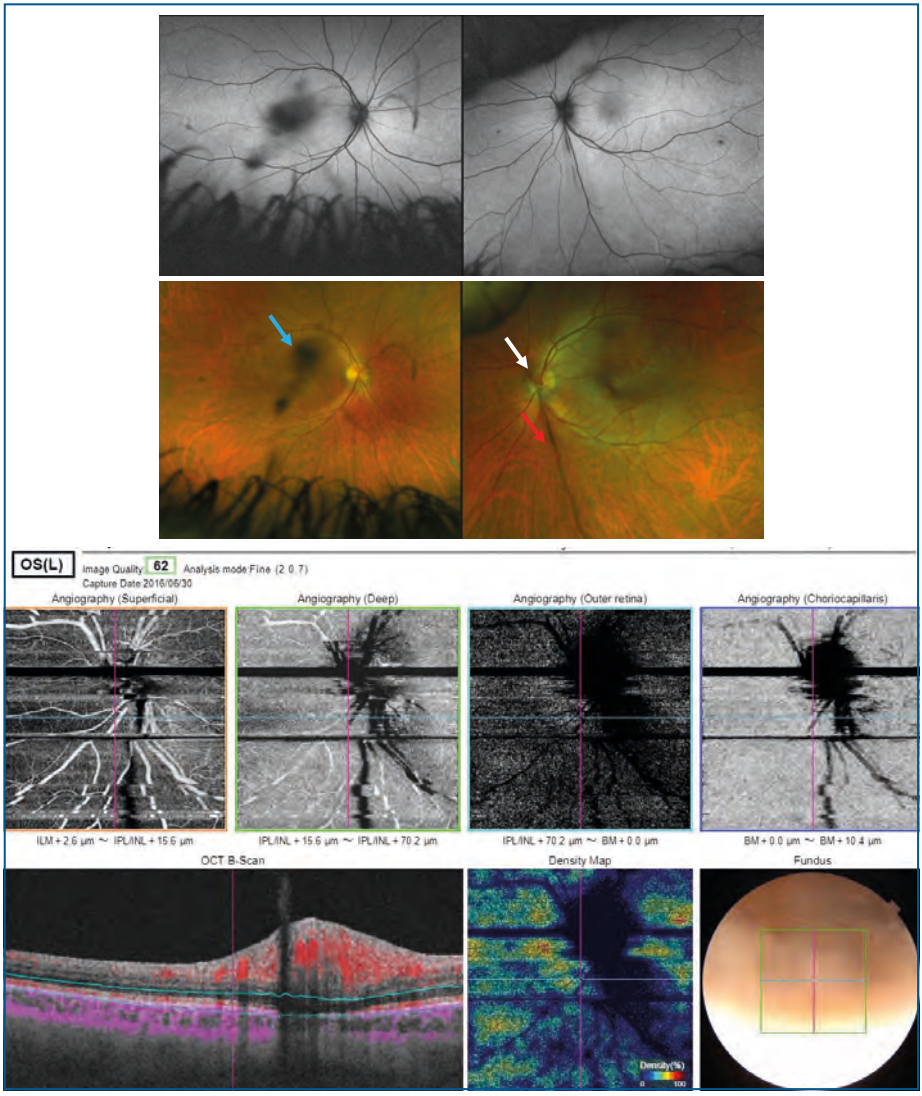

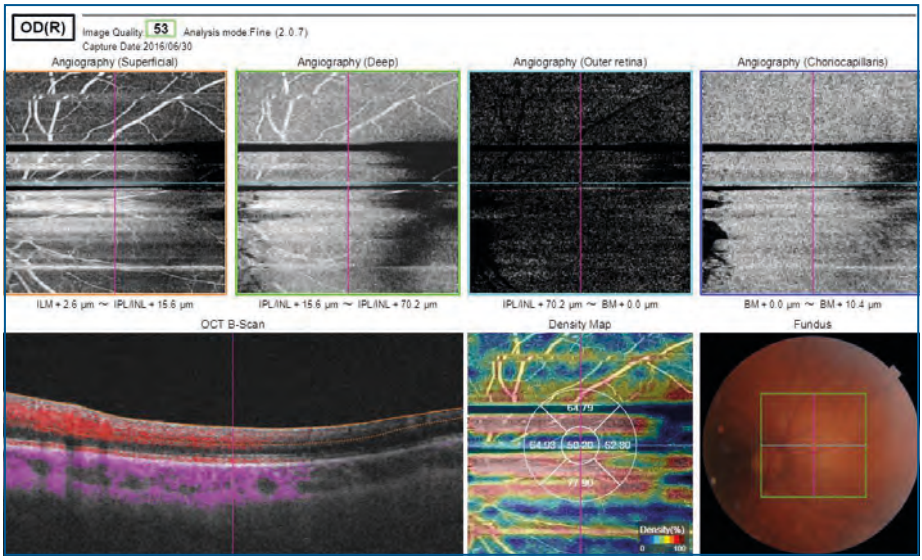

Figure 3-10. Multimodal imaging of a 29-year-old male with Leber's hereditary optic neuropathy and post vitritis (blue arrow). SLO colored fundus photo as well as autofluorescence show the papillitis (white arrow) and vasculitis (red arrow) of the left eye. However, due to a low BCVA it was not possible to get reliable images. In cases with poor visual acuity, performance of fluorescein angiography might be more appropriate, as this method does not require the patient to fixate or a long time.

3.9. Move the segmentation

Segmentations in standard machines are performed by detecting natural layers of the retina when they are visible; otherwise, false information will be presented. Therefore, you should always move the segmentation lines over the whole scan. Do not rely on the images prepared by the software.

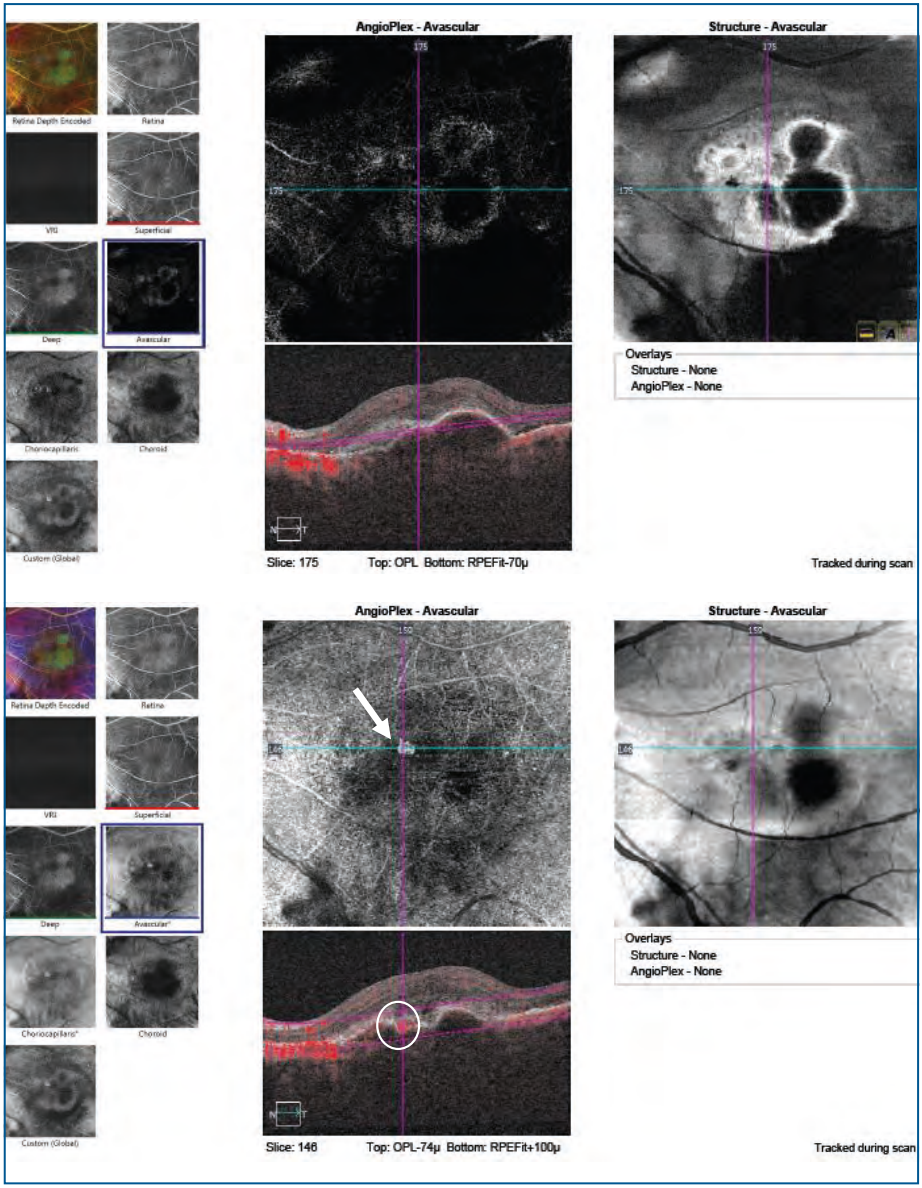

Figure 3-11. OCTA reports on left eye. 69-year-old male. In the image above, you can see an original segmentation produced by the machine. Below type 2 CNV the bright spot that is visible within the circle on a B-scan and corresponding to a bright lesion on an OCTA image (arrow) is a CNV lesion that was captured only after a modification of segmentation lines.

3.10. Choroid is not visible unless there is a destruction of RPE

In general, study of the choriocapillaris/choroid is limited, as it is obscured by the structures above such as drusen or other deposits but more importantly by RPE. Therefore, in order to analyze an OCTA image an en-face OCTA image must be examined as well. A high signal can be a result of noise rather than neovascularization. Why are the vessels dark in the choroid when they should actually be white, as white indicates motion? Melanosomes of the choroid backscatter light so that the choroidal vessels are imaged dark. As was mentioned in the principles section, there is also fringe washout.

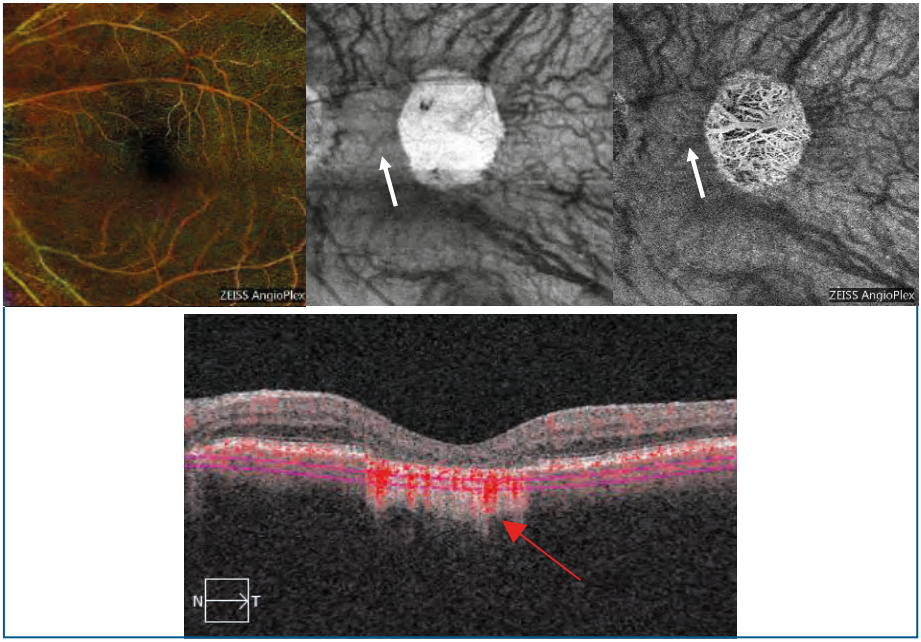

Figure 3-12. OCTA images of the macular and submacular region of left eye. 71-year-old female. Normally, it is impossible to see vessels in the choroid due to the high velocity of blood flow in the choroid and interference from the RPE. Hyper-transmission of A signal: backscattering due to loss of RPE (red arrow) is also present. Submacular atrophy is clearly visible on the B-scan under the areas with the loss of RPE. The large choroidal vessel is shown in the choroid as a shadow under a present RPE (white arrow) and white under the atrophic lesion.

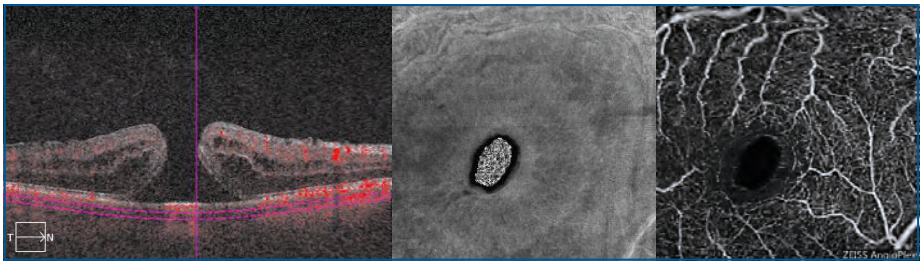

Figure 3-13. OCTA images of macula of right eye. In this 39-year-old male, The choriocapillaris is well visualized due to a macular hole and subsequent loss or RPE and other retinal layers. Such A well-defined circular lesion may also be misdiagnosed as CNV; however, they have the same shape as the hole suggesting another origin.

3.11. The navigation bar on different scans does not always correspond to the same places

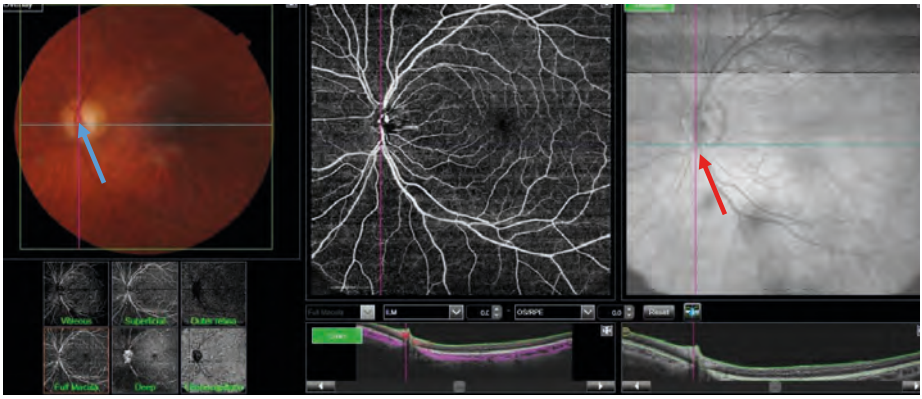

Figure 3-14. The possibility of acquiring a fundus photo together with the OCTA is a great feature and many consider this one of the biggest advantages of DRI OCT Triton; however, sometimes the images do not correspond to each other. In this example of a healthy patient, the navigation bar on the fundus photo (blue arrow) is crossed in the middle of the disc whereas in the en-face image the navigation bar is located inferior to the disc (red arrow). This is because the photo is taken after the OCTA scan.

3.12. Colored B-scan can tell you a lot

A B-scan scan with color-coded flow is a great feature and examining it is as important as looking at an OCTA en-face. A B-scan can give you information about structural changes affecting flow and can also help to distinguish artifacts.

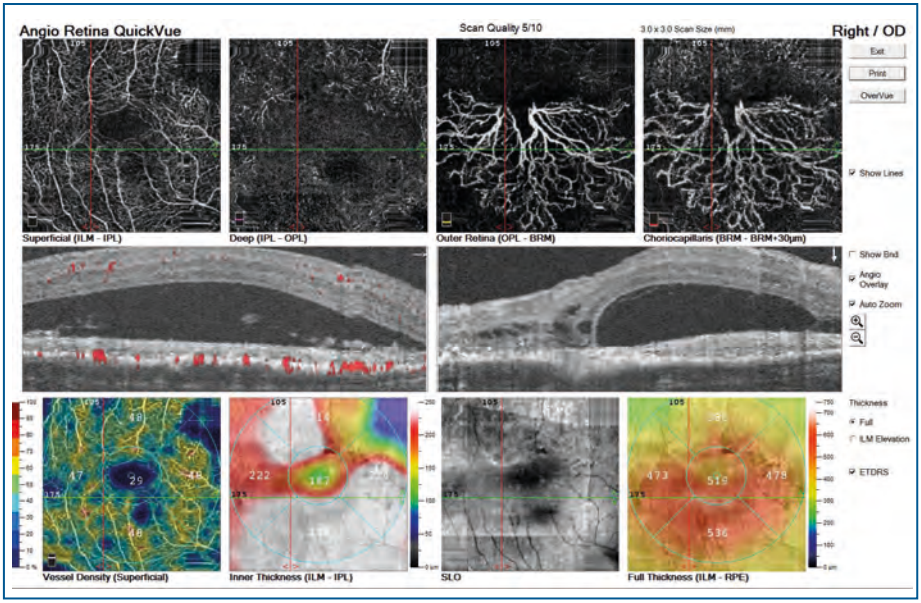

Figure 3-15. Multimodal imaging of right eye. In this patient, the program was able to reveal an impressive large lesion in the outer retina; the color-coded B-scan shows high flow colored red suggesting an active CNV which is confirmed by presence of large amount of subretinal fluid.

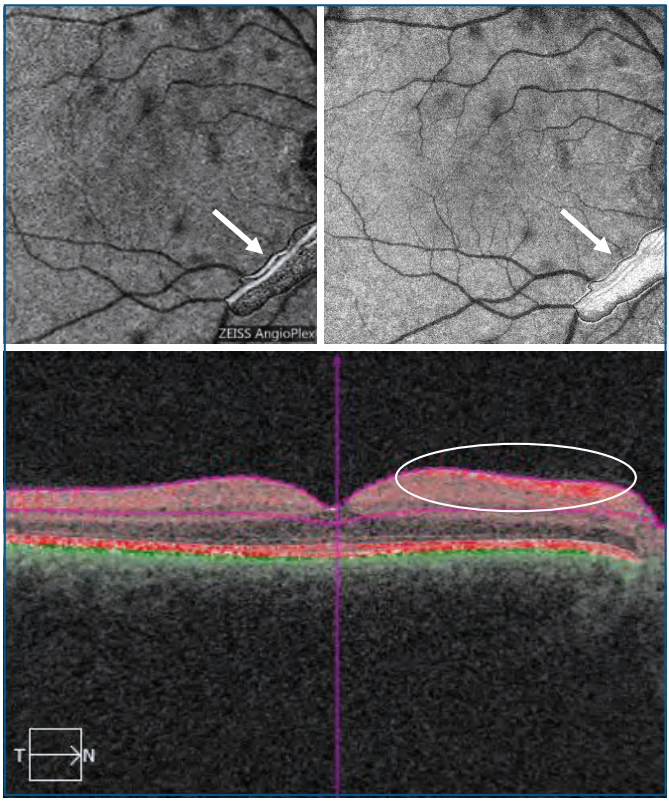

Figure 3-16. OCTA images of right eye. In this healthy 23-year-old female, a structure is visible in the lower quadrants (white arrows) that looks like a CNV but on closer inspection of the B-scan we can see that a very high flow (red intensity) is visible within the nasal side of RNFL (circle). This artifact comes from the high reflectance of this layer. Note the bicolor B-scan with the red flow above the RPE and green below.

3.13. OCTA scarcely visualizes vessels under the blood

Although SS-OCT has greater penetration than SD-OCT due to the infrared spectrum that is used, nonetheless large hemorrhages or blood clots will make this system totally useless in imaging what lies below.

If you have an intraretinal hemorrhage, you will probably not be able to visualize vessels beneath.

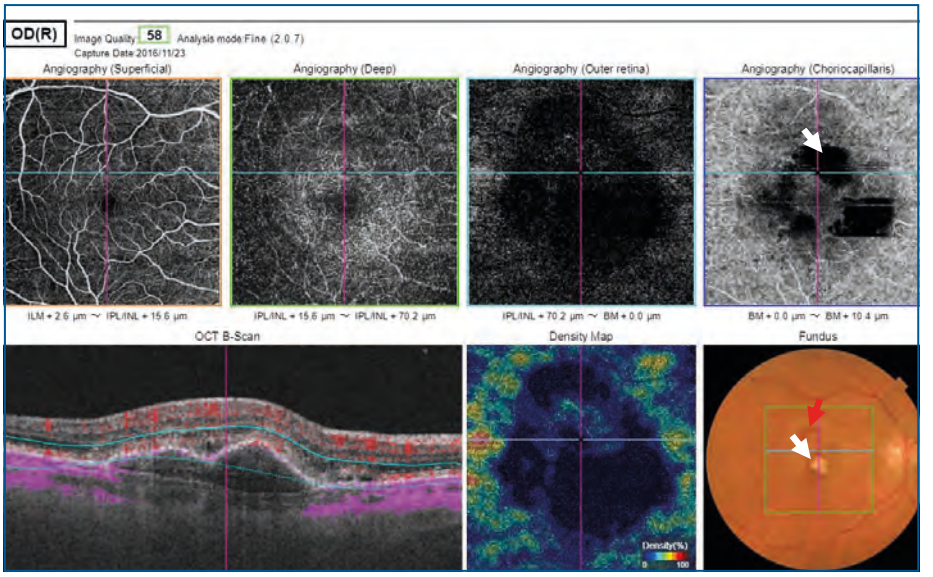

Figure 3-17. Multimodal imaging of right fundus. In this 71-year-old female with vascular AMD and mixed CNV, the lesion is invisible partially by improper segmentation and partially due to the presence of a blood clot (white arrow) and blood (red arrow). This is seen in the choriocapillaris segment where obstructed areas are colored dark (white arrow).

3.14. Choroidal segmentation may appear to be like CNV due to retinal atrophy

As mentioned in the 9th rule, you can clearly see choroid and choriocapillaries in eyes with destroyed RPE, sometimes such a projection may be misdiagnosed as CNV.

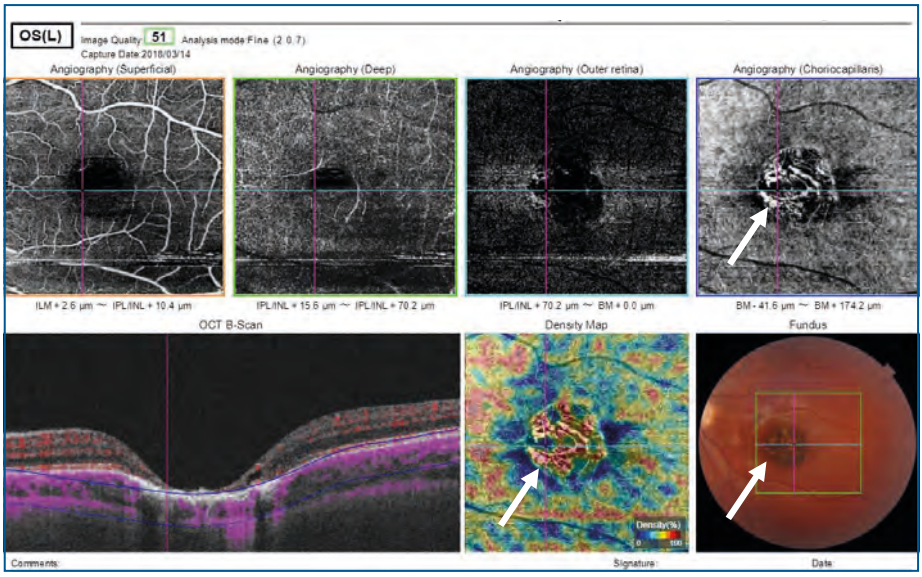

Figure 3-18. OCTA report on left fundus. In this 9-year-old female with a congenital toxoplasma scar, there is backscattering due to destruction of the retina and RPE accompanied by choroidal atrophy. Note that the area normally occupied by choriocapillaris has large choroidal vessels. The vessels are also visible in the outer segment.

3.15. Density maps in DME cannot be relied upon

In large diabetic macular edema, sometimes under the macula there might be an increase in flow suggesting CNV. This is especially visible on a density map. However, in such cases you cannot rely on this map.

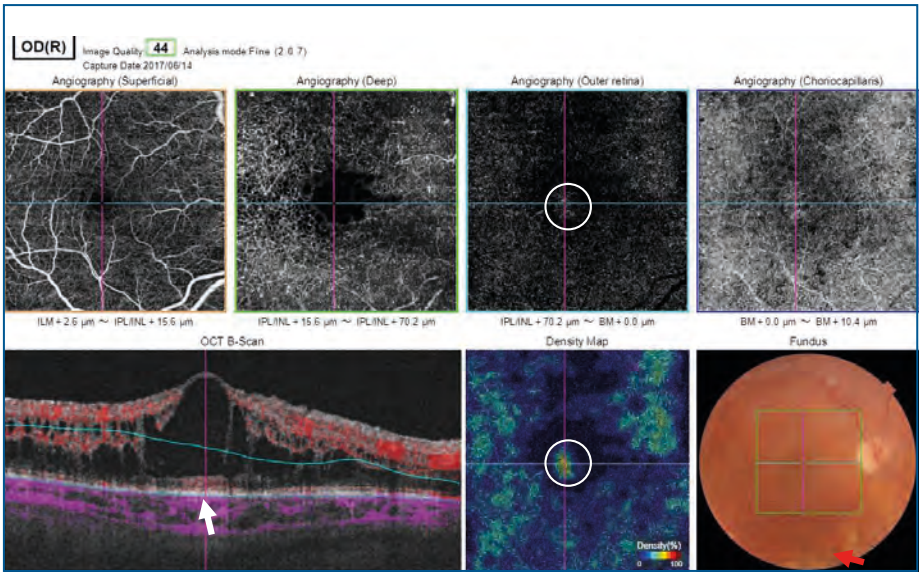

Figure 3-19. OCTA report on right eye. OCTA shows multiple areas with loss of flow corresponding to cysts. Furthermore, there is increased flow under the macula (arrow and circles). The increased flow under the macula is best shown on a density map. However, it is likely to be artifactual rather than CNV-related. Note the presence of laser burns in the periphery on the right eye (red arrow).

4. Artifacts

Whenever there is an image, there are artifacts which disturb the graphic. This is especially true for sophisticated computer methods such as OCTA, as they are more prone to disturbances than a simple photo registered on a membrane. Since we acquired our Triton with OCTA in October 2015 there has been significant development associated with image quality; however, artifacts are still a problem in OCTA and some were mentioned in the previous chapter.

4.1. Projection artifacts

Large vessels can be projected into the layers lying below the retina.

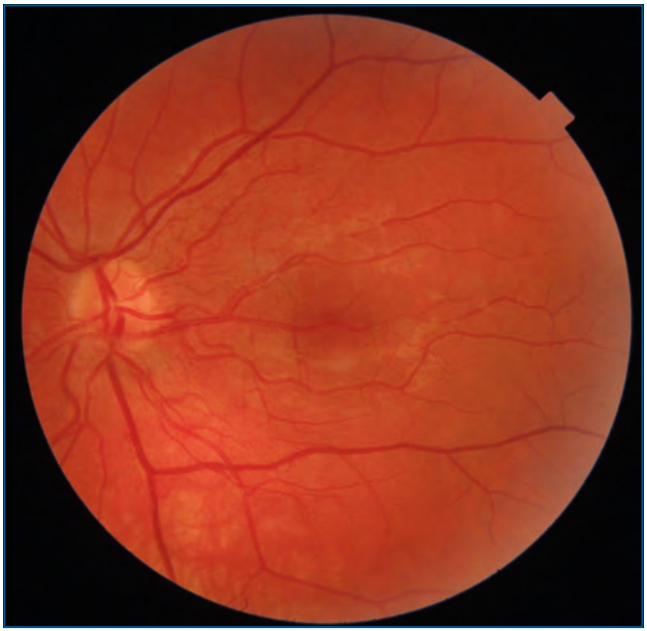

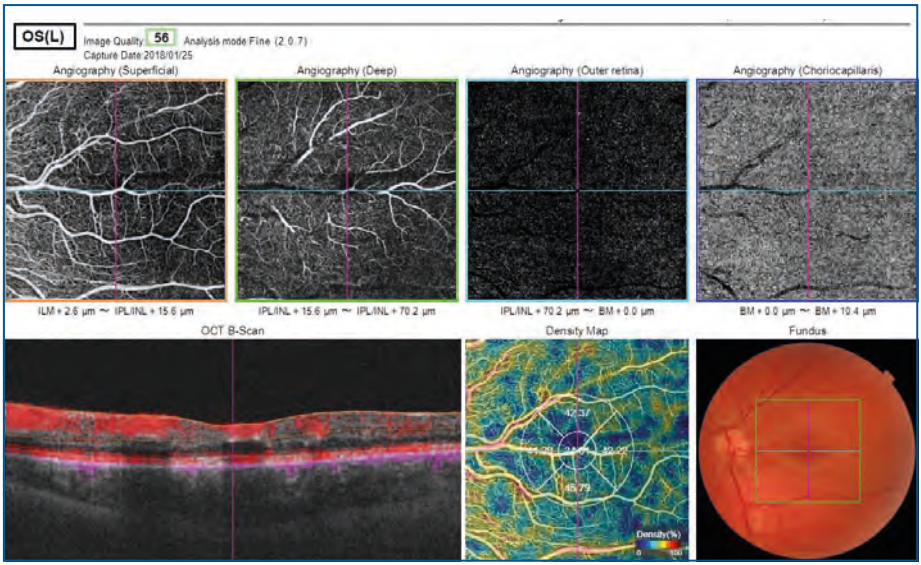

Figure 4-1. OCTA report on left eye. OCTA of a 29-year-old female with a macro vessel running through the macula. As the retina does not have a normal thickness, the segmentation in the deep vascular complex shows the presence of large retinal vessels. The projection artifact is again displayed in the outer retina and choriocapillaris is displayed as dark vessels.

4.2. Eye movement

As the patient loses fixation, eye movements are interpreted as blood movement and so it leads to the creation of white lines. This was at the beginning of the use of OCTA; however, this once major challenge is no longer so prominent.

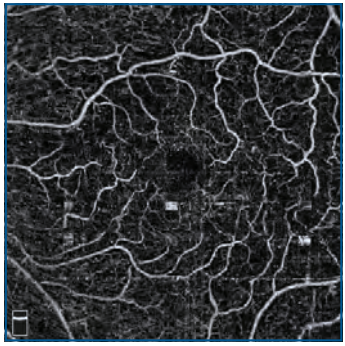

Figure 4-2. OCTA segment of left eye with visible white dots that are motion artifacts.

4.3. Pseudo vascularized epiretinal membrane

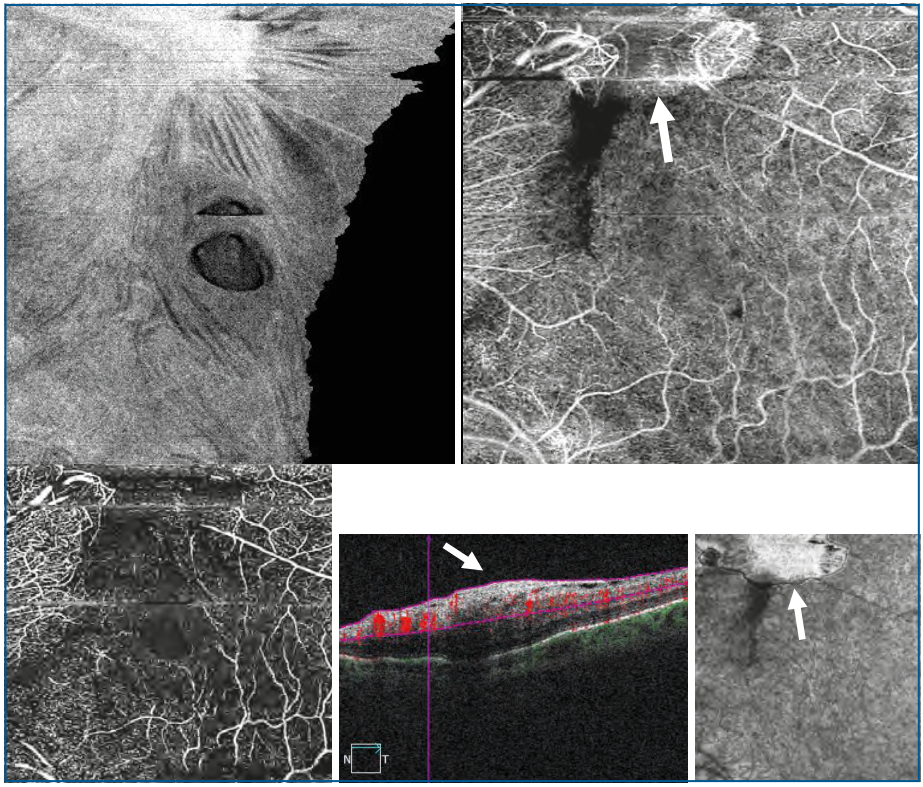

Figure 4-3. OCTA images of left eye. This seems like a neovascular membrane; however, if you look at the B-scan as well as the en-face OCT you can distinguish wrinkles of the ERM. As ERM possesses high reflectance it can lead to a decorrelation signal as it does in this case and this is clear on the superficial and sub-RPE slab (arrows).

5. Vein occlusion

The second most common vascular retinal condition is retinal vein occlusion. The most important risk factors are smoking, diabetes, hypertension and open angle glaucoma. In OCTA, DVC is more affected than SVC; however, much of the microvascular circulations may be obscured by the presence of hemorrhages.

Table 5-1. Comparison of imaging techniques for diagnosis and assessment of BRVO.

	OCTA	OCT	FA	Fundus photo
Ischemic size	+	-	+	-
Edema Size	-	+	+	+
Size of occlusion	-	-	+	+

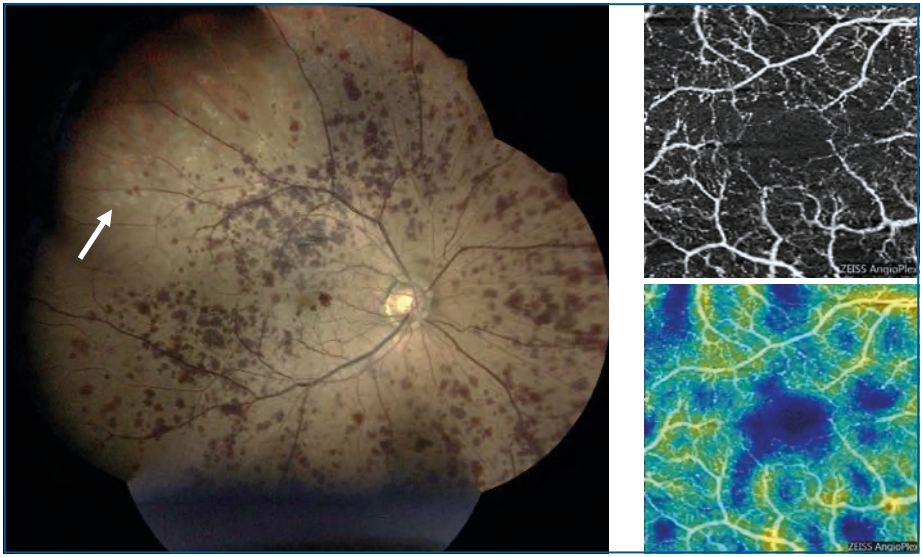

Figure 5-1. Multimodal imaging of right fundus. Merged colored SLO image of a 67-year-old male with CRVO of the right eye with the appearance of retinal hemorrhages. There is a majority of non-perfusion/inflammatory without major leakage. On the OCTA, there is FAZ enlargement and loss of its circular shape. Moreover, there is a loss of visible perfusion on the hot-cold color map, and vascular abnormalities such as microaneurysm and capillary telangiectasia may also be present. Note the photocoagulation burns in the superior temporal quadrant (arrow).

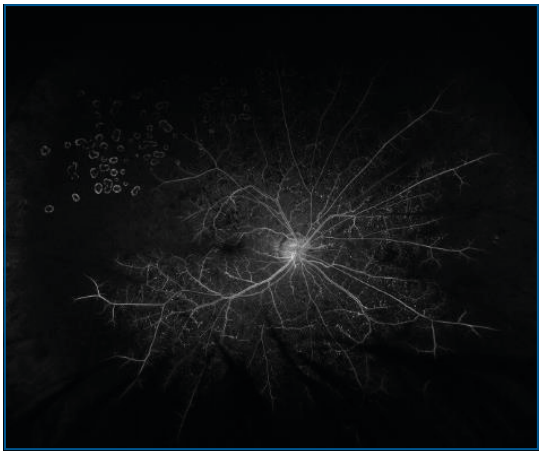

Figure 5-2. FA images of right eye. The venous and late venous FA images show an area of perfusion loss, enlargement of FAZ and vascular leakage, extensive capillary dropout and microaneurysms. After performing FA we decided to perform a full photocoagulation.

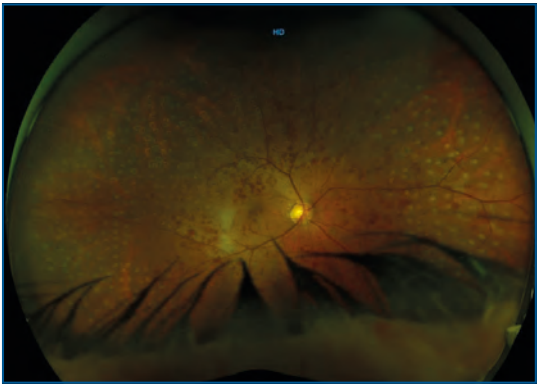

Figure 5-3. Ultra-wide field of right fundus. Laser burn marks are seen in the whole periphery.

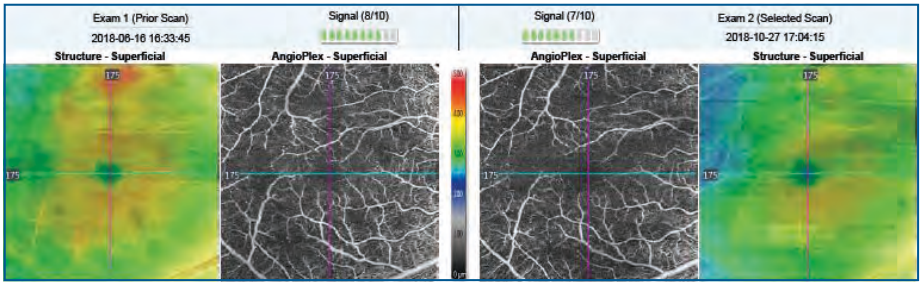

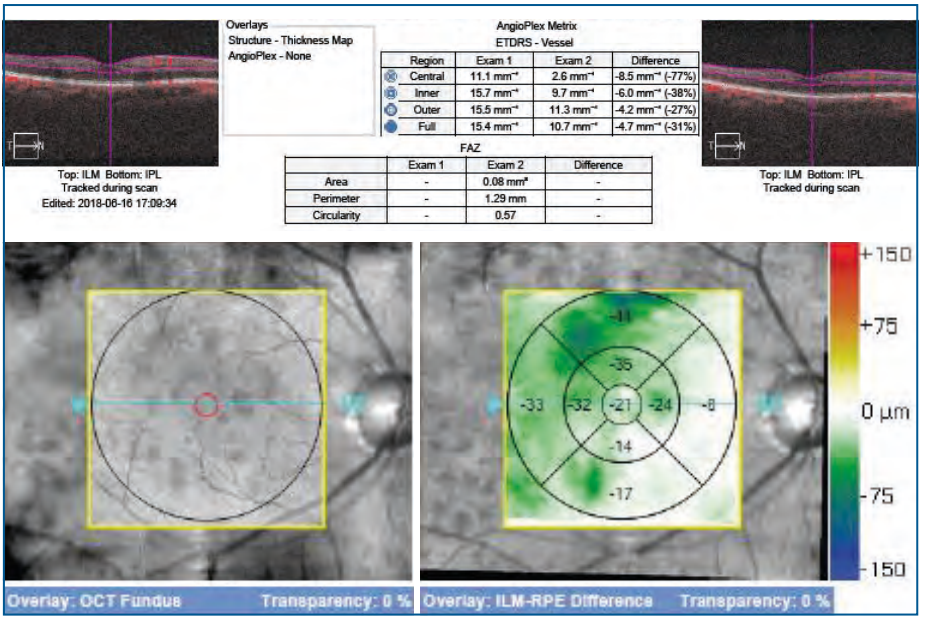

Figure 5-4. Comparison of two OCTA scans. 51-year-old female. Although there is a visible decrease in the macular thickness from 323 to 302 µm, there is also a loss of perfusion seen on the comparison report.

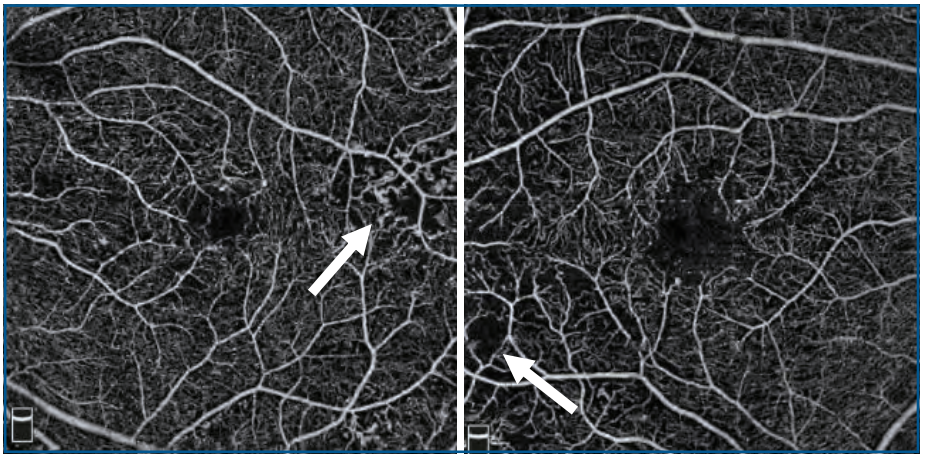

Figure 5-5. Bilateral OCTA images of the superficial segment In this patient after BRVO collateral vessels are visible in the temporally in the left eye capillary non-perfusion is visible inferotemporally in the right eye.

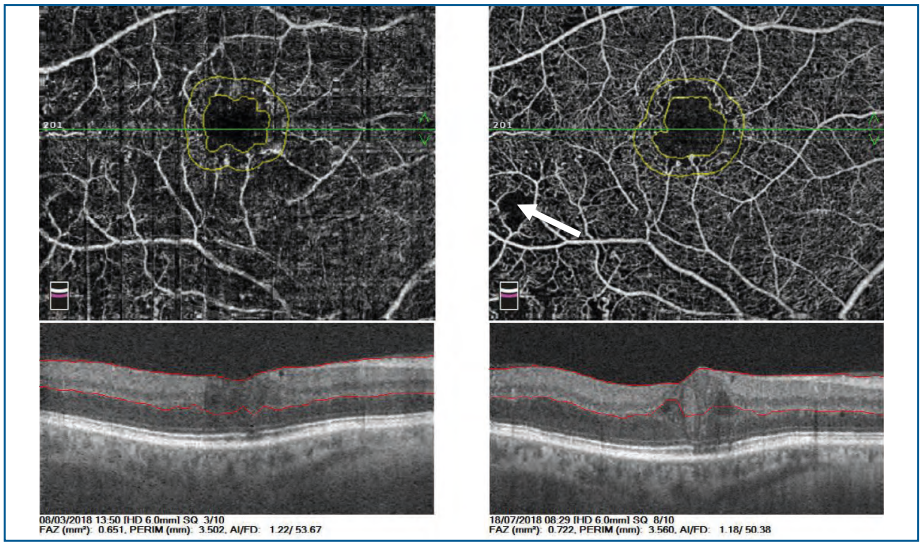

Figure 5-6. Comparison of two superficial segments over 4 months in the same patient, showing enlargement of the FAZ from 0.651 to 0.722 mm² as well as the presence of avascular zones (arrow).

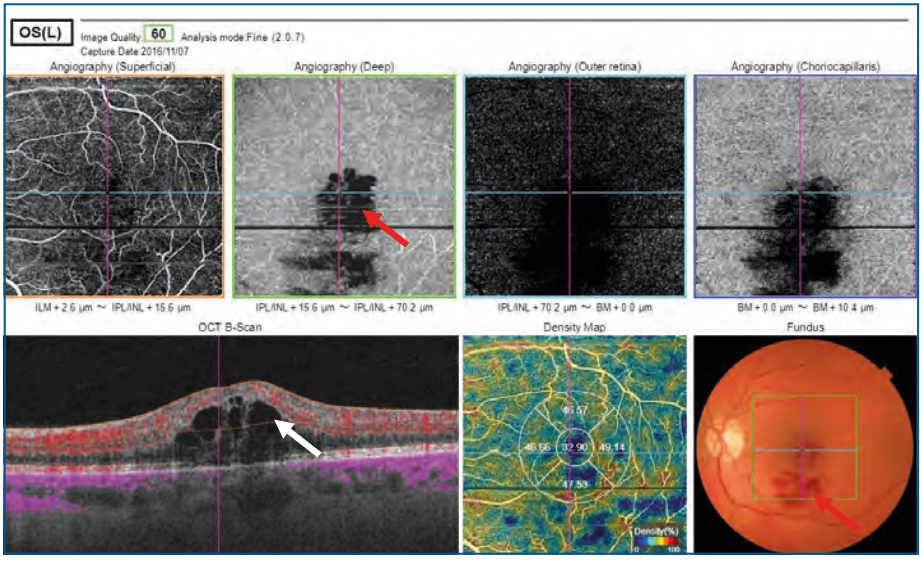

Figure 5-7. OCTA report on left fundus. 48-year-old male. In this patient with BRVO with intraretinal hemorrhage, the B-scan shows multiple cystoid spaces, and a macular edema (white arrow). Again, blood (red arrow) is blocking the decorrelation signal emanating from the outer layers of the retina as well as the choroid.

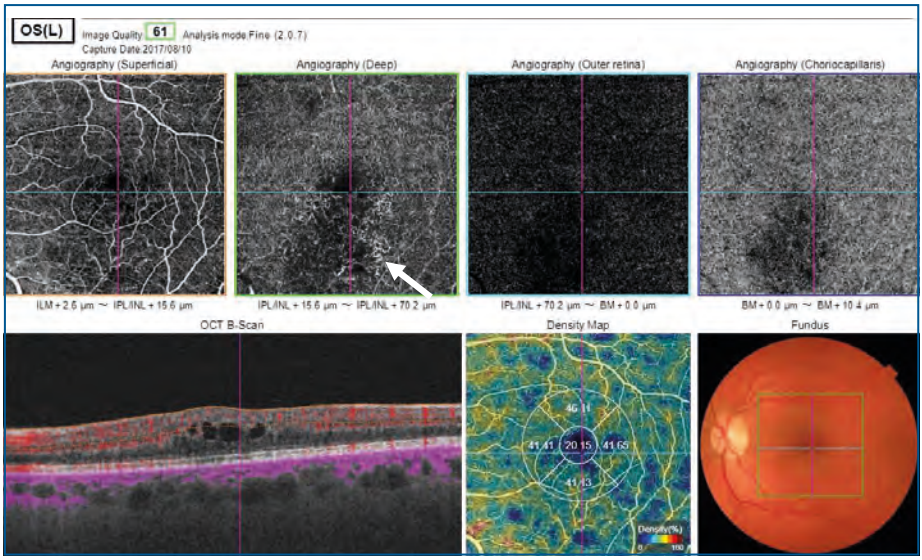

Figure 5-8. OCTA report on left fundus. Same patient. After several EYLEA injections and yellow laser treatment, the fundus photo shows less prominent blood presence; however, still dilated tortuous veins (arrow) and collateral vessels are visible, especially in the deep segment. B-scan shows accumulation of fluid in cysts.

Key features of BRVO

Enlargement of FAZ, vascular abnormalities and often presence of neovascularization. The segmentation is almost always performed incorrectly. The inner-retinal layers are usually obscured by blood.

6. Diabetic retinopathy

Diabetic eye disease is one of a leading causes of blindness in developed countries. When it affects the posterior pole, it can be divided into proliferative and non-proliferative diabetic retinopathy and diabetic macular edema. OCTA can facilitate imaging of the microvascular changes and neovascularization. This is especially useful as alteration in the DVC cannot be visualized in the FA. DME is associated with the presence of microaneurysms and microvascular changes. As DME is often cystoid, the intraretinal fluid can obstruct the imaging of the deeper layers.

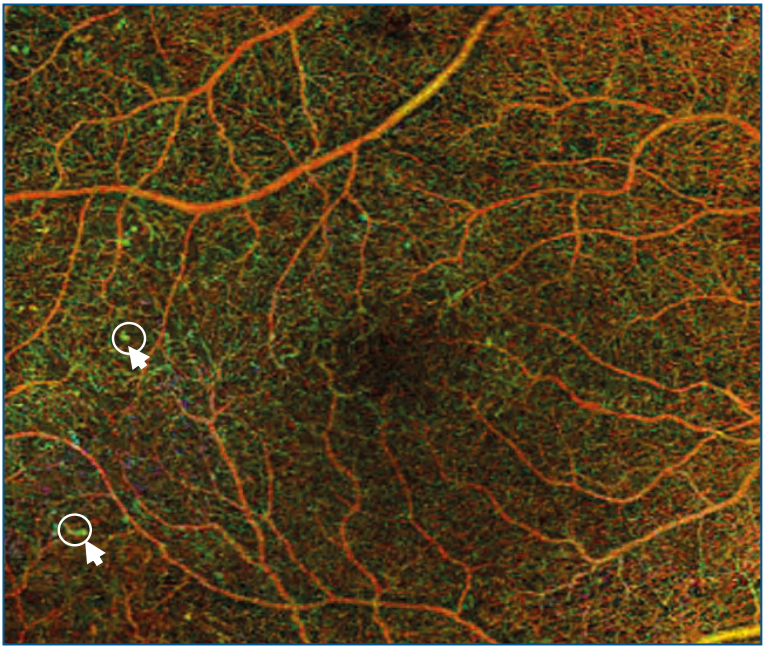

Figure 6-1. Color-coded merged image of the whole retina in NPDR. Multiple microaneurysms are visible in both DVC in SVC (white arrows).

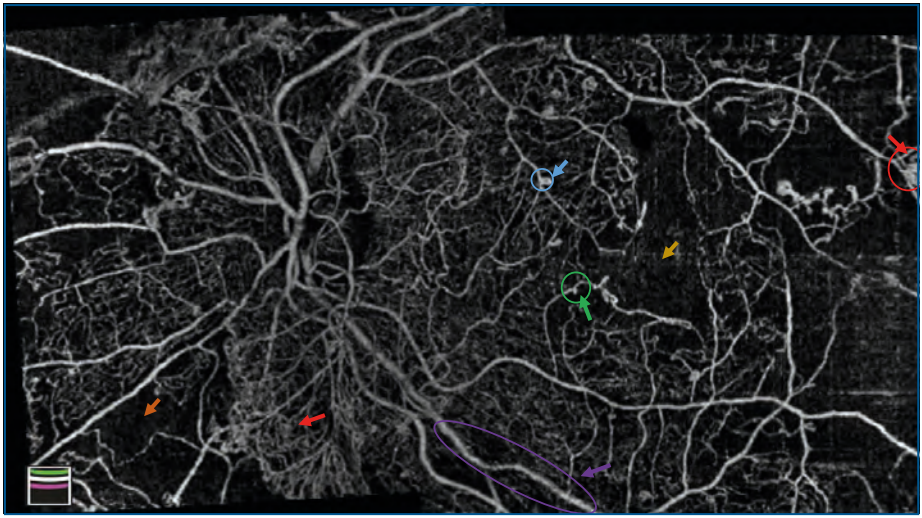

Figure 6-2. Composite image of PDR in diabetes type 1 32-year-old female. With multiple diabetic changes: neovascularization, venous bedding, microaneurysm, vascular loop, destruction of FAZ, loss of perfusion.

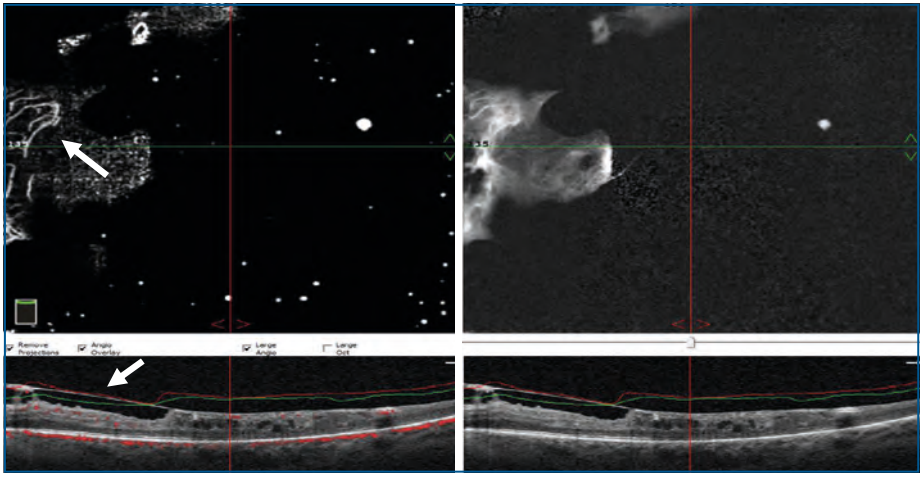

Figure 6-3. OCTA images of a vitreo retinal interface of a patient with a PDR showing parts of an epiretinal vascularized membrane.

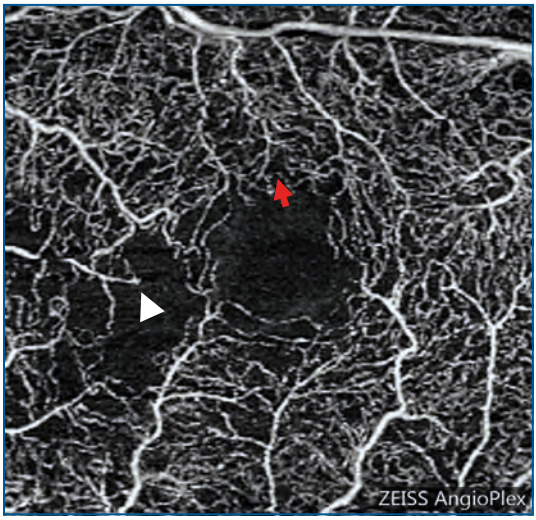

Figure 6-4. OCTA scan of the right eye of a 42-year-old male. 3×3 mm image of SVC of a patient with type 2 DM. Destruction of FAZ (red arrow) and perifoveal areas with perfusion loss (arrow head) and foveal microvascular tortuosity.

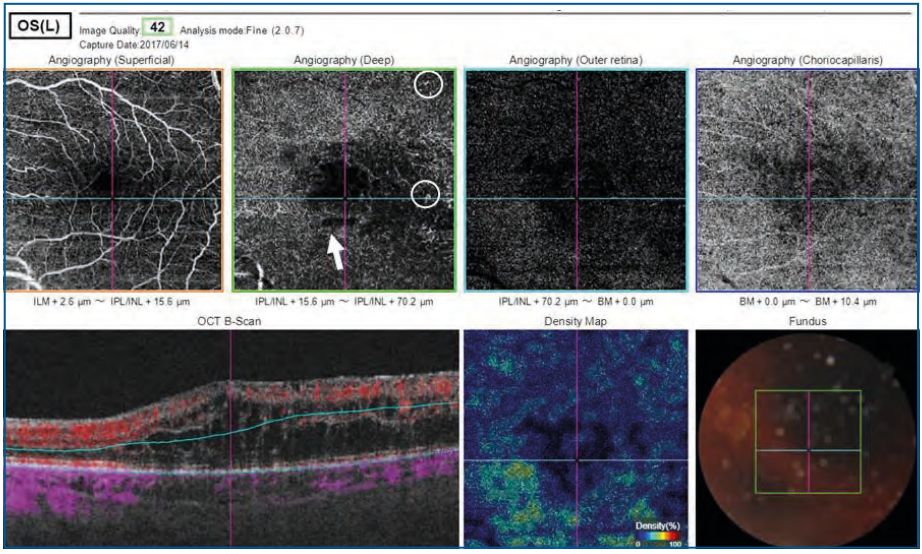

Figure 6-5. OCTA report of the left eye. DME of a left eye, 48 year old male. B-SCAN scan shows the presence of cystoid macular edema with multiple intraretinal fluid spaces. OCTA scan shows the loss of flow (arrow) due to artifactual absorption of a light by cysts and microaneurysms (circles) in a deep capillary.

7. CNV

The most obvious application of OCTA is detection of CNV in vascular AMD. This is firstly because of the sheer number of patients with vascular AMD in developed countries and secondly, because the current CNV classification is based on the location of the lesion and OCTA enables the visualization of vascular changes at the required level.

Based on fluorescein angiography and OCT, the CNV was classified as either type 1 which was sub-RPE, type 2 within the subretinal space (between retina and RPE) or type 3 intraretinal also called retinal angiomatous proliferation RAP. In the OCTA, type 1 will be positioned below RPE and above Bruch's membrane, sometimes accompanied by PED. Type 2 will be positioned above the RPE within the avascular zone, also called the outer retina. Type 3 starts in the deep layers of the retina and extends to the outer layers and subsequently leads to the retinal choroidal anastomoses. RAP can be bilateral and have no choroidal component. Its incidence is 10-20% of vascular AMD. It is usually seen as a high flow line on a flow scan which is hyper-reflective on a B-scan, but it can also be associated with PED and fluid accumulation.

To date, there is no consensus on whether OCTA can be used to differentiate between active and inactive lesions. It seems that the presence of fine vessels at the edge of the lesion, and a dark halo around the CNV as well as intraretinal fluid and the presence of a hemorrhage suggests an active CNV. An inactive CNV looks more like a tree in the winter.

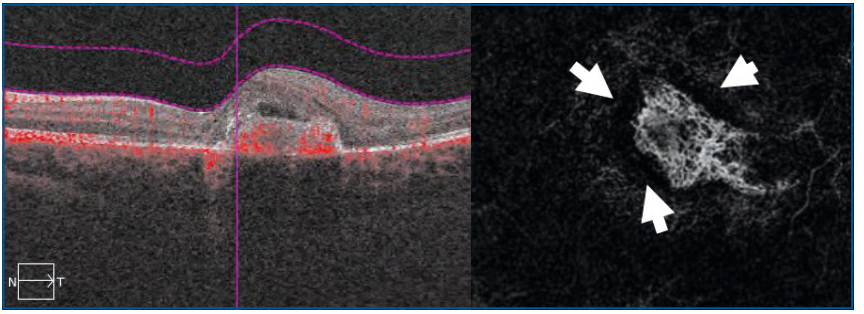

Figure 7-1. OCTA images of left fundus. The presence of a dark halo around the CNV (arrows) in the outer retina as a sign of active CNV.

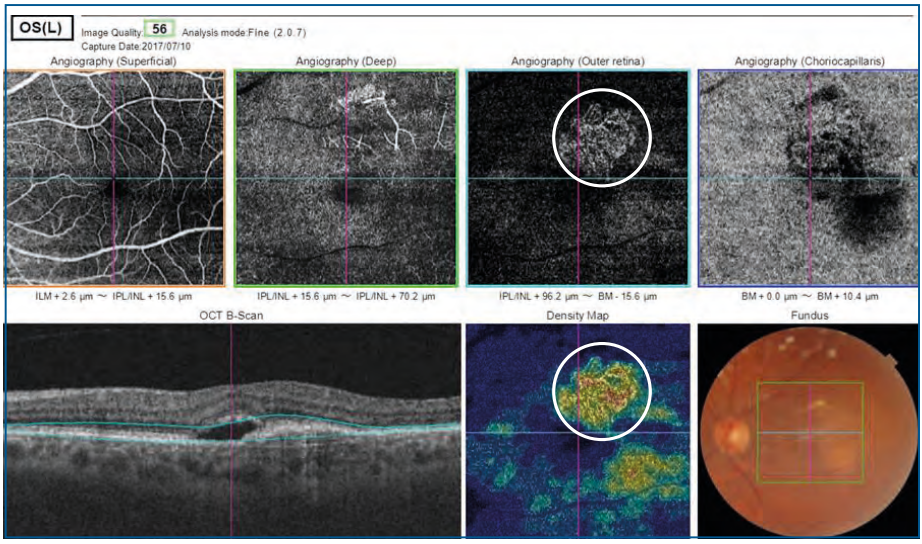

Figure 7-2 OCTA report on the left fundus of a 63 year old female. Type 1 CNV is seen on a B-scan with the presence of subretinal fluid and PED. On a density map and outer retina clear bush like structure is present (circle).

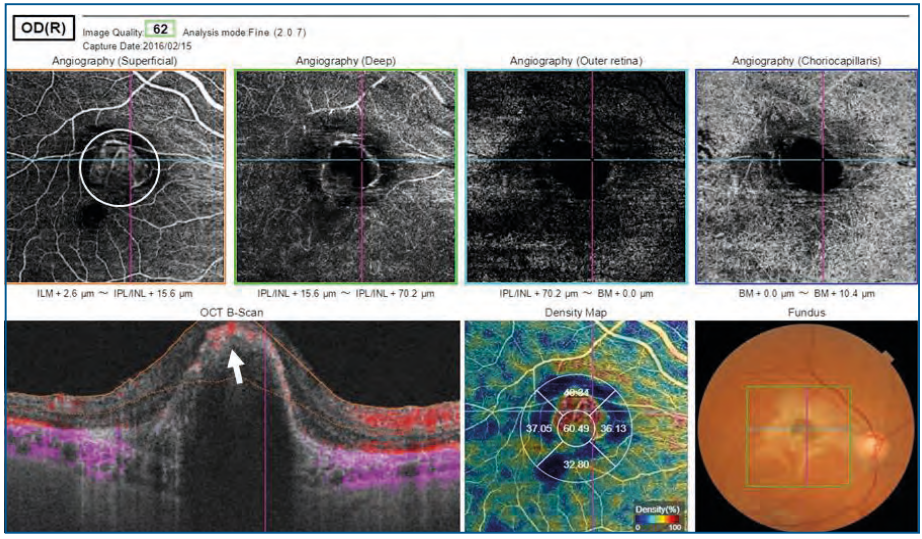

Figure 7-3. OCTA report on right fundus. On the B-scan, the sub-RPE hyporeflective lesion (arrow) as well as the presence of hyper-reflective material on the undersurface of the RPE indicates fibrovascular PED. The lesion can be seen in a superficial scan (circle) due to a massive elevation of the retina. Furthermore, a scar is clearly distinguished and visible on the fundus photo.

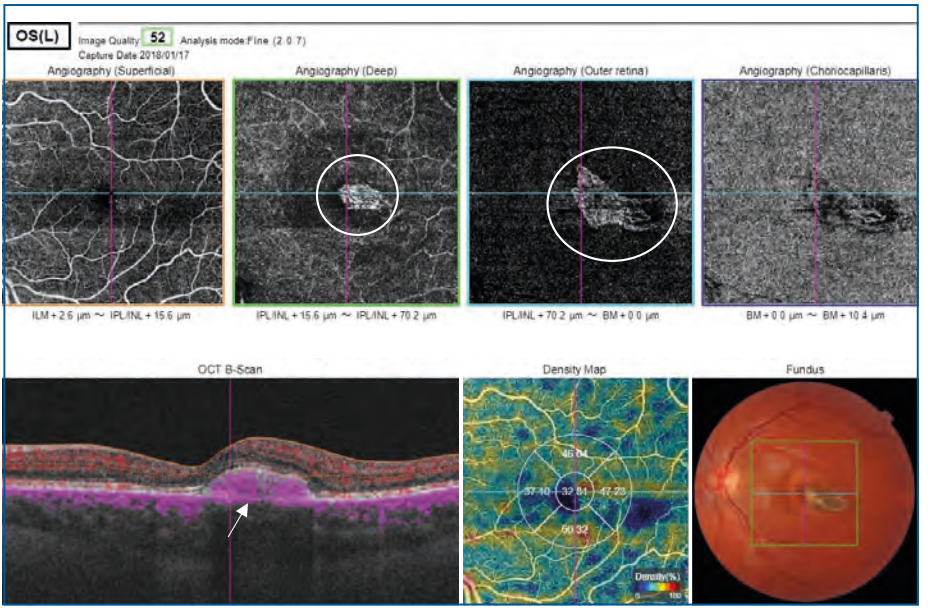

Figure 7-4. OCTA report on left fundus. Composed image of CNV B-scan and fundus photo of a 17-year-old female with an idiopathic CNV lesion (circles). There is the presence of intra-retinal fluid, and CNV seen on all displayed segments except for the superficial.

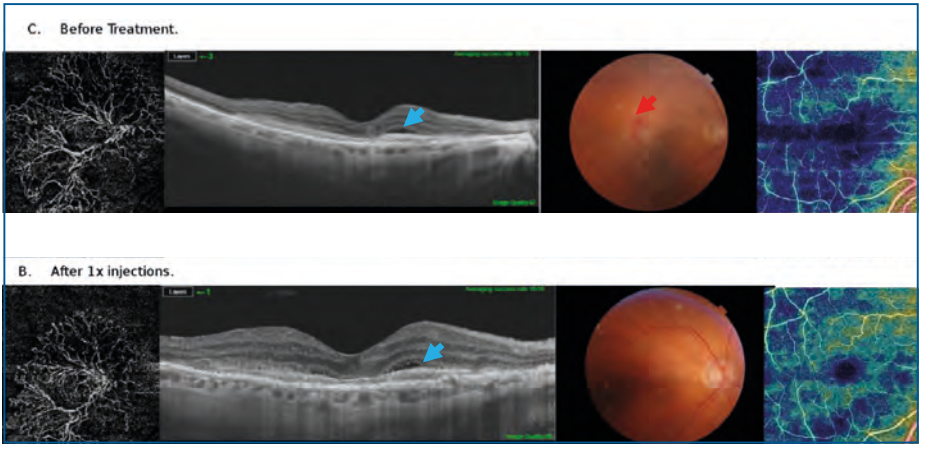

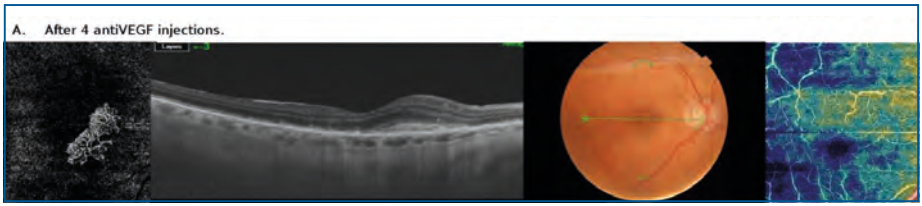

Figure 7-5. Images of right eye. 73-year-old female. Report shows the response of type 2 CNV following anti-VEGF injections. The pre-injection layer is displayed at the top of the image. The overall size of the lesion shrinks but it becomes more dense. Also, the decrease in fine vessels in the periphery of the lesion also tends to shrink. In the fundus photo, there is a hemorrhage (red arrow) visible before treatment as a sign of VEGF activity as well as intraretinal fluid within the retina (blue arrows). After 4 injections, the blood is gone as well as the fluid; however, there is choriocapillaris loss. Reprinted from Wylęgała A et al. Doi: 10.1155/2018/8595278

A positive feature is the possibility to assess a change during treatment with anti-VEGF agents.

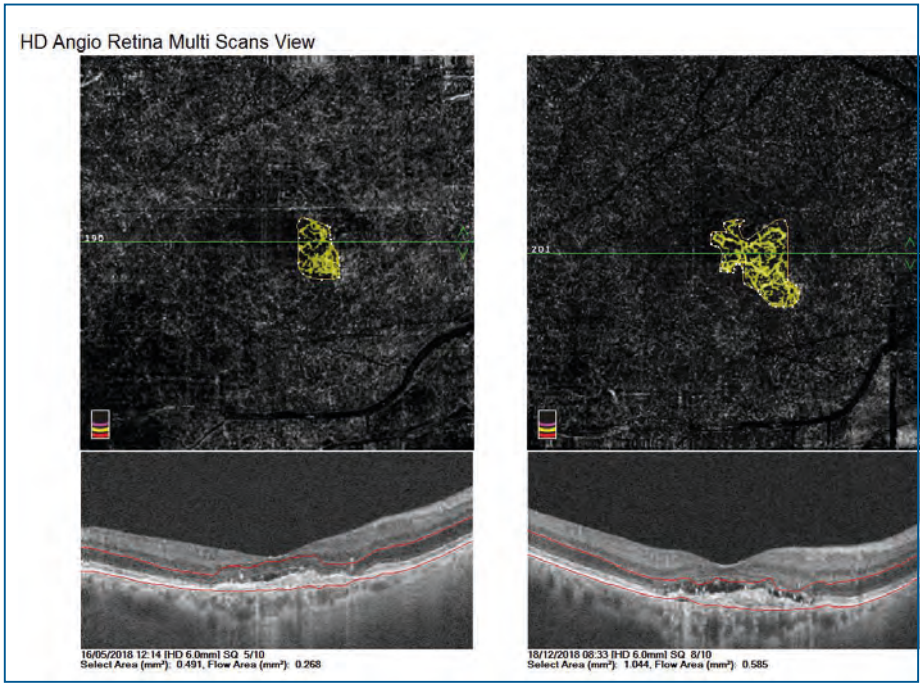

Figure 7-6. Comparison of OCTA reports. In some cases, despite the treatment the lesion can grow bigger from 0.491 mm² to 1.044 mm².

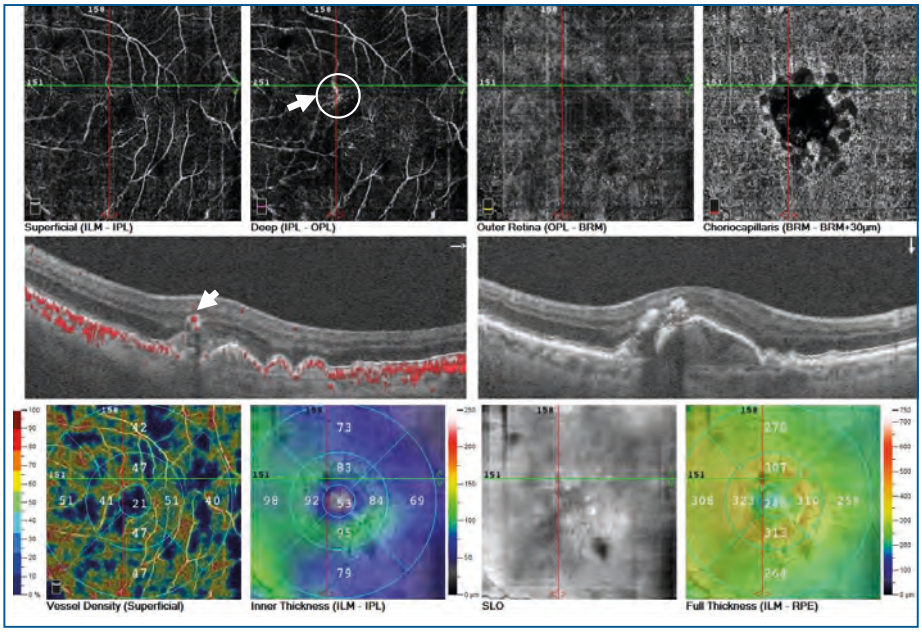

Figure 7-7. Multimodal images of left fundus. 65-year-old male with RAP. En-face OCTA in a deep capillary complex showing a single vessel (circle and arrow) that is dilated and much brighter compared to the surrounding area. This corresponds to the outer retina.

8. Secondary CNV

8.1. Secondary CNV with CSR

CSR can be characterized by the presence of serous retinal pigment epithelium detachment. This disease can be classified into two subcategories: acute and chronic. It is the chronic type that leads to secondary CNV. This is common in young and middle-aged men, with type A personality and exogenous steroids.

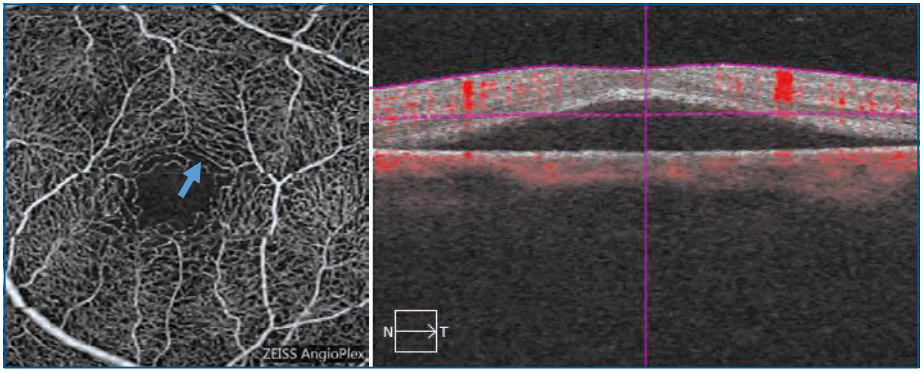

Figure 8-1. OCTA images of left fundus. Example of an acute CSR, with dome-shaped elevation of the retina and shaggy photoreceptors. There are no signs of secondary CNV, while there is some thinning in perimacular vessel density (arrow).

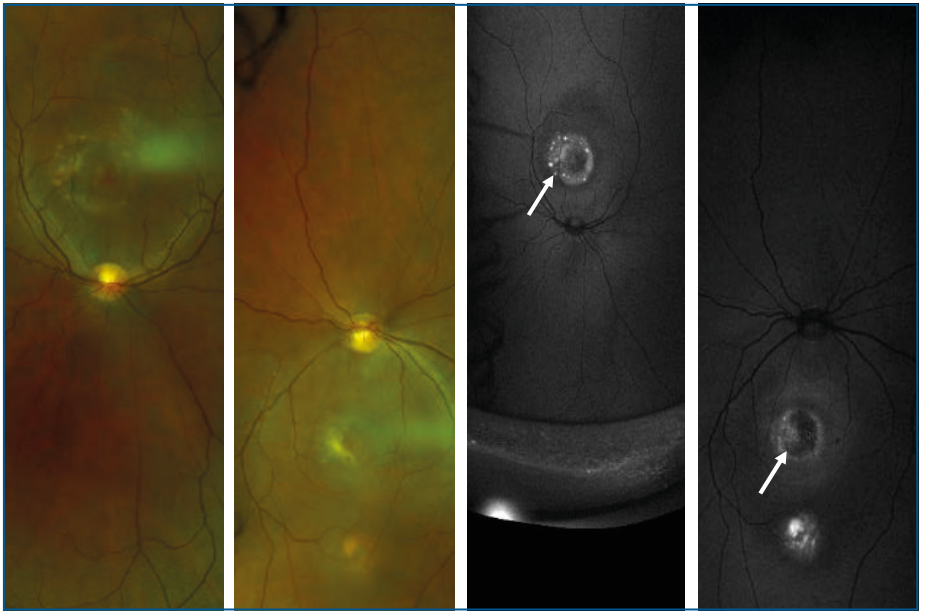

Figure 8-2. Wide-field color fundus and autofluorescence photo of a patient with bilateral CSR. AF photo shows hyperfluorescent lesion in the maculae as well as hyperfluorescent image in the left eye temporally to the macula as well. In this case due to the presence of secondary CNV visible in OCTA images, FA was not necessary.

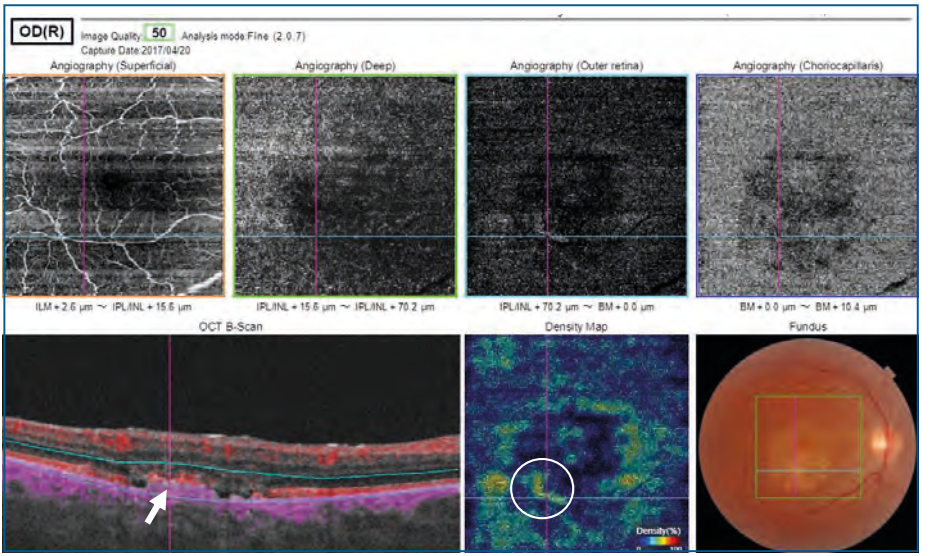

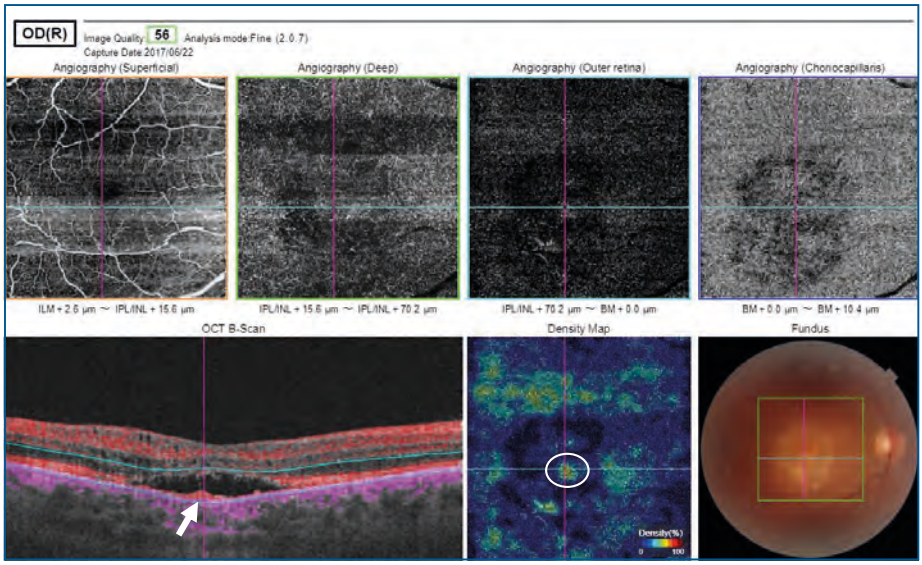

Figure 8-3. OCTA reports on right eye. In this 30-year-old male OCTA showed PED, subretinal and intraretinal fluid (right eye) and secondary CNV. CNV is best seen in the density map (circle), showing the CNV in the warm colors (circle). Picture above before and below after Avastin therapy.

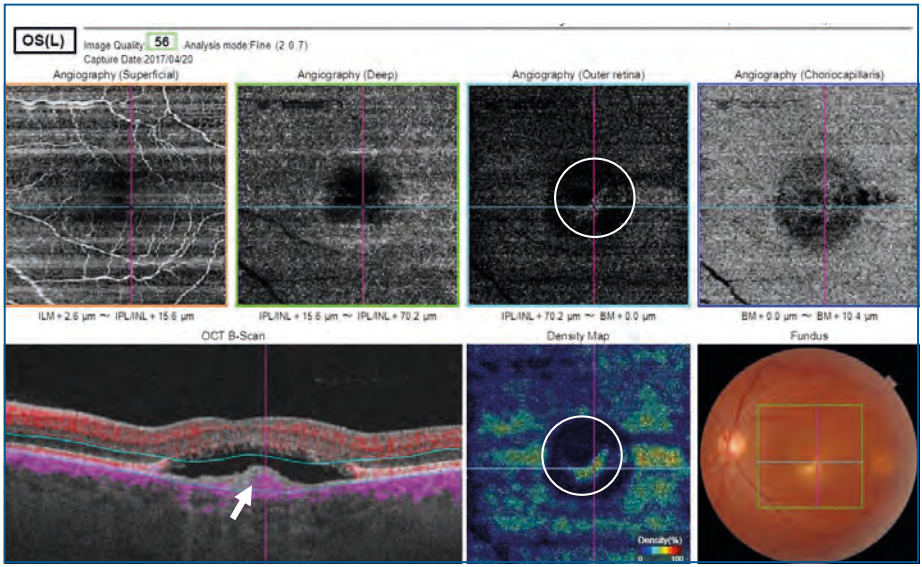

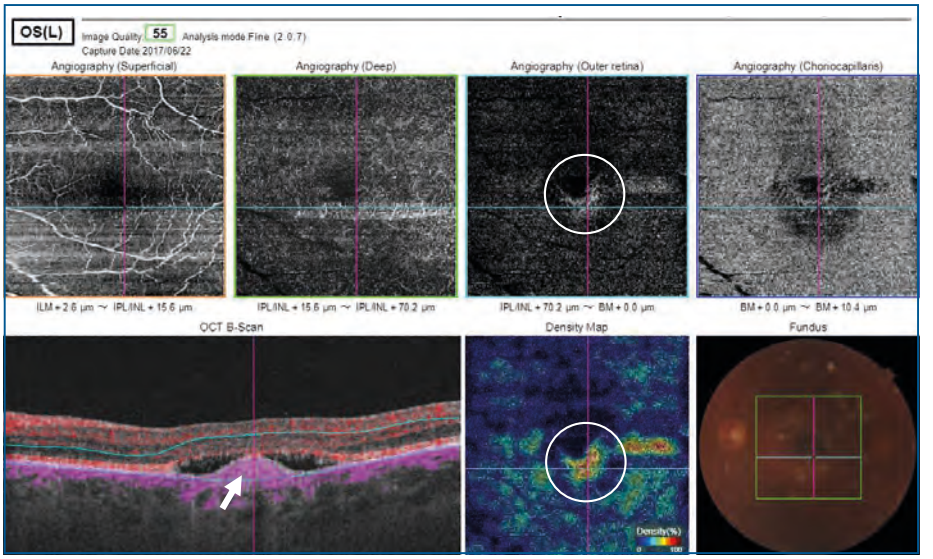

Figure 8-4. OCTA reports on left eye before (above) and after (below) anti-VEGF therapy. 30-year-old patient. B-scan shows PED and CNV lesion (arrow) with subretinal fluid. Despite the therapy, the lesion is bigger; best seen in density map (circle). Another example of chronic CSR with a lesion localized on a B-scan. Note the presence of subretinal fluid.

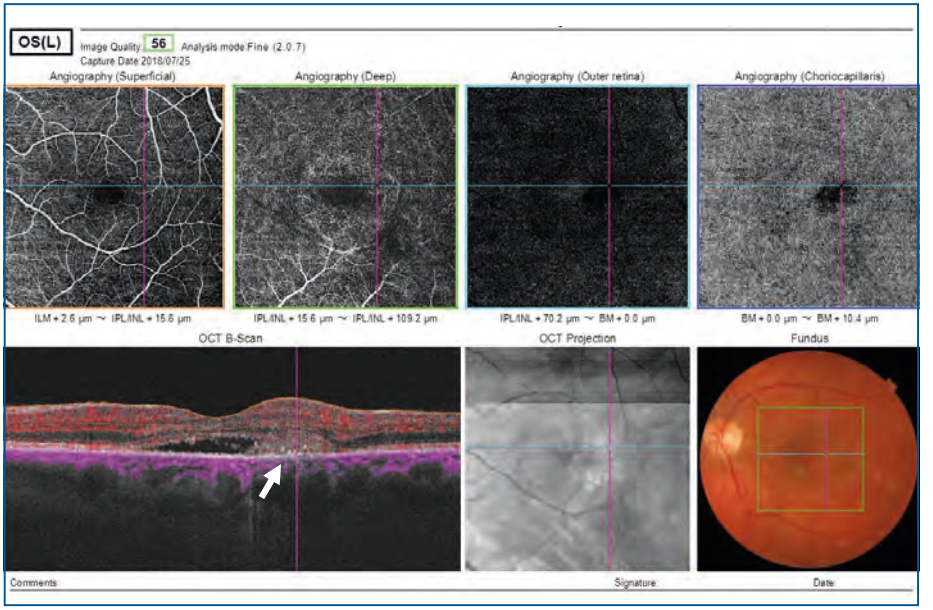

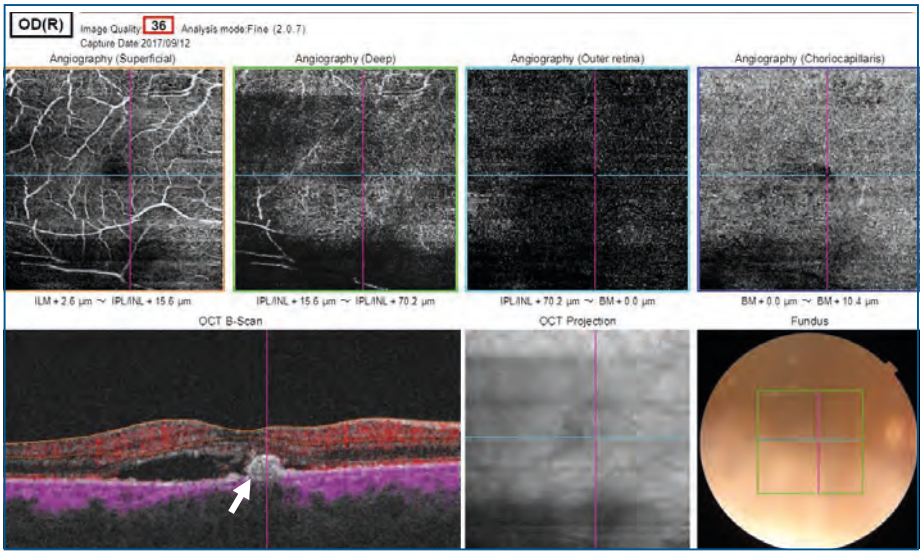

Figure 8-5. OCTA reports on both eyes. In this bilateral case of chronic CSR, B-scan shows the presence of PED, subretinal lesion (arrows) and fluid. 37-year-old male. In this patient, although there is a well-defined lesion resembling CNV in the example above, no vessels are visualized.

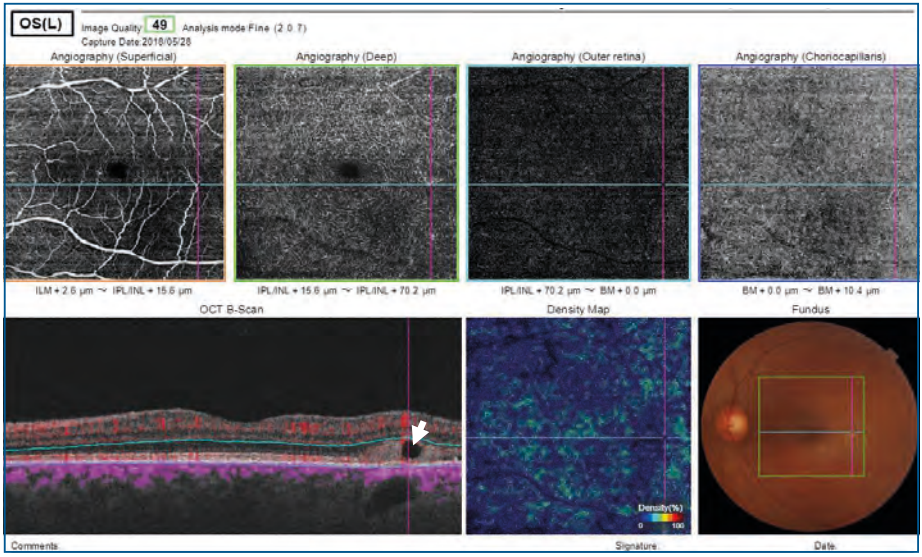

Figure 8-6. OCTA report on left eye. In this 43-year-old male with an inner-retinal cystoid cavity (arrow) and subretinal tissue corresponding to a yellowish scar on the fundus photo. No CNV was detected.

Key points

OCTA can act as a simple tool that allows differentiation of neovascularization in CSR. CNV can be paramacular and can vary in size.

8.2. Choroidal neovascularization caused by degenerative myopia

Pathological myopia is defined either as Axial length >26 mm and/or a refractive error of more than -6D together with degeneration of the posterior segment caused by the elongation of the globe. It is considered one of the major causes of vision deterioration. CNV is usually classic or type 2. OCTA is very useful to create an image of the CNV; however, as in wet AMD, we cannot say whether a CNV is active or not based on the OCTA scan. Moreover, the larger than normal

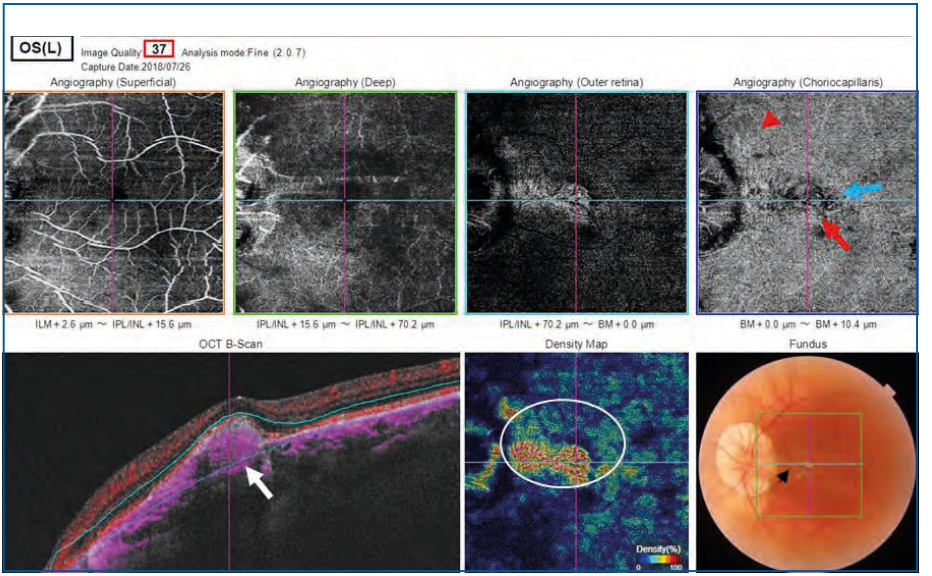

Figure 8-7. OCTA report on left eye. 38 year-old female. B-scan shows dome-shaped hyper-reflective lesion with increased flow, loss of RPE and choriocapillaris (white arrow). Moreover, dark areas of chorioretinal atrophy are also visible on the choriocapillary segmentation (red arrows) as well as larger choroidal vessels under the atrophy (blue arrow). Due to segmentation error, this lesion is not well-defined but seems to have a lot of interlacing vessels. Fundus photo shows larger peripapillary atrophy of the RPE and choriocapillaris and a lacquer crack (arrow).

size of the globe results in many segmentation errors; therefore, to get the best image of the CNV, it is essential to place the upper segmentation slab above the RPE.

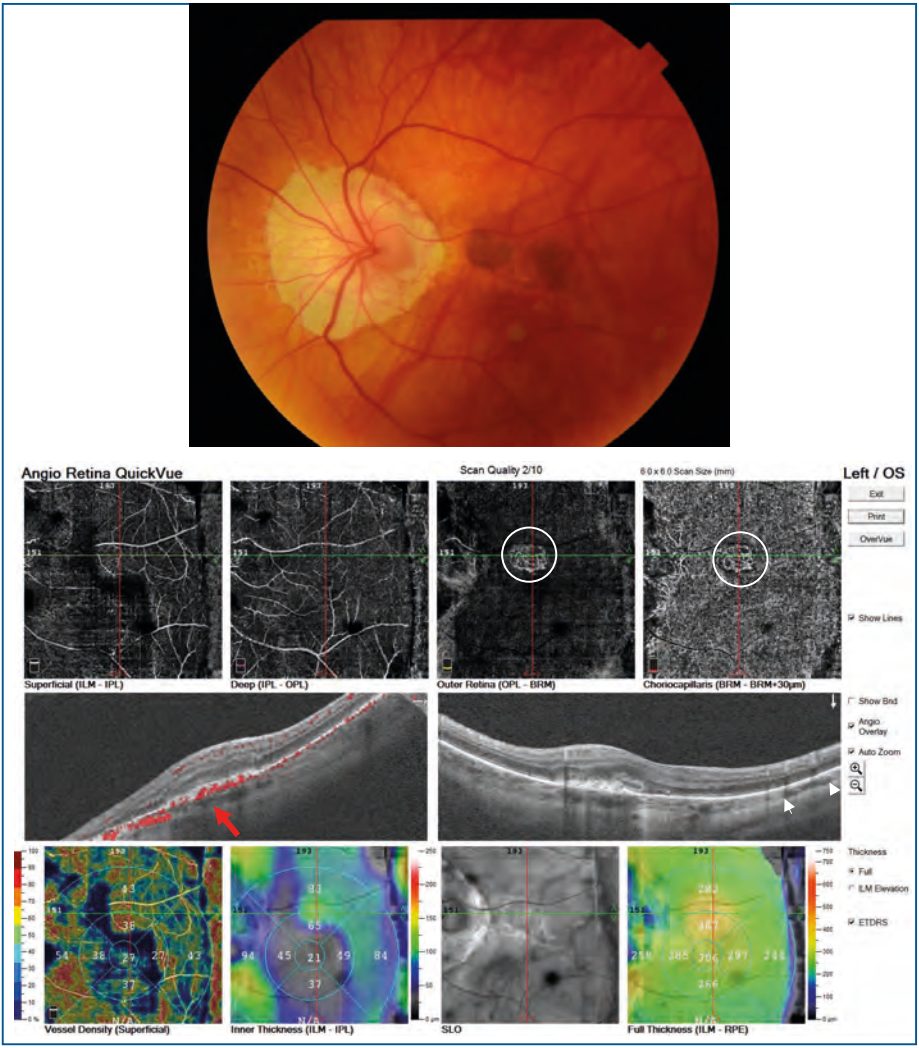

Figure 8-8. Multimodal images of the left eye of a 56-year-old woman diagnosed with CNV in macular region caused by myopic degeneration. Fundus photo shows choroidal vessels well visible due to thinning of the retina, as well as oval appearance of the optic disc. Obvious neovascular image demonstrated on the outer retinal layer. CNV is well-defined and circular-shaped with many tangled vessels. B-scan break of retinal pigment epithelium, choriocapillaris atrophy under lesion. Note chorioretinal atrophy area between 2 white arrowheads.

Key points

CNV caused by degenerative myopia can be seen in choriocapillaris section with manual selection over RPE. CNV has a circular shape with tangled and or interlacing vessels. Due to choriocapillaris atrophy, larger choroidal vessels are visible in choriocapillaris segment.

8.3. CNV caused by angioid streaks

Angioid streaks are dehiscences in Bruch's membrane and look like red bands with irregular borders that radiate from the optic nerve head. They can be associated with multiple disorders: pseudoxanthoma elasticum, Ehlers-Danlos syndrome, Paget's disease, sickle cell anemia, hypertensive and cardiovascular disorders and thalassemia. The most common cause of visual function deterioration is secondary CNV. CNV can appear as tangled or interlacing. According to some studies, the interlacing appearance is associated with more active CNV. It is important in cases with angioid streaks to perform FA.

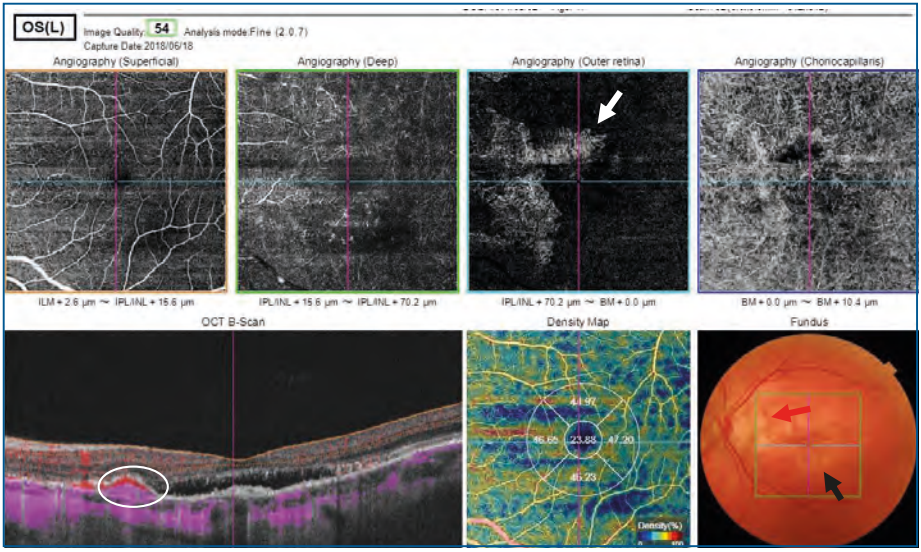

Figure 8-9. OCTA report on left eye. 47-year-old female patient with secondary CNV due to angioid streaks. Color fundus photo shows angioid streaks (red arrow) and pigmentary changes in the fundus of left eye (black arrow). B-scan shows a hyper-reflective subretinal lesion with intraretinal fluid with the presence of high flow lesion perifoveal (circle) and no flow subfoveal. OCTA shows irregular foveal sparing and poorly defined tangled neovascular network.

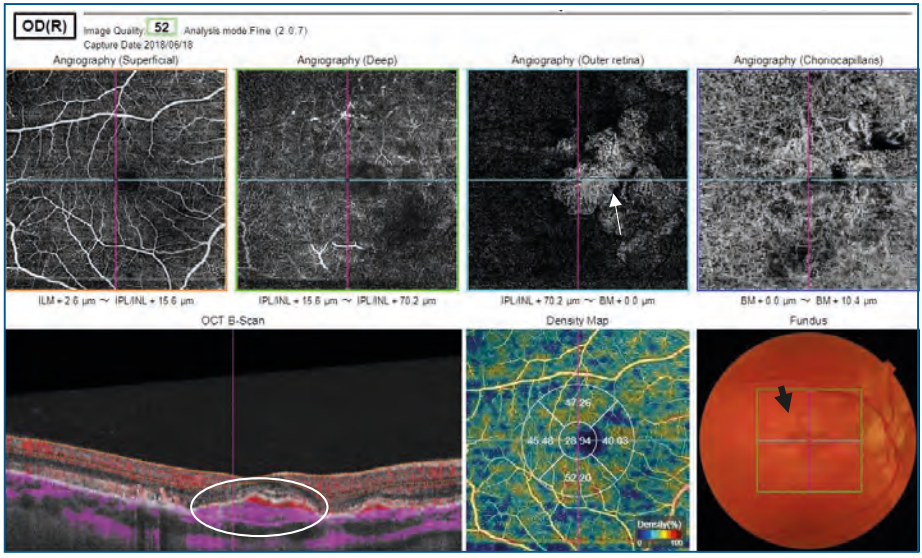

Figure 8-10. OCTA report on the right eye in the same patient. Color fundus photo shows pigmentary changes of the fundus (black arrow). B-scan shows hyperfluorescent subretinal lesions with intraretinal fluid (circle). OCTA shows the presence of macula involving irregular, poorly demarcated interlacing CNV. In the center, OCTA shows no flow in some regions, probably due to sub-threshold speed of flow (arrow).

Key points

OCTA helps to diagnose neovascular lesions in chronic CSR. Myopic CNV is typically dome-shaped on a B-scan and tangled or interlacing.

CNV in angioid streaks can involve the fovea and is usually irregularly tangled or interlacing. Unlike vascular AMD, the lesion can be located outside the macula.

9. Dry AMD

Dry AMD is a disease of the posterior segment with RPE and Bruch's membrane alterations and deposition of drusen. Currently, AMD is divided into early with medium drusen, intermediate with large drusen and severe with either exudative or atrophic form. Small drusen are considered a normal aging change.

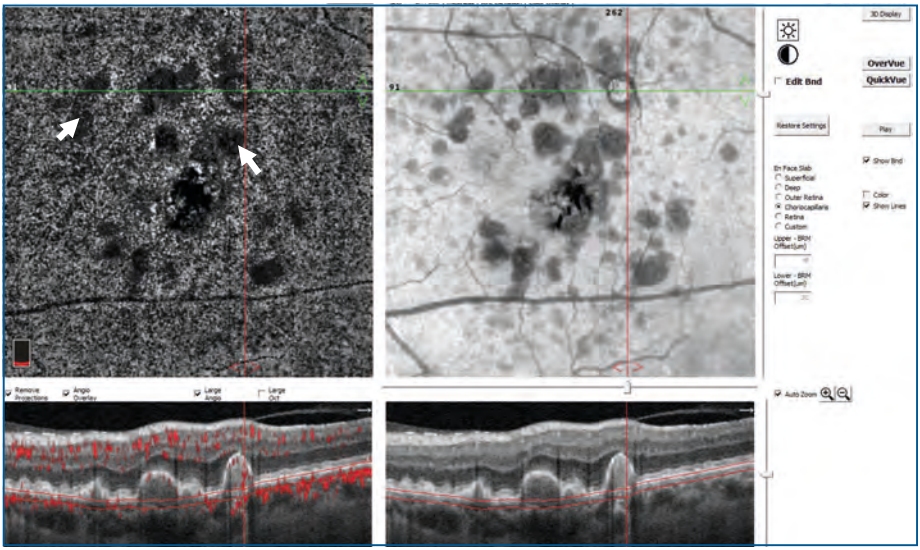

Figure 9-1. OCTA image of a patient with drusen. Bottom: B-scan showing many hyper-reflective deposits under the RPE. The red parallel lines show segmentation for the top images. Drusen shown on the B-scan vary in size and characteristics, despite their presence there is an intact ellipsoid zone. Top: OCTA of choriocapillaries showing flow depletion (arrow).

As mentioned in chapter 3, drusen can create a flow signal and be mistakenly diagnosed as CNV.

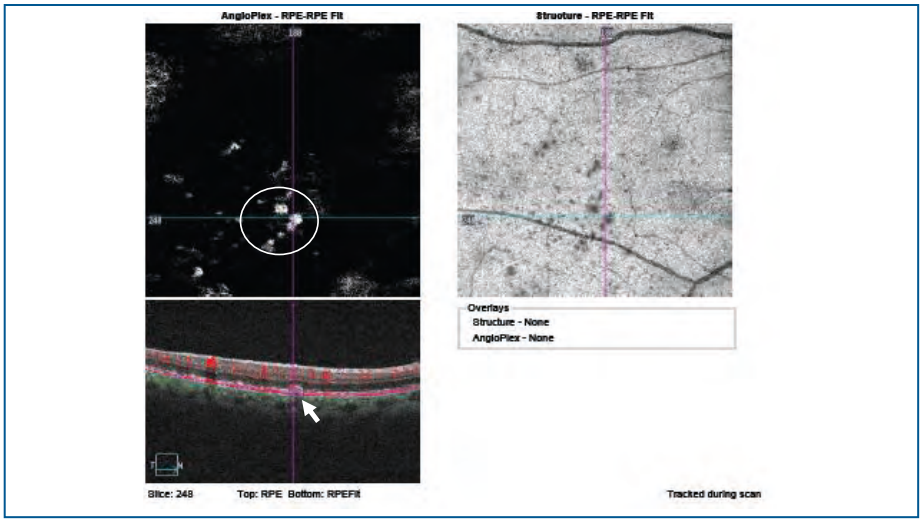

Figure 9-2. OCTA images of right fundus. B-scan shows multiple drusen (arrows) which are generating a flow signal on an OCTA avascular segment (circle).

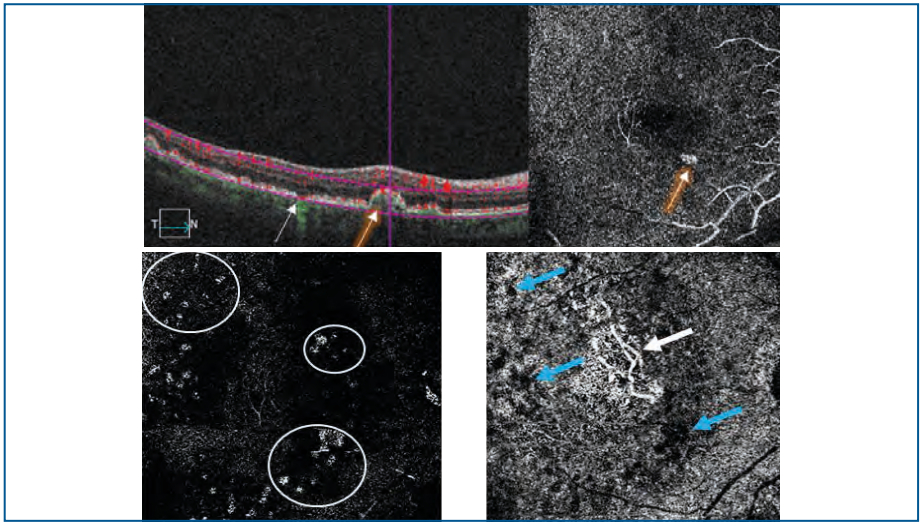

Figure 9-3. Macular atrophy with hyper-transmission of signal (white arrow). 72-year-old female. Additionally, multiple deposits are seen modifying RPE and the retina. Image of a deep segment showing the flow signal from the large drusen (glowing arrow) with some segmentation errors. Bottom left: Avascular image with multiple hyper-reflective drusen (circle) which correspond to a lack of flow (blue arrows) on the choriocapillaries on the right. Furthermore, there is a large vessel (white arrows) visible.

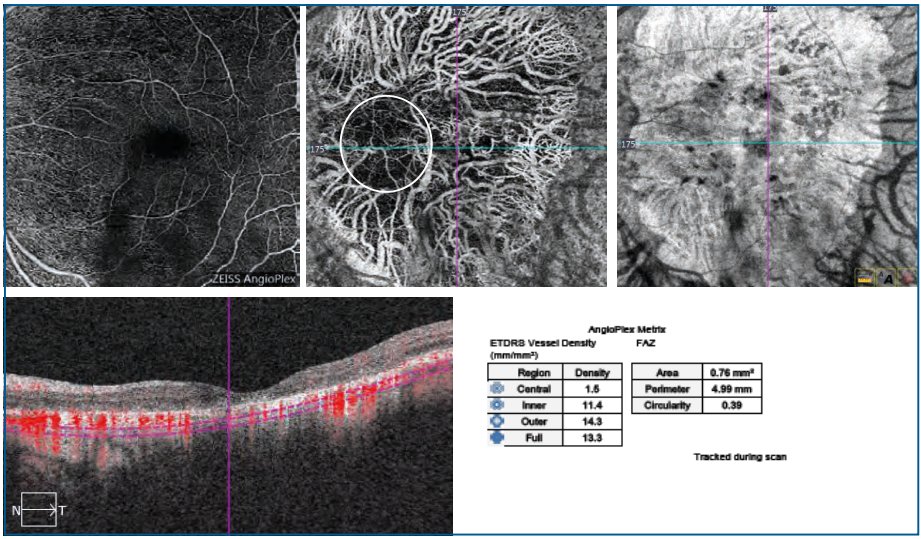

Figure 9-4. OCTA images of left eye. OCTA and B images of 67-year-old female with geographic atrophy. There is a very good picture of large choroid vessels. The macular atrophy also leads to rarefication or even loss of vessels in the choroid (circle). GA leads also to FAZ enlargement (up to 0.76 mm^2) in the superficial complex.

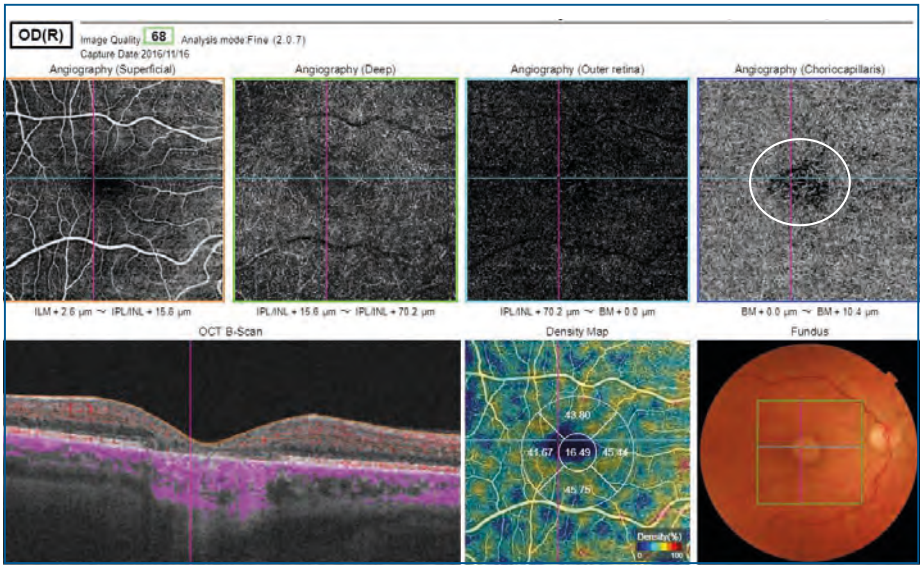

Figure 9-5. OCTA report on right fundus. 43-year-old male. There is a clear macular atrophy visible in this patient who underwent pars-plana vitrectomy with inverted flap technique due

to a macular hole. There is an enlargement of FAZ and rarefication of vessels in choriocapillaris (circle). B-scan shows destruction of photoreceptors in the macula and backscattering of light.

Key points

There is a choriocapillaris dropout under drusen. Geographic atrophy leads to enlargement of FAZ. In extensive geographic atrophy, there is even a rarefication of the choroidal vessels.

10. Optic Disc

Retinal ischemic diseases may create neovascularizations on a disc (NVD) or shunt vessel collaterals also known as optociliary shunt vessels. Why is it important to differentiate these findings? Because the presence of NVD suggests an uncontrolled disease and requires laser therapy, whereas the presence of collaterals implies self-regulatory mechanisms. OCTA is an especially good tool for this, because you can see the vessels in their respective 3D locations. NVD will be best displayed using vitreous segmentation as the vessels will tend to rise above the vitreous while collaterals will be on a superficial segment. OCTA is more useful in determining those two entities, as in the fluorescein angiography these are hard to differentiate due to hyperfluorescent leakage from leaking new vessels that can accompany shunts.

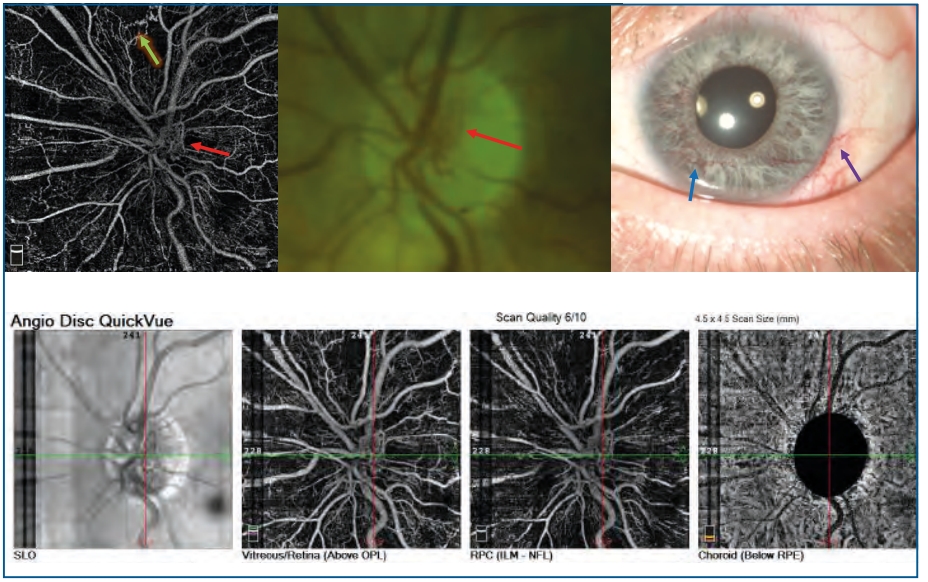

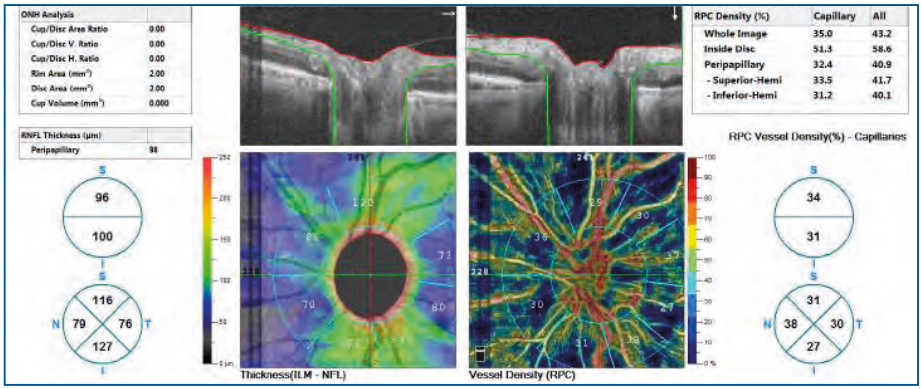

Figure 10-1. Multimodal images of a 58-year-old male with diabetic neovascularization on conjunctiva (violet arrow), iris (blue arrow) and optic disc collaterals. Fundus photo shows the presence of abnormal vessels on a disc (red arrow) that are clearly displayed on the OCTA image (red arrow). Furthermore, the glowing green arrow displays the venovenous shunt. Density map shows capillary loss around the disc as blue areas. There is a slight bulge on the B-scan related to new vessels, despite the fact that the new vessels are flat, suggesting collaterals rather than NVD.

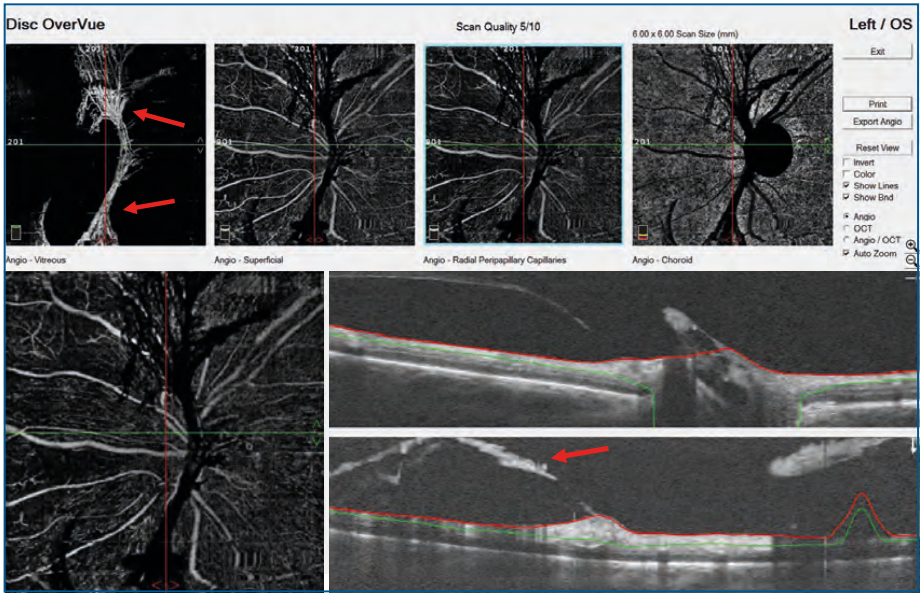

Figure 10-2. In this 64-year-old female with HbA1 of 12 %, the huge neovascularization on the disc (red arrows) is best seen on the Angio vitreous segment (top left). Note that this creates a shadowing artifact on the scans below. On a B-scan, this neovascular tissue tends to be hyper-reflective and extends from the optic disc.

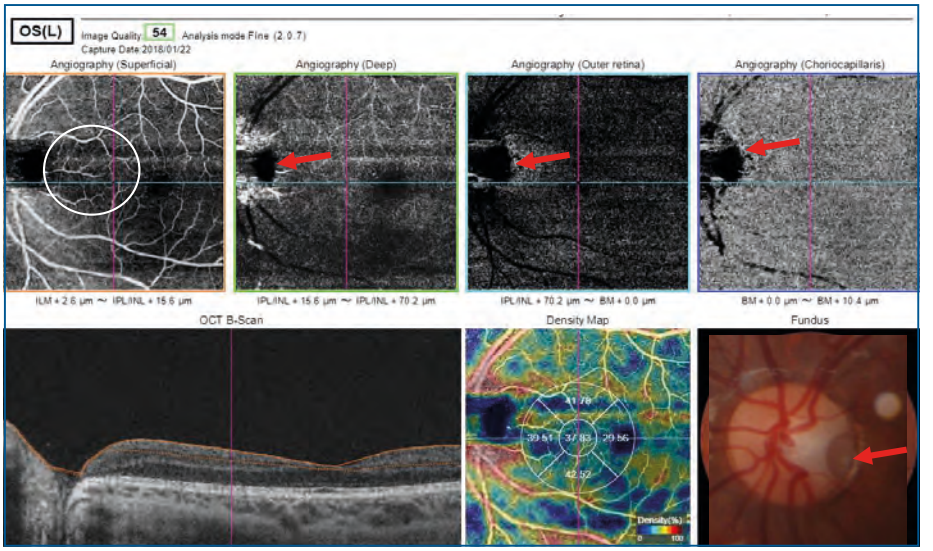

Figure 10-3. Multimodal images of left eye. 9-year-old female. Optic pit may be a result of imperfect closure of the superior edge of the optic fissure. OCTA is useful in differentiating the presence of intra/subretinal fluid in cases of optic disc pits from CNV. Fundus photo showing an optic pit (red arrow) in 9-year-old girl. OCTA shows a lack of vessels within the pit (red arrows) on the disc and the absence of RPCP at the level of the pit (white circle).

Drusen: Optic disc drusen are associated with elevated discs and comorbidities such as central artery or vein occlusion and non-arteritic anterior ischemic neuropathy. Drusen can be associated with attenuation of RPCP, and a decrease in vessel density probably due to contraction of the vessels.

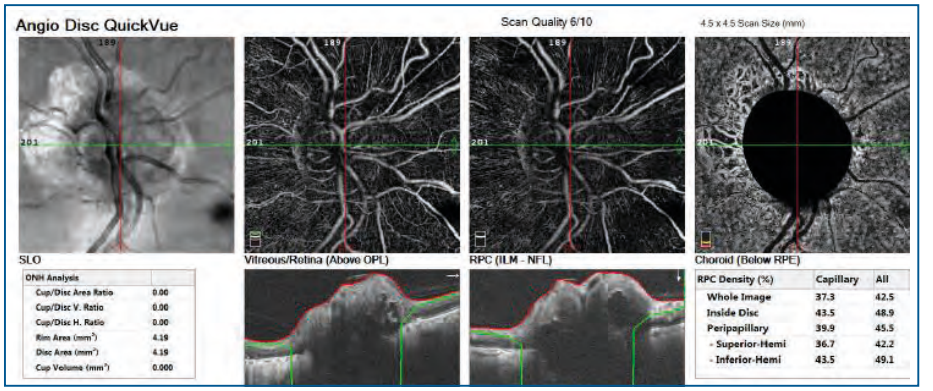

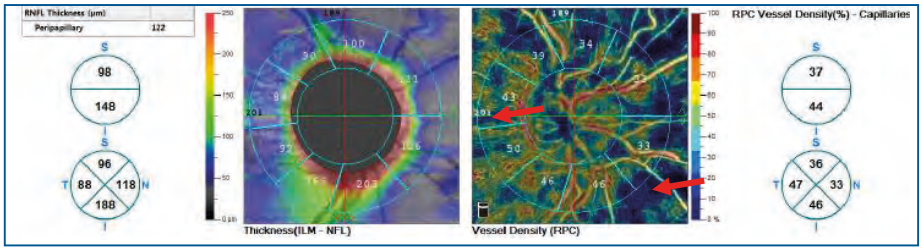

Figure 10-4. OCTA report on right optic disc. In this patient with bilateral optic disc drusen peripapillary decrease in the vessel density (red arrows). Moreover, a decrease in density is also found within the optic nerve.

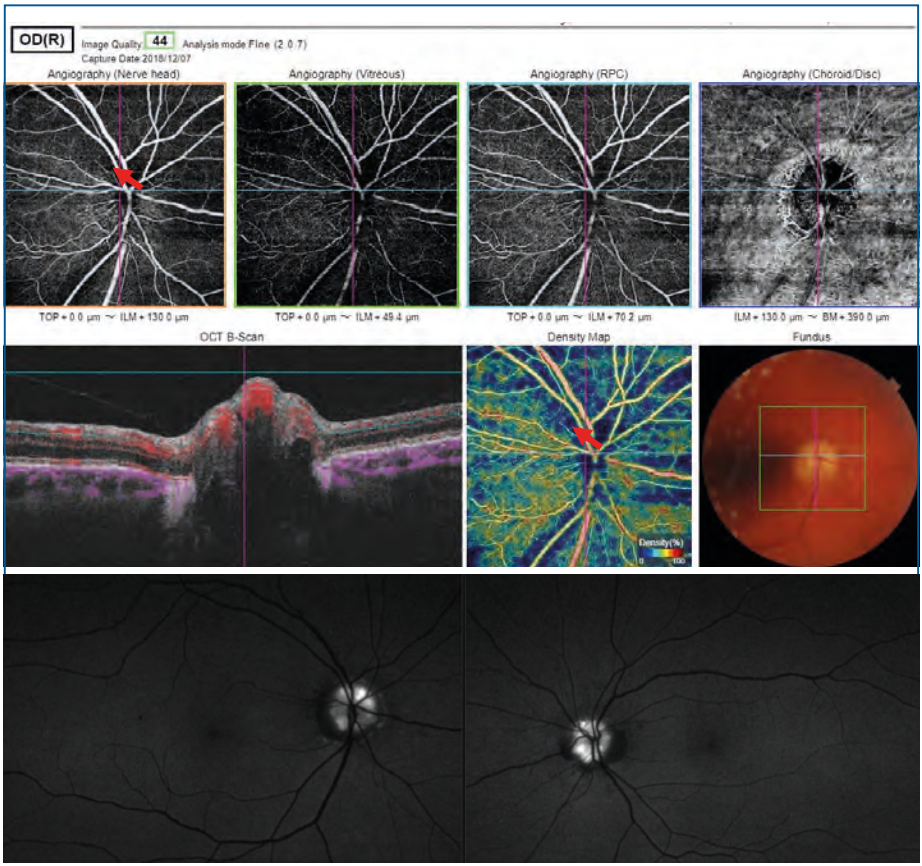

Figure 10-5. Multimodal imaging of right eye with autofluorescent image of both eyes. 60-year-old male. AF shows the presence of optic disc drusen. OCTA report on the right eye showing capillary dropout in the superior quadrants (red arrow).

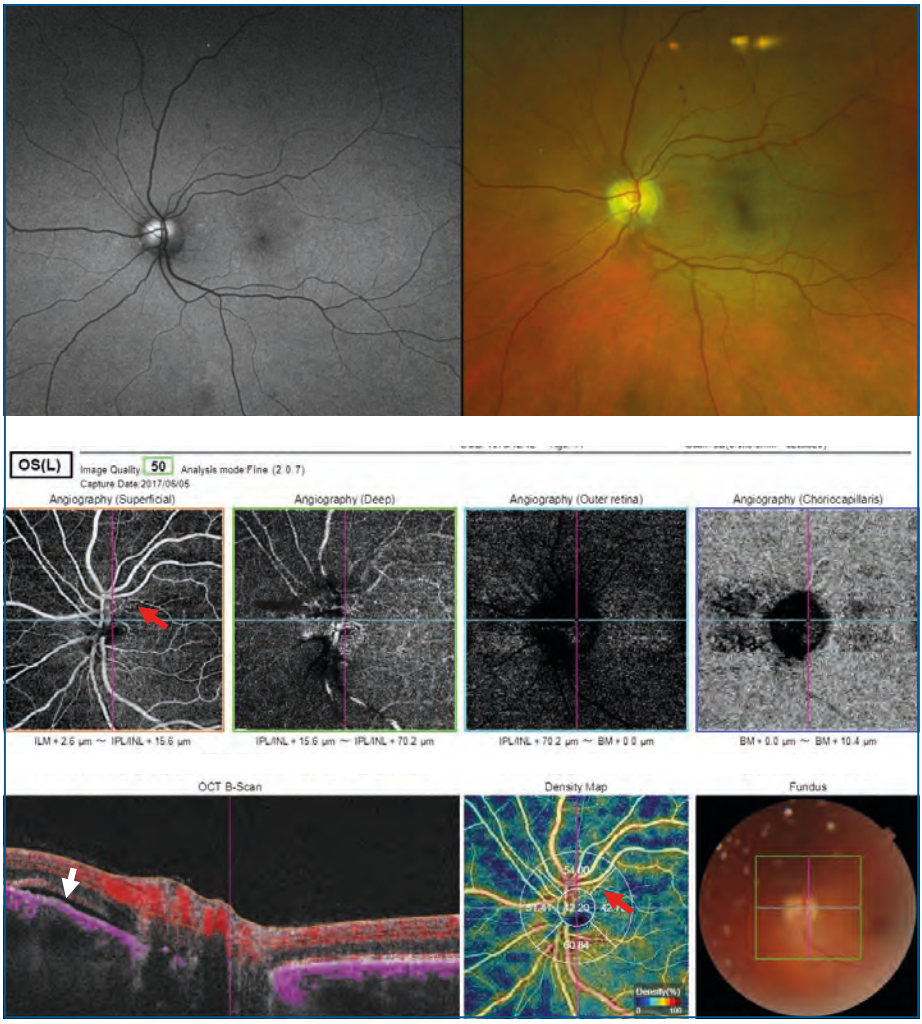

Figure 10-6. Autofluorescence and colored SLO image of 41-year-old patient post hypertensive crisis. Hyperautofluorescence was detected in the superior quadrants of the disc. Subretinal fluid is visible on the B-scan (white arrow) as well as artifactual loss of capillaries. No CNV was observed within in the superior quadrants (red arrows).

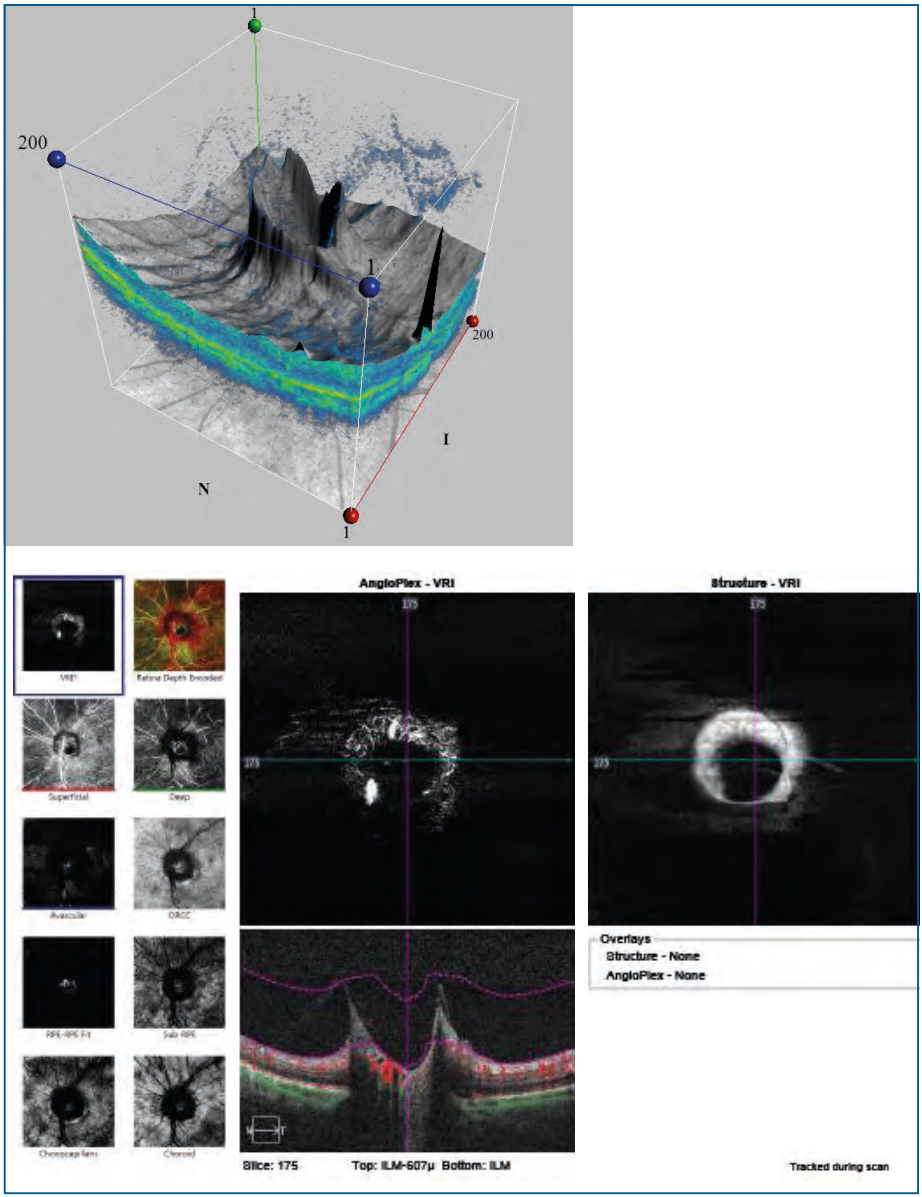

Figure 10-7. OCTA reports on optic disc. 63-year-old male. 3D image shows the presence of extensive budging of the optic disc. In this patient with type 2 diabetes, OCTA helped to distinguish between NVD and vitreopapillary tractions. In this photo, there is lack of flow on the VRI segment indicating that this is an optic disc tractional syndrome.

Key points

Optic disc drusen can cause thinning in peripapillary vessels probably due to compression by extracellular material. Optic pits lead to destruction of RPCP at the level of the pit. NVD will grow into the vitreous and will be best visualized on a vitreoretinal segment, whereas collaterals are best visible on a superficial segment.

11. Fundus Abnormalities

OCTA can also be utilized in other retinal diseases involving vessels. One such condition are posterior segment malignancies. OCTA can show enlargement of FAZ in the deep layers as well as a decrease in vascular density or presence of CNV.

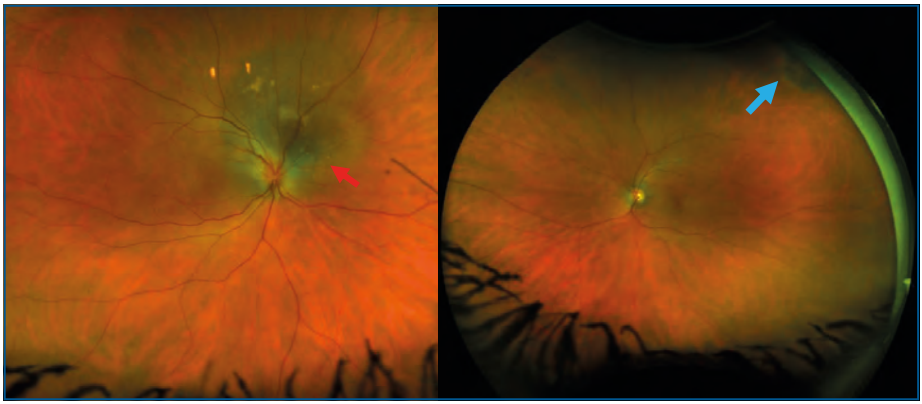

Figure 11-1. Color fundus photo. 48-year-old female. Pigmented superior peripapillary lesion with pigmentary changes which was diagnosed as a malignant melanoma of the right eye (red arrow) causing papilledema. Note the presence of melanotic change in the superior temporal retina of the left eye (blue arrow).

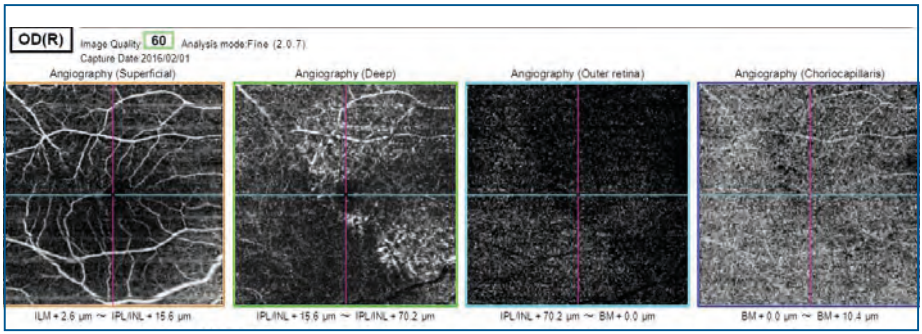

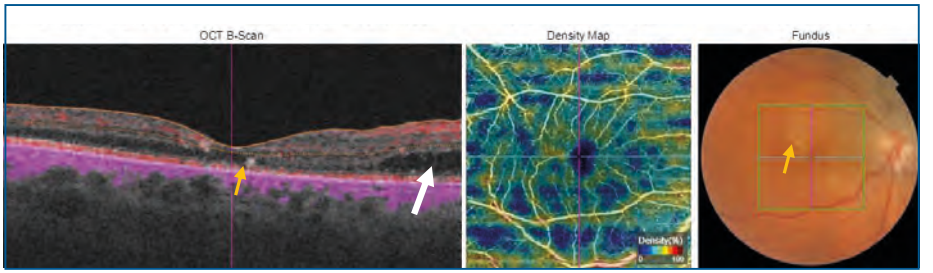

Figure 11-2. OCTA report on right eye. B-scan shows presence of intraretinal fluid (arrow), and some hyper-reflective material corresponding to hard exudates (yellow arrows) on a fundus photo. Density map shows disrupted FAZ. There is also choriocapillaris dropout.

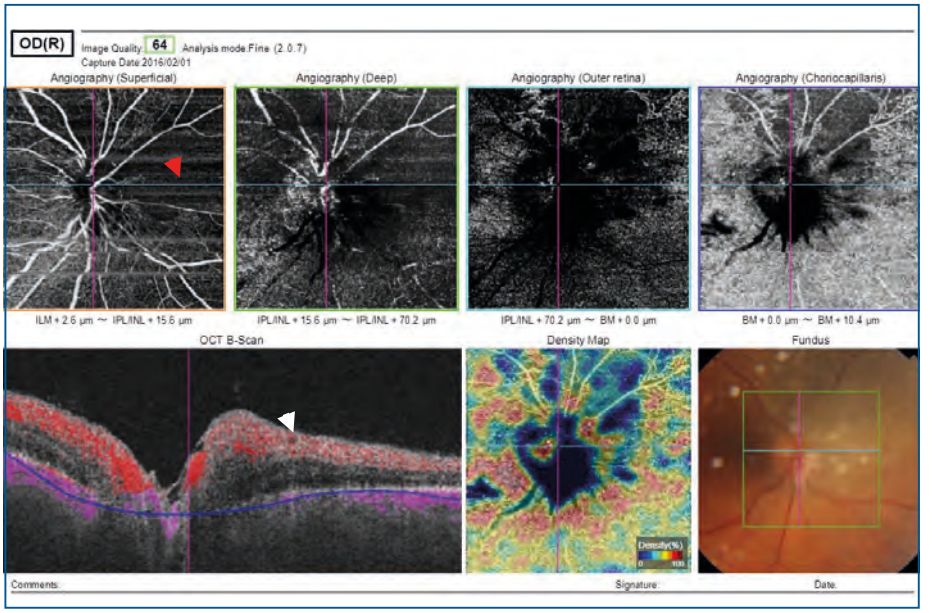

Figure 11-3. OCTA report on right eye. B-scan demonstrates papilledema and intraretinal fluid (white arrowhead). There is a general destruction of microcirculation of the superonasal quadrants (red quadrant)

After proton beam therapy.

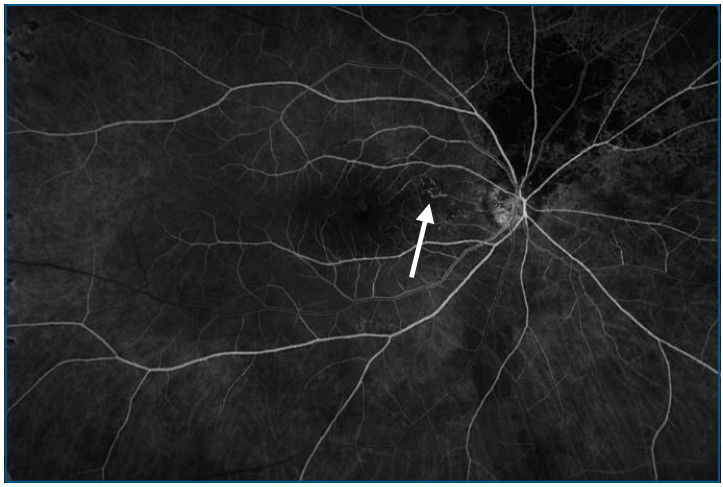

Figure 11-4. Fluorescein angiography of the same eyes as in the former examples. Fluorescein Angiography demonstrates perfusion loss and vascular abnormality: nasal to the macula (arrow)

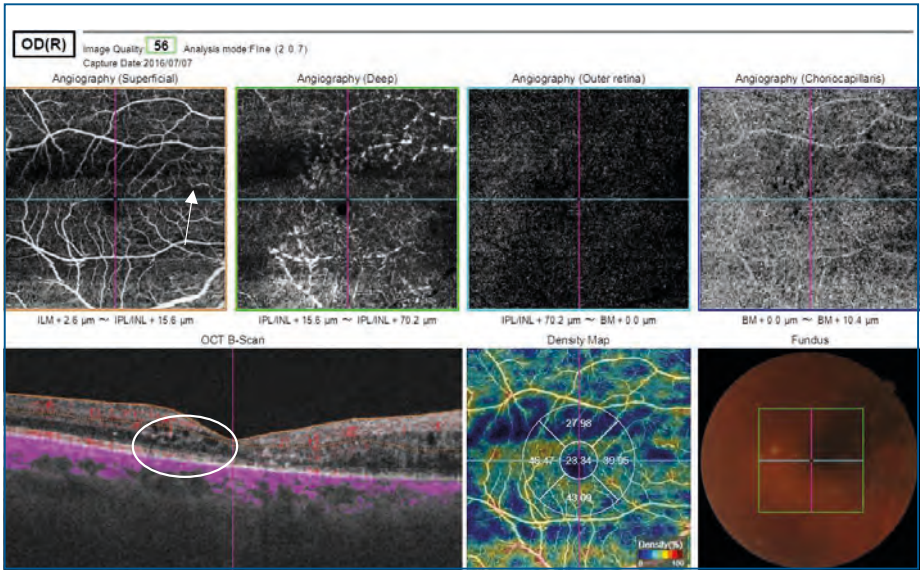

Figure 11-5. OCTA images of the same eye. OCTA shows perfusion loss with vascular collaterals and shunts. B-scan shows resolution of the fluid space with more intraretinal fluids as well as hyper-reflective hard exudates. Note the increased opacity in the fundus photo due to cataract formation.

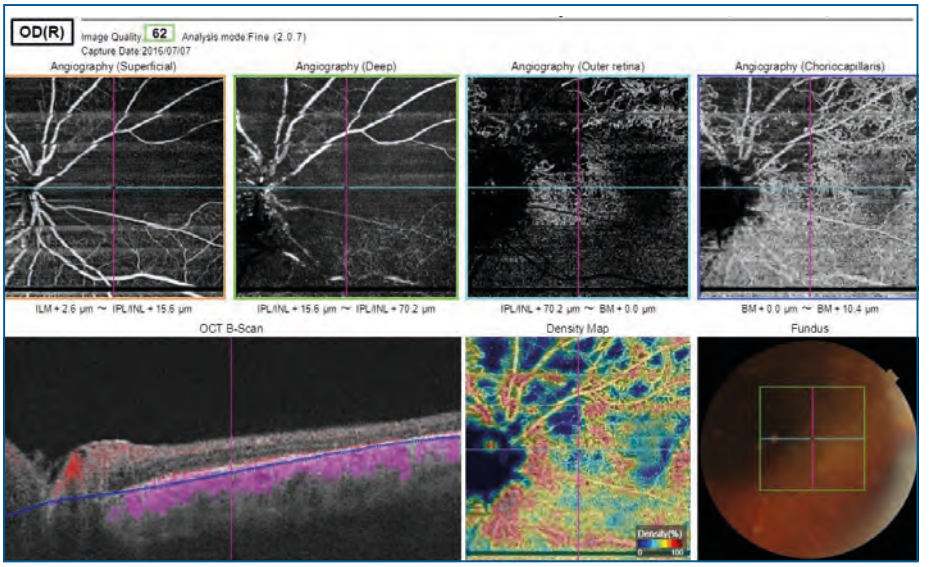

Figure 11-6. OCTA report on the same patient. B-scan demonstrates resolution of the edema of the optic disc. Compared to the previous scan, there is a slight increase in capillary dropout in the choriocapillaris segment. Furthermore, she also received anti-VEGF and yellow laser was applied.

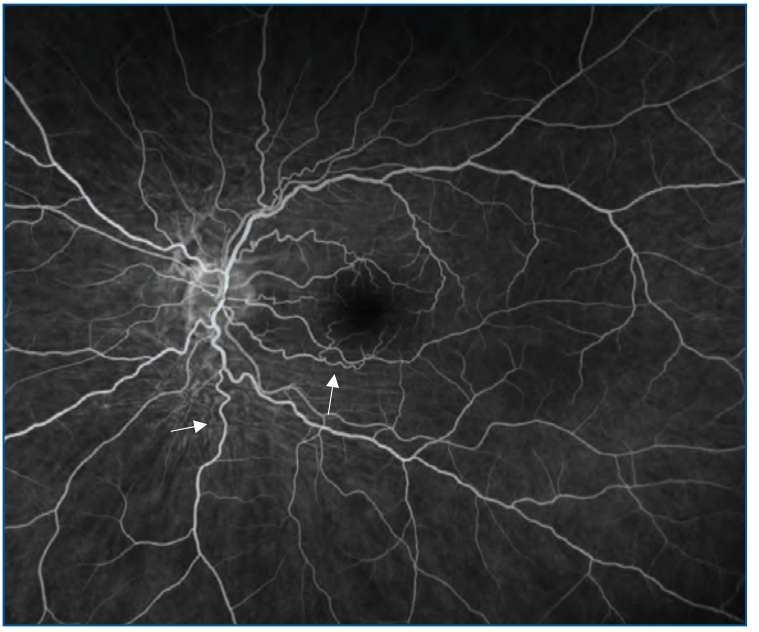

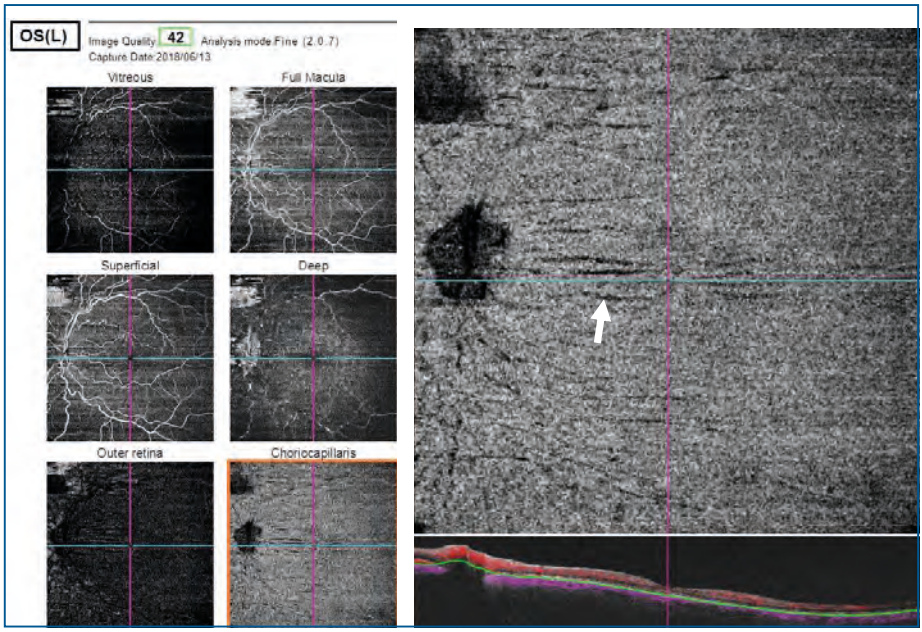

Figure 11-7. Multimodal imaging of left eye. 43-year-old male. In this patient with hypertensive retinopathy, choroidal folds are visible in the FA as well as in the choriocapillaris segment (arrows). Moreover, increased tortuosity is seen in the superficial retina segment.

12. Inflammation

OCTA can be successfully used in inflammatory diseases of the posterior pole. The most obvious application is in the detection of CNV from inflammatory infiltrates. Furthermore, there is a possibility to assess capillary loss in choriocapillaris.

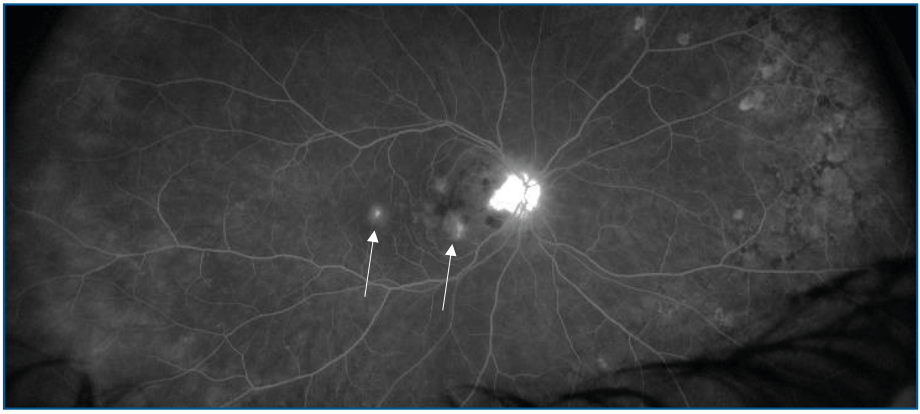

Figure 12-1. FA of a patient with papillitis and uveitis. 63-year-old woman who underwent biologic, azathioprine and anti-VEGF treatment. Leakage is seen around the disc together with hyperfluorescence and within some perifoveal lesions with visible staining and leakage (arrow).

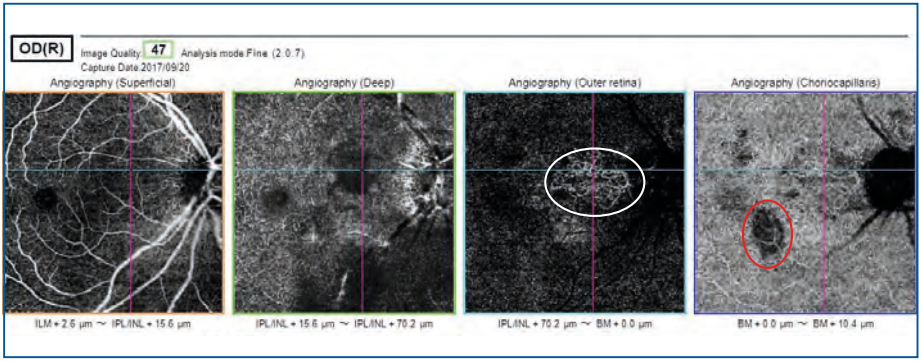

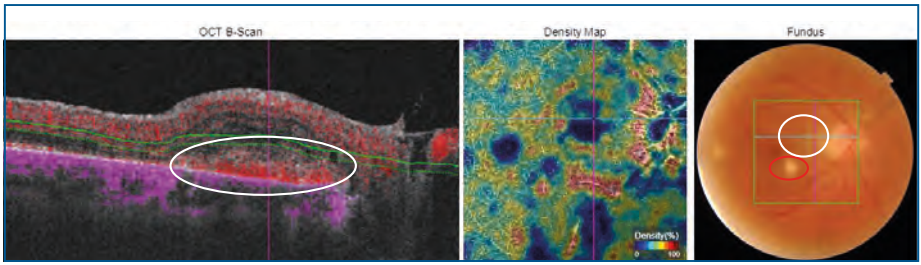

Figure 12-2. OCTA report on the same patient with panuveitis and choroiditis, showing irregular choroidal neovascularization close to the optic disc (white circles). The B-scan shows increased flow, hyper-reflective lesion with the presence of intraretinal fluid. The granuloma located inferiorly to the macula shows no flow, suggesting its pure inflammatory origin with no signs of CNV (red circle).

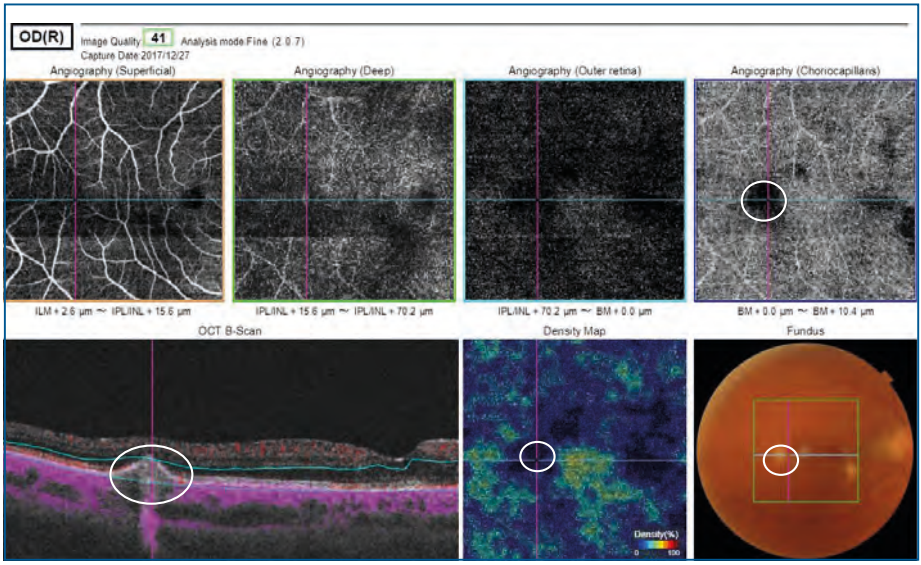

Figure 12-3. OCTA report on right eye. In this lesion temporally to the macula (circles) there is infiltration of inflammatory material, however it is not neovascular. Unlike the images above, this lesion is also more homogenous than CNV.

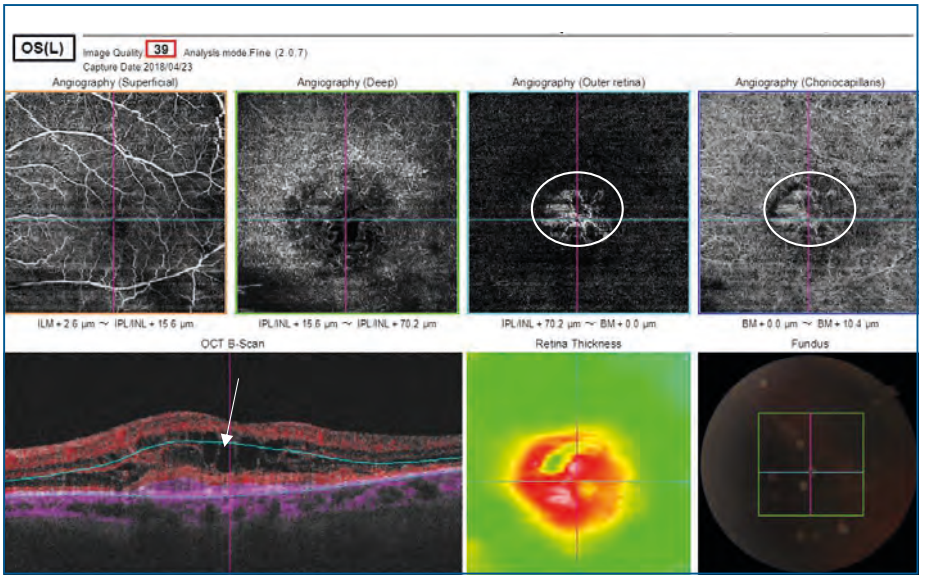

Figure 12-4. OCTA report on left eye. Example of uveitis in a 63-year-old female with CNV close to the optic disc with increased flow and a hyper-reflective lesion (circles) in the B-scan under a cystoid macular edema (arrow). Note that the CNV is circular.

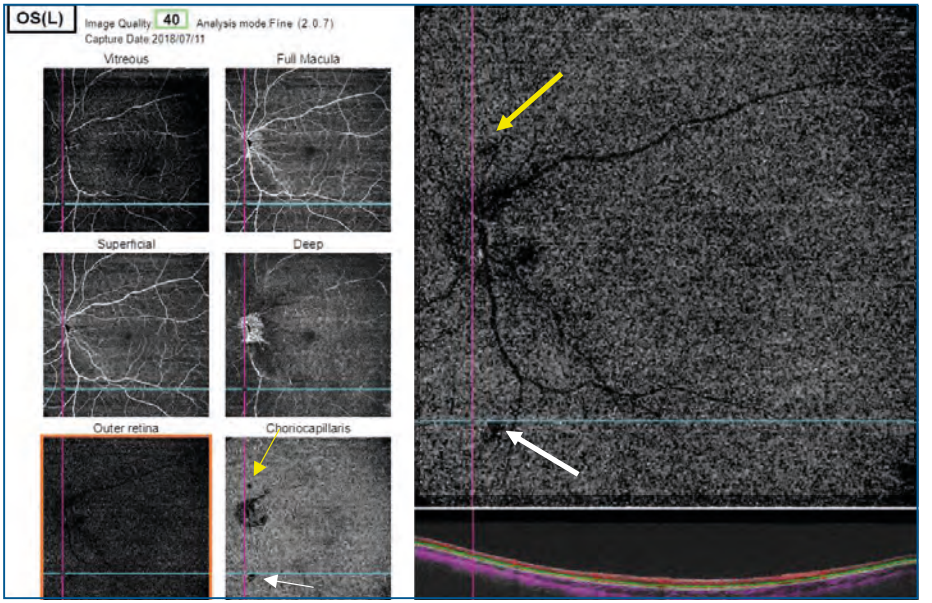

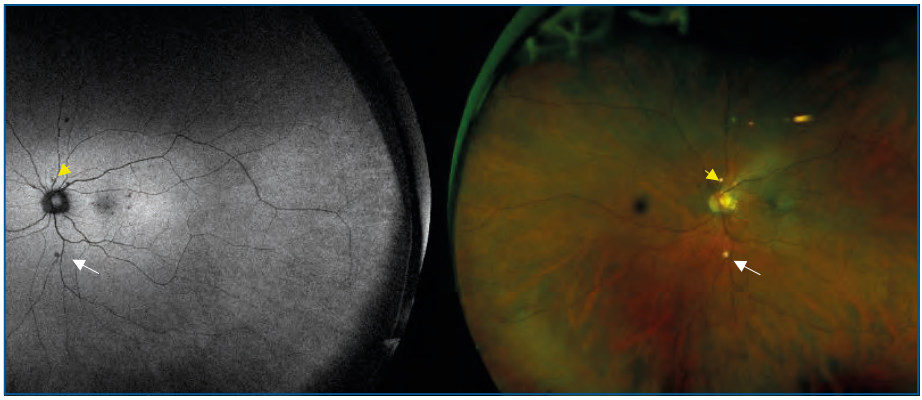

Figure 12-5. Multimodal imaging of left eye. In this 32-year-old female with history of retinal inflammation, bright yellow, hypoautofluorescent spots (yellow and white arrows) correspond to capillary dropout seen in choriocapillaris; also visible in the outer retina as darker spots. No CNV was detected.

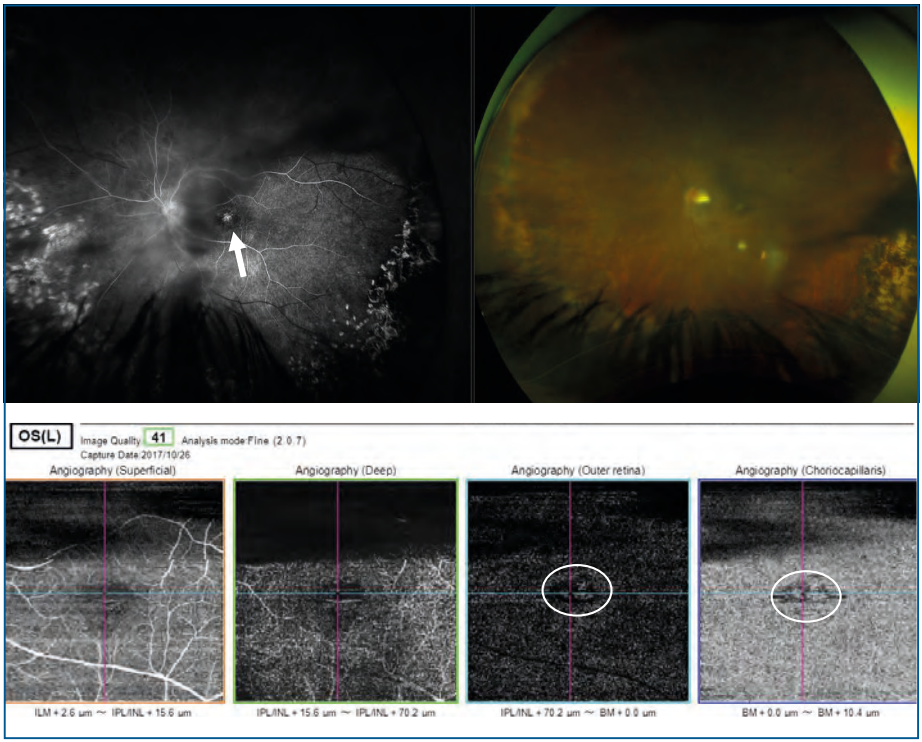

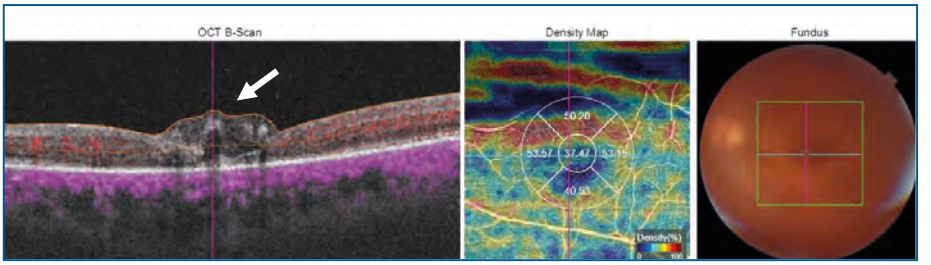

Figure 12-6. Multimodal image of left eye. 35-year-old male after pars planitis. FA shows decrease in visibility due to floaters subsequent to previous vitritis and vitreous hemorrhage with macular (arrow) and peripheral staining of laser burns and retinal degeneration. Although there is an identifiable lesion on the B-scan (arrow) in the macula, it generates no signal, yet it is absorbing light and not allowing a full flow signal from the choriocapillaris (circles).

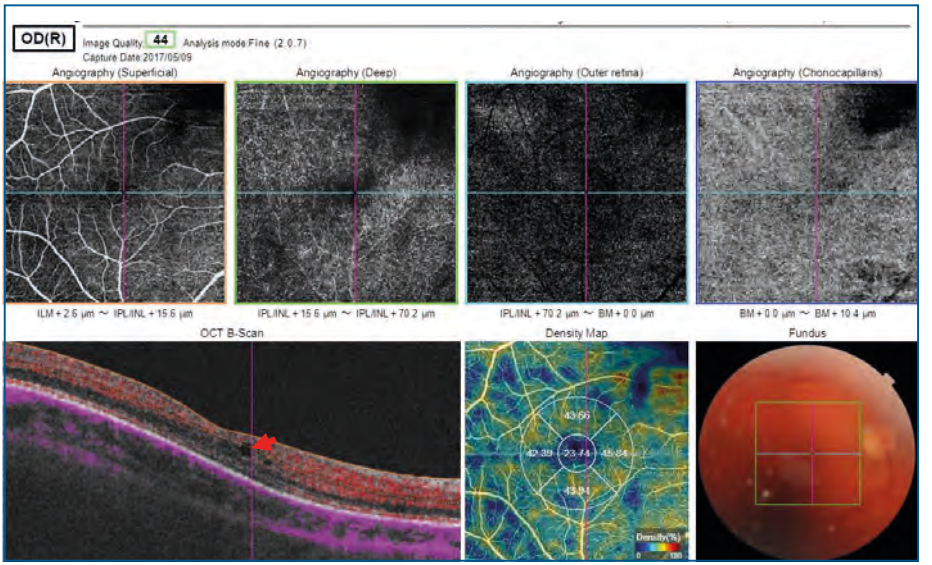

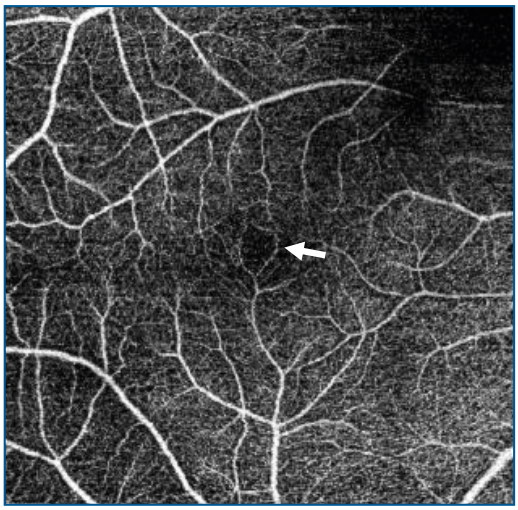

Figure 12-7. OCTA report on right eye of 34-year-old female. Report and superficial segment of uveitic patient. Some patients have small FAZ area, that can be misinterpreted as a vascular infiltration of the FAZ (white arrow). Moreover, in the B-scan some intraretinal fluid is visible (red arrow). Fluid can be a result of leaking vessels that can not be visualized on OCTA.

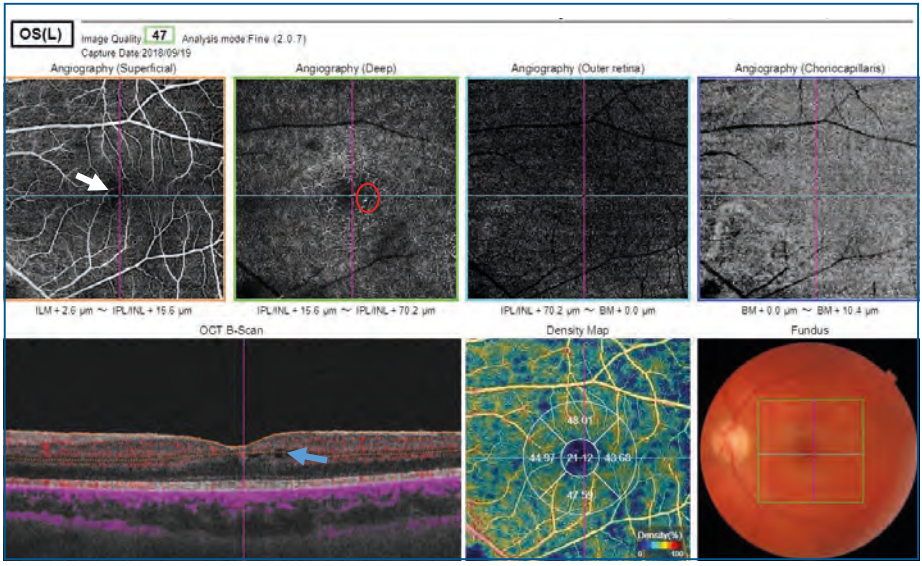

Figure 12-8. OCTA report on left eye. Retinitis and uveitis with multiple cysts in the B-scan (blue arrow) and FAZ vessel infiltration (white arrow) in the superficial segment and a microaneurysm (red circle) in the deep segment.

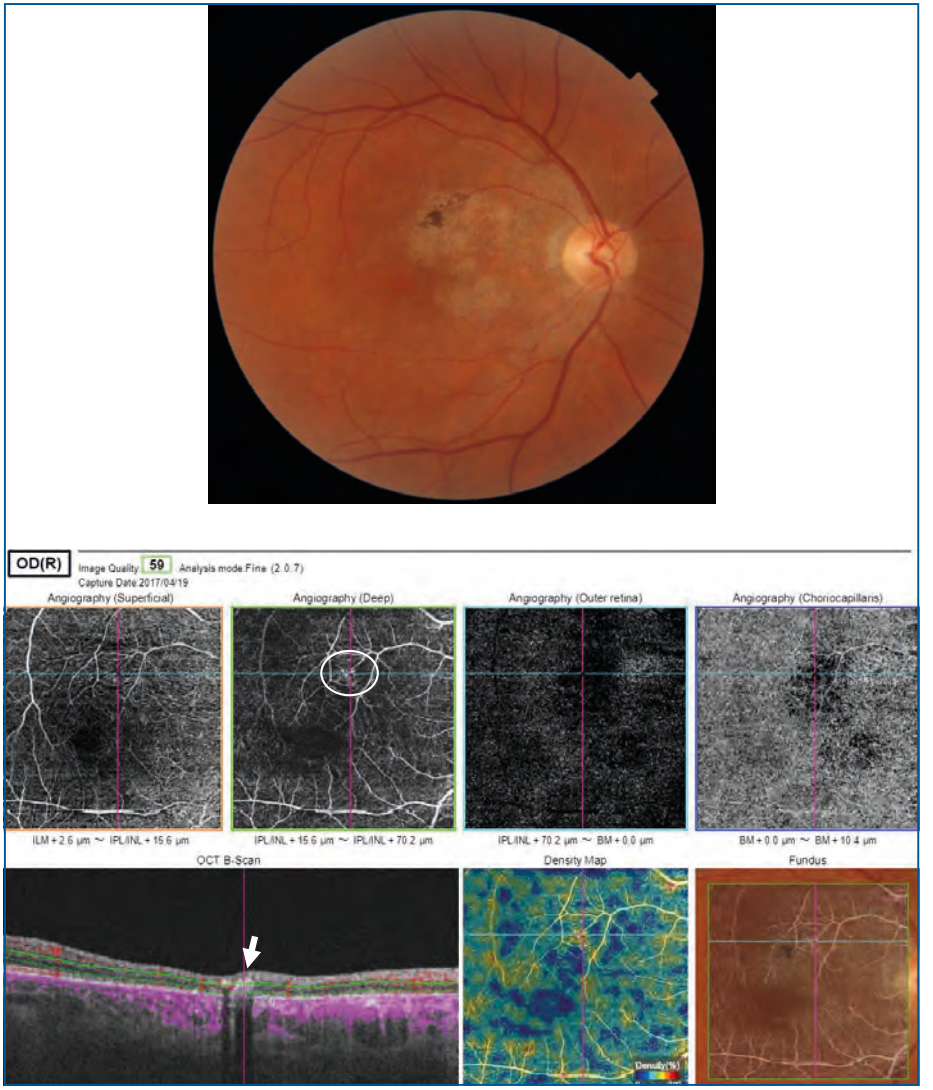

Figure 12-9. OCTA report on right eye. A traumatic case post battery explosion that created thinning of the retina and abnormal vessels within the scar. Pigmentary lesions in the fundus photo and retinal scars are not associated with CNV.

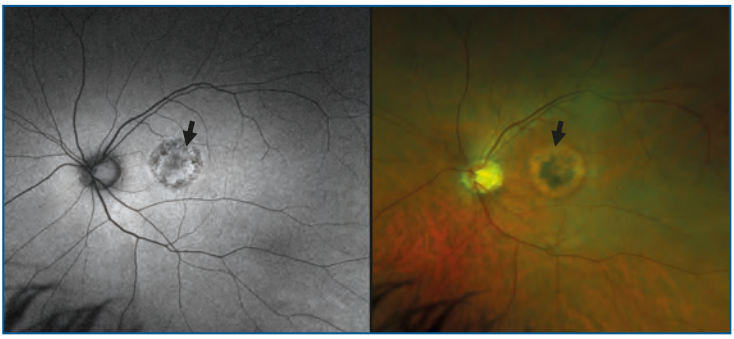

Figure 12-10. Fundus autofluorescence and SLO colored image of 35 years old patient with Kryll's disease or Acute Retinal Pigment Epitheliitis (ARPE). There is a hypofluorescent halo surrounding the macular hyperpigmentation seen in the color fundus photo.

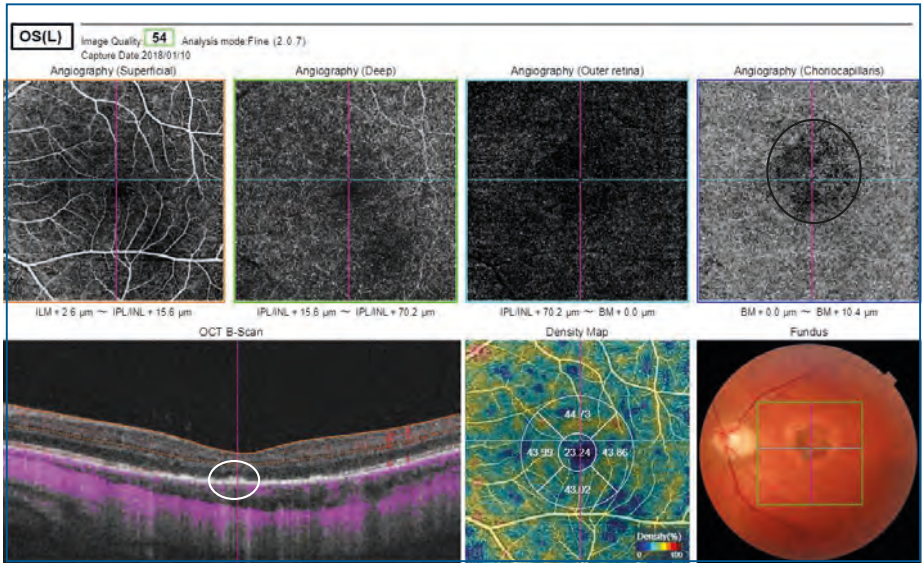

Figure 12-11. OCTA report on left eye. 35-year-old male with ARPE. In the fundus photo, an area of pigmentation is surrounded by a hypopigmented halo (arrows). B-scan shows hyper-reflective tissue (circle), which can be seen above the RPE, and disruption of the ellipsoid zone. There is a visible vessel void in the choriocapillaris (circle) segment, probably due to absorption of the signal by the pigmentary lesion.

Key points

Uveitis can lead to choroidal neovascularization which can be clearly shown on OCTA images.

13. Inherited diseases

Inherited diseases of the retina, of which Stargardt dystrophy and Retinitis Pigmentosa (RP) are the most common, can have variable appearance in OCTA. Stargardt is distinguished by the presence of choroidal atrophy, while in RP there is dislocation of the vascular networks.

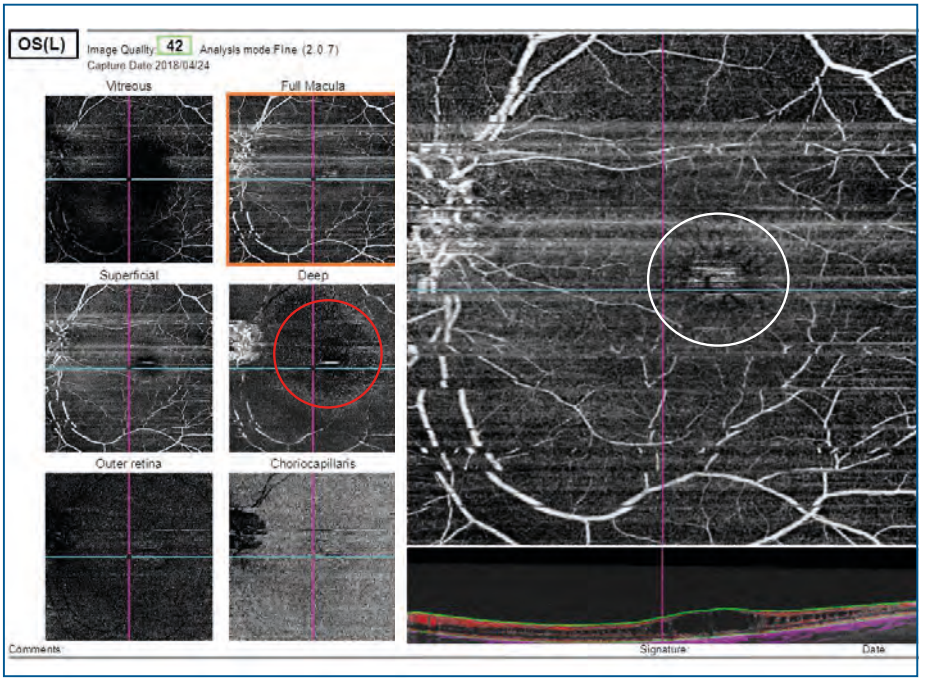

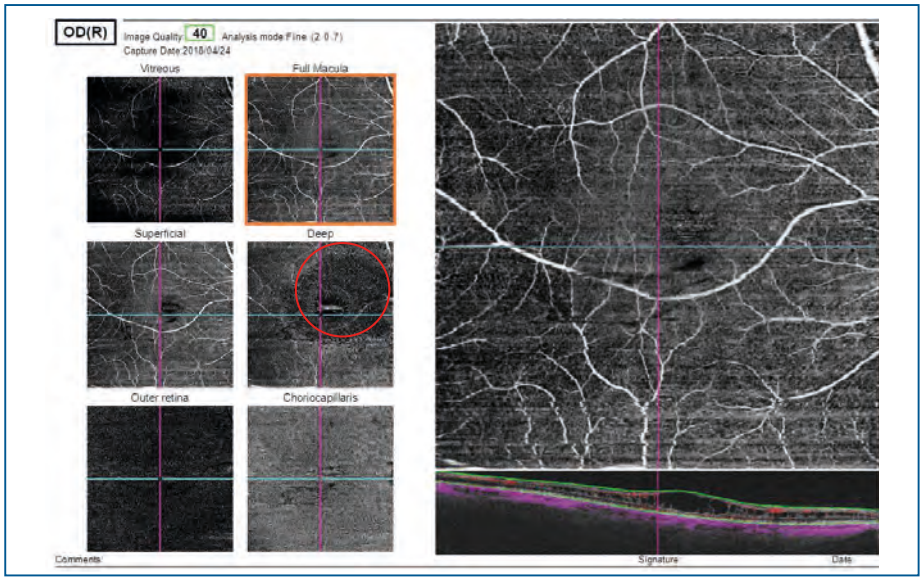

Figure 13-1. OCTA report on both eyes. Bilateral OCTA scan of X-linked retinoschisis with hyporeflective areas in the inner nuclear and outer plexiform layers. 37-year-old male. Schisis in the left eye revealed a spoke-like pattern in the foveal region (white circle). There is also a decrease in vessel density in the deep layers, probably due to cyst displacement (red circle). Note the presence of many motion artifacts due to low visual acuity.

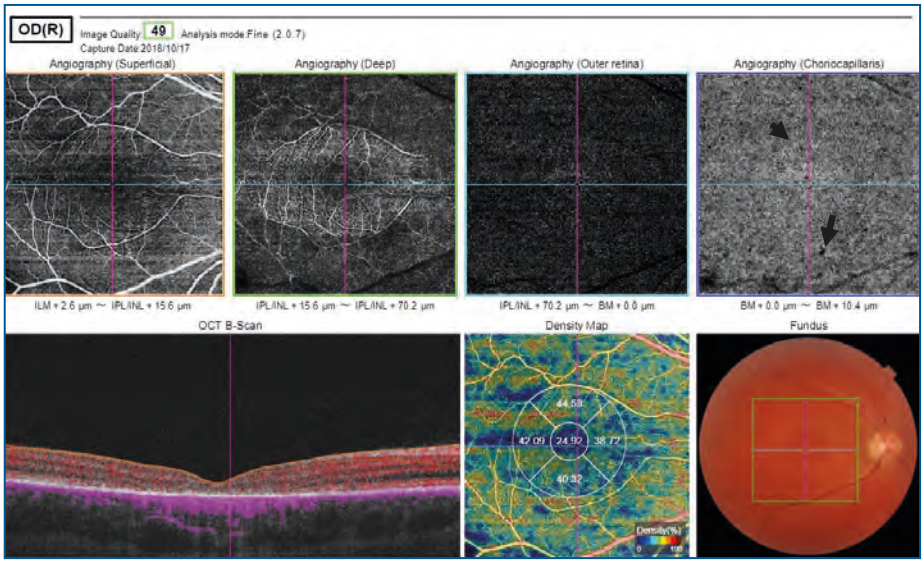

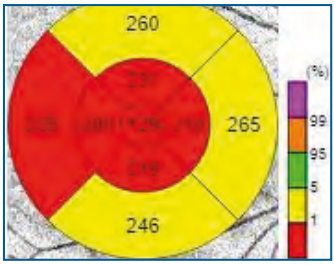

Figure 13-2. Images of a 17-year-old patient with fundus flavimaculatus, Stargardt disease. B-scan together with EDTRS macular thickness displays profound macular atrophy. OCTA of choriocapillaries shows depletion of small vessels.

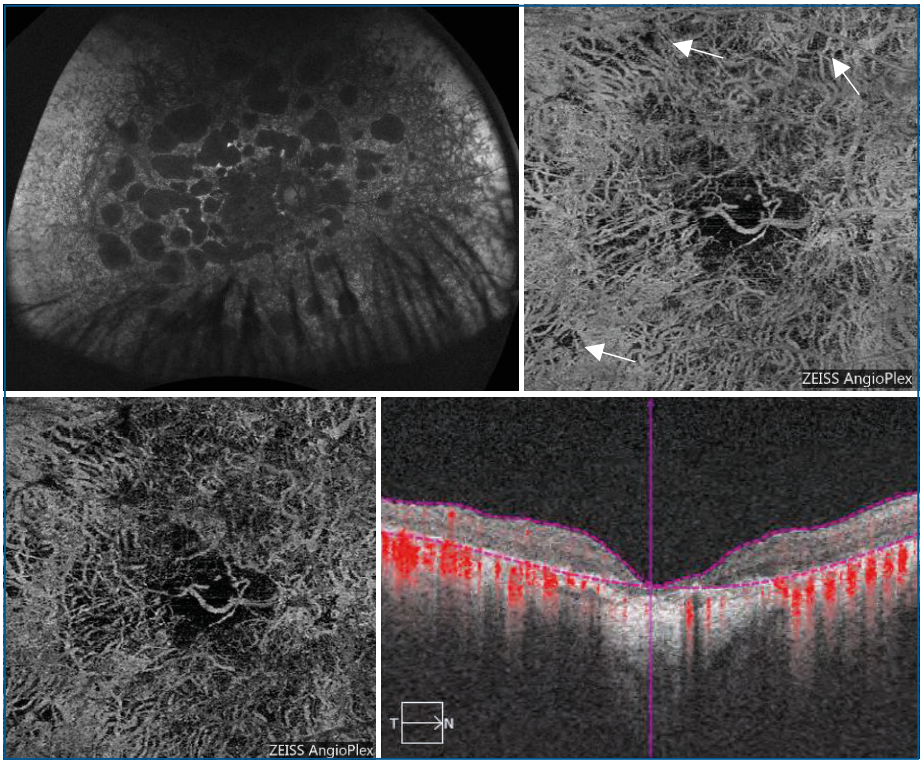

Figure 13-3. Images of advanced Stargardt disease in a 31-year-old patient. Fundus autofluorescence reveals large areas of hypoautofluorescence. Color-coded B-scan shows limited flow in the choroid under the atrophic fovea, which corresponds to the rarefication of the choroid vessels shown in the choriocapillaris segments second left (arrows). There is an increased FAZ in the superficial segment.

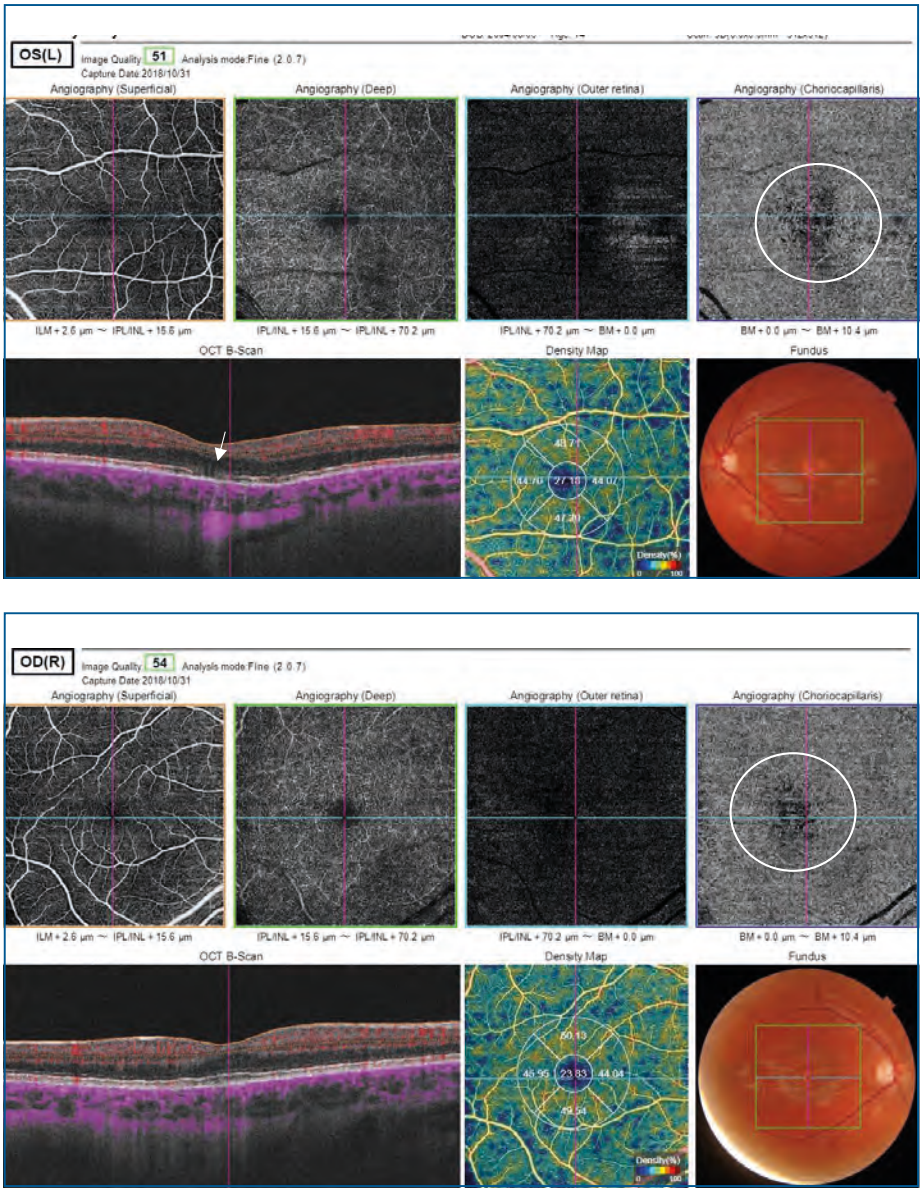

Figure 13-4. Retinitis pigmentosa (RP) in a 14-year-old boy. Both eyes are affected. Fundus photo shows macular atrophy, B-scan shows destruction of outer retina, especially in the left eye (arrow), and pallor of the optic disc in the right eye. Moreover, rarefication of the choriocapillaris in OCTA image (circles).

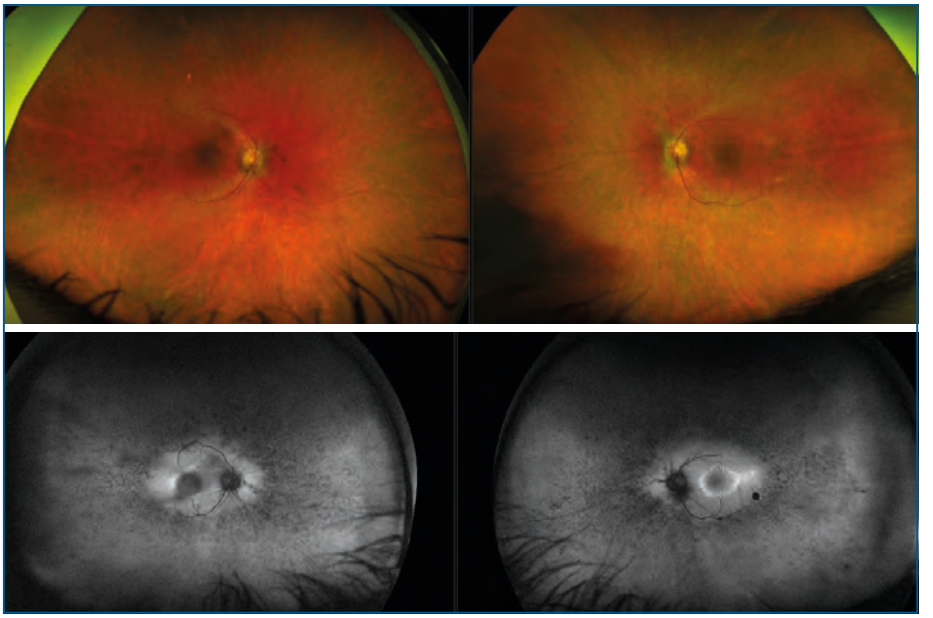

Figure 13-5. Wide-field images of both eyes. 25-year-old patient with rod-cone dystrophy. Color fundus photo shows pigmentary changes in the periphery, as autofluorescence shows abnormal fundus appearance around the macula and disc with macular edema and hypoautofluorescence further away.

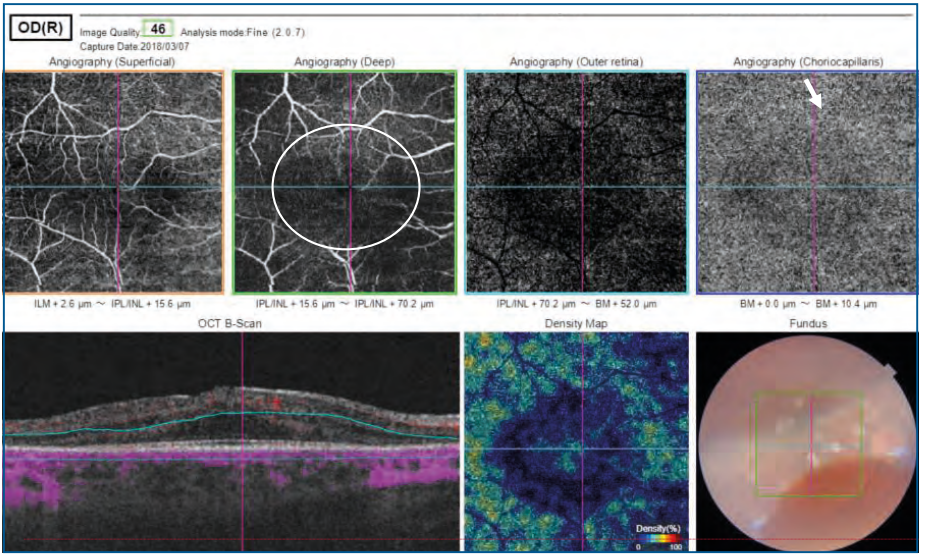

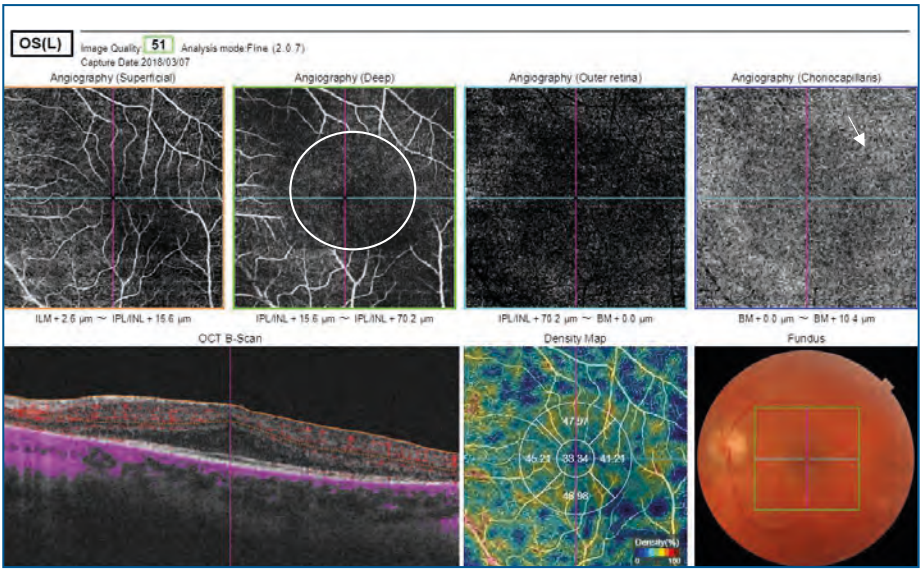

Figure 13-6. OCTA reports on left and right eyes. The same patient. Both B-scans show the presence of macular edema; however, there are no signs of neovascularization. On the deep segment of the both scans, there is the presence of wrong segmentation so the segments in the center show DVC due to its elevation (circle), whereas periphery shows only SVC. Furthermore, the choriocapillaris shows flow void areas (arrows).

14. Macular Telangiectasia 2

Macular telangiectasia 2 (MacTel) is a bilateral disorder that affects the paramacular region of the retina. It usually affects people in the fifth and sixth decade. It is occult and non-exudative. Its OCT findings include macular thinning, hyporeflective cavitations, development of full-thickness macular holes in the absence of vitreoretinal traction, and atrophic changes in the outer retinal layer. The superficial layer can be intact despite the presence of abnormal vessels in the deep layers.

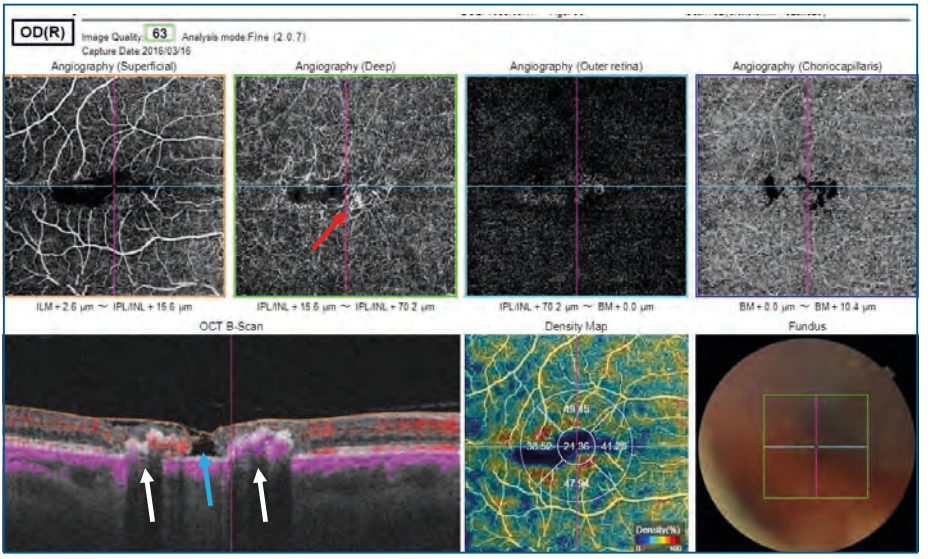

Figure 14-1. OCTA report on right eye. 60-year-old male. OCTA increased vascular caliber and increased flow voids in SVC and DVC, destruction of FAZ with vessel infiltration. Widened and telangiectatic vessels are present in the DVC (red arrow). In the B-scan, there are hyper-reflective crystalline deposits (white arrows), a macular hole (blue arrow) and destruction of the ellipsoid zone.

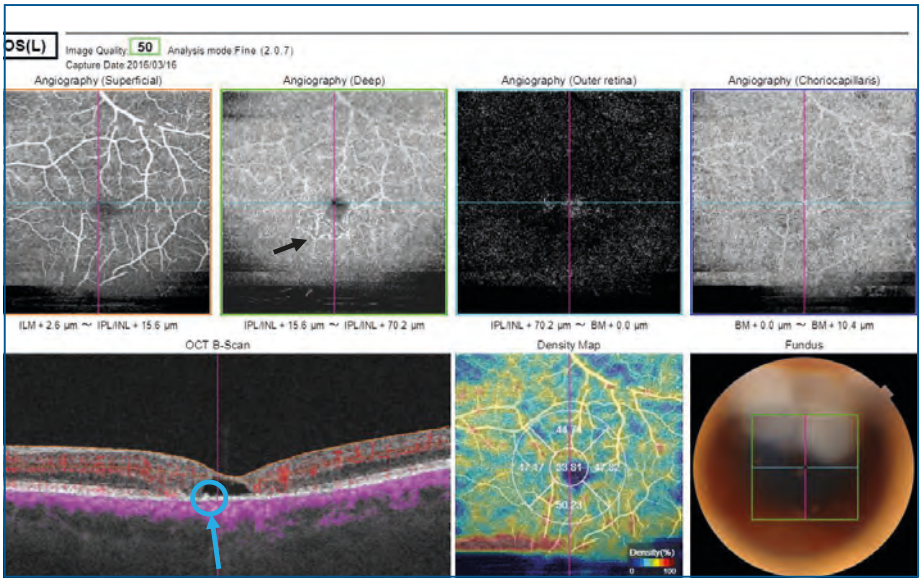

Figure 14-2. Left eye of the same patient presents intraretinal fluid disruption of inner and outer segment of photoreceptors and hyperplastic RPE migration (blue arrow). In the OCTA, a right angle vein is seen in the deep segment.

Key points

OCTA shows telangiectatic vessels together with right angle veins. In advanced cases, there might be choriocapillaris loss.

Index

References

Bousquet E. et al. 2018. Optical coherence tomography angiography of flat irregular pigment epithelium detachment in chronic central serous chorioretinopathy. *Retina* **38**, 629–638.

Campbell J.P. et al. 2017. Detailed Vascular Anatomy of the Human Retina by Projection-Resolved Optical Coherence Tomography Angiography. *Sci. Rep.* **7**, 1–11.

Cicinelli M.V. et al. 2018. Optical coherence tomography angiography in dry age-related macular degeneration. *Surv. Ophthalmol.* **63**, 236–244.

Cole E.D. et al. 2017. The Definition, Rationale, and Effects of Thresholding in OCT Angiography. *Ophthalmol. Retin.* **1**, 435–447.

Corbelli E. et al. 2018. Optical coherence tomography angiography features of angioid streaks. *Retina* **38**, 2128–2136.

Fang P.P. et al. 2016. Technische Grundlagen der OCT-Angiographie. *Der Ophthalmol.* **113**, 6–13.

Farecki M.L. et al. 2017. Characteristics of type 1 and 2 CNV in exudative AMD in OCT-Angiography. *Graefe's Arch. Clin. Exp. Ophthalmol.* **255**, 913–921.

Flores-Reyes E., Hoskens K., Mansouri K. 2017. Optic Nerve Head Drusen: Imaging Using Optical Coherence Tomography Angiography. *J. Glaucoma* **26**, 845–849.

Gaier E.D. et al. 2017. Focal capillary dropout associated with optic disc drusen using optical coherence tomographic angiography. *J. Neuro-Ophthalmology* **37**, 405–410.

Huang D. et al. 1991. Optical coherence tomography. *Science* **254**, 1178–81.

Kalkman J. 2017. Fourier-Domain Optical Coherence Tomography Signal Analysis and Numerical Modeling. *Int. J. Opt.* **2017**, 1–16.

Lane M. et al. 2016. Visualizing the choriocapillaris under drusen: Comparing 1050-nm swept-source versus 840-nm spectral-domain optical coherence tomography angiography. *Investig. Ophthalmol. Vis. Sci.* **57**, OCT585-OCT590.

Makita S. et al. 2006. Optical coherence angiography. *Opt. Express* **14**, 7821.
Nalcı H. et al. 2017. Optic Coherence Angiography Findings in Type-2 Macular Telangiectasia. *Türk Oftalmol. Derg.* **47**, 279–284.
Nicolò M. et al. 2017. Choroidal vascular flow area in central serous chorioretinopathy using swept-source optical coherence tomography angiography. *Investig. Ophthalmol. Vis. Sci.* **58**, 2002–2010.
Querques L. et al. 2017. Optical coherence tomography angiography of myopic choroidal neovascularisation. *Br. J. Ophthalmol.* **101**, 609–615.
Roisman L., Goldhardt R. 2017. OCT Angiography: an Upcoming Non-invasive Tool for Diagnosis of Age-Related Macular Degeneration. *Curr. Ophthalmol. Rep.* **5**, 136–140.
Schwartz S.G., Monroig A., Flynn H.W. 2017. Multimodal images of chronic branch retinal vein occlusion. *Int. Med. Case Rep. J.* **10**, 159–162.
Singh A. et al. 2017. Morphological differences between optic disc collaterals and neovascularization on optical coherence tomography angiography. *Graefe's Arch. Clin. Exp. Ophthalmol.* **255**, 753–759.
Spaide R.F. et al. 2018. Optical coherence tomography angiography. *Prog. Retin. Eye Res.* **64**, 1–55.
Spaide R.F., Fujimoto JG, Waheed NK. 2015. Image artifacts in optical coherence tomography angiography. *Retina* **35**, 2163–2180.
Winegarner A. et al. 2018. Retinal microvasculature and visual acuity after intravitreal aflibercept in eyes with central retinal vein occlusion. *Retina* **38**, 2067–2072.
Wojtkowski M. et al. 2002. In vivo human retinal imaging by Fourier domain optical coherence tomography. *J. Biomed. Opt.* **7**, 457.
Wylęgała A. et al. 2016. Optical coherence angiography: A review. *Medicine (Baltimore).* **95**, e4907.
Wylęgała A. 2018. Principles of OCTA and Applications in Clinical Neurology. *Curr. Neurol. Neurosci. Rep.* **18**, 96.
Wylęgała A. 2017. Zastosowanie angio-OCT w chorobach tylnego odcinka oka. in Wylęgała E, (Ed.) *Zastosowanie optycznej koherentnej tomografii w okulistyce*. Górnicki, Wrocław, pp. 97–109.
Wylęgała A., Wylęgała E. 2018. Anti-vascular endothelial growth factor and macular atrophy: an unanswered question. *Ann. Eye Sci.* **3**, 61–61.
Wylęgała A., Wylęgała F., Wylęgała E. 2018. Aflibercept Treatment Leads to Vascular Abnormalization of the Choroidal Neovascularization. *J. Healthc. Eng.* **2018**, 1–5.